Jasmine Anne Quiambao

Candidate

Civil Engineering

Department

This thesis is approved, and it is acceptable in quality and form for publication:

Approved by the Thesis Committee:

Dr. Kerry Howe, Chairperson

Dr. Jorge Gonzalez – Estrella

Dr. Jośe M. Cerrato

Co-occurrence of microplastics, uranium and arsenic in heavy metal-contaminated freshwaters and their potential interaction

by

Jasmine Anne Y. Quiambao

Bachelor of Science in Chemical Engineering
University of New Mexico, 2020

THESIS

Submitted in Partial Fulfillment of the
Requirements for the Degree of

Master of Science

Civil Engineering

The University of New Mexico
Albuquerque, New Mexico

May 2022

Acknowledgements

I am very thankful and blessed for being surrounded by amazing people who constantly show love and support throughout my career. I would not be the person I am today, and I would not be where I am now if it was not for the people who helped and guided me. This acknowledgment is not enough to show how much I appreciate each one of you.

To my committee members, Dr. Kerry Howe, Dr. Jośe Cerrato Corrales, and Dr. Jorge Gonzalez Estrella. Thank you for allowing me to work with all of you. I am grateful for witnessing how great each of you is in your profession. I am very amazed by the passion, commitment, and intelligence you have in your career. I would like to thank all of you for giving me genuine support and guidance throughout my research. With your dedication to helping students grow personally and professionally, I have gained so much knowledge that I will continue to carry throughout my career. Each of you has contributed to my life differently. I would like to thank Dr. Kerry Howe for believing in me, for the opportunity to continue my research, and for encouraging me to always do my best. I would like to thank Dr. Jośe Cerrato Corrales for sharing his passion for his work, for helping me finish my research, and for supporting me in everything I do. I would like to thank Dr. Jorge Gonzalez Estrella for giving me the opportunity to work on this fascinating research topic, for guiding me all throughout, and for giving me valuable advice that I will always remember. I am very lucky to have good mentors who want nothing but the best for their students. Thank you for being there during all my successes and challenges. Thank you for believing in me.

To my research group colleagues, I would like to thank you for all the amazing memories we shared together inside and outside work. I will forever cherish all the hard times, laughs, and victories we shared together. This is the best group anyone could ask for. As we move on with our lives, let's continue to strive harder and support each other.

To my friends, thank you for lifting me up during my hard times and for celebrating with me during my triumphs. Thank you for always being there for me, for making me feel supported, loved, and cared for.

To the most important people in my life, my family. I would like to thank my parents for always encouraging me to follow what my heart desires. Thank you for always believing in me and trusting me with all my life decisions. I am forever grateful to both of you. Thank you for all the sacrifices, hard work, and for doing everything for our family. I appreciate all that you do. I would also like to thank my two brothers for all the love and laughers we share. My family has given me unconditional love and support throughout my life. I will keep chasing my dreams and make them proud.

Co-occurrence of microplastics, uranium and arsenic in heavy metal-contaminated freshwaters and their potential interaction

by

Jasmine Anne Quiambao

B.S. Chemical Engineering, 2020

University of New Mexico

M.S. Civil Engineering, 2022

ABSTRACT

This study identified microplastics and heavy metals in fields sites of freshwater systems in New Mexico and evaluated the interactions of arsenic (As) and uranium (U) with commercial microplastics for acidic and neutral pH in laboratory-controlled conditions. The potential interaction of microplastics with other contaminants is not well-established. Microplastics could interact with heavy metals in ecosystems with naturally elevated background concentrations of metals or affected by anthropogenic activities. Previous studies have found heavy metal contamination in freshwater systems in New Mexico near abandoned mine sites. The objective of this study is (1) to identify and characterize microplastics from metal contaminated freshwater systems in New Mexico and (2) to evaluate the interaction of As and U with commercial microplastics in laboratory-controlled conditions. Freshwater samples from Tingley Beach, the Rio Grande, and Laguna Pueblo, NM were collected and treated. Stereomicroscopy and micro-Fourier Transform Infrared (FTIR) spectroscopy were utilized to identify microplastics from the field samples while Inductively Coupled Plasma Mass Spectrometry (ICP-MS) was utilized to quantify heavy metals. The laboratory-controlled experiments were conducted with commercial

poly(methyl-methacrylate) (PMMA), polyethylene (PE), and polystyrene (PS) microplastics exposed to 0.02 – 0.2 mM of As and U solutions, separately. Field data indicated microplastics occurrence and elevated heavy metal concentrations in freshwater systems in New Mexico. Laboratory experiments showed no interaction of commercial microplastics with As at pH 3 and pH 7 and U at pH 3. However, U precipitates formed at pH 7 and deposited onto the microplastics surface. These results indicate that microplastics can accumulate and may be acting as nucleation site for U precipitates. Aqueous chemistry analyses indicated that the precipitates formed are potentially sodium-compreignacite and schoepite. The results of this study advance the understanding of the occurrence and interactions of microplastics and heavy metals in freshwater systems in New Mexico, potentially facilitating the transport of metals through the environment and increasing toxicity effects.

Table of Contents

List of Figures

List of Tables

Chapter 1: Research Overview

1.1 Research Introduction. This study assesses the reactivity of microplastics with heavy metals. Microplastics (MPs) are broadly defined as plastic materials with a diameter <5 mm (Carr et al., 2016; Jingyi Li et al., 2018; Zhao et al., 2014; Zou et al., 2020), while nanoplastics (NPs) are defined as plastic materials with <0.1 μm in size; both are considered as major sources in aquatic environments (Ateia et al., 2022). The word microplastics used in the whole document will represent MPs with <5 mm and NPs with <0.1 μm unless specified for methodology uses. Microplastics with a diameter <150 μm are of particular concern given their small size and their potential to be ingested (Cox et al., 2019; *Microplastics in Drinking-Water*, 2019). The consensus is that microplastics are ubiquitous in the environment (Schymanski et al., 2018; Song et al., 2015; Fayuan Wang et al., 2019; Wong et al., 2020; Zhao et al., 2014). Previous studies have found microplastics in the surface water of inland rivers of different continents (Z. Fu & Wang, 2019; Kataoka et al., 2019; Naqash et al., 2020; Zhang et al., 2018), glaciers (Horton & Barnes, 2020), sediments of remote lakes around the world (Sruthy & Ramasamy, 2017; Triebskorn et al., 2019; Yuan et al., 2019), or remote marine environment atmosphere (Trainic et al., 2020) among other sites. The prevalence of microplastics enables their interaction with several contaminants. Such interactions are of concern due to potential enhancement of toxic effects and transport of contaminants through the environment.

Several freshwater systems in the state of New Mexico near abandoned mine sites are contaminated with heavy metals (Blake et al., 2015, 2017). For instance, water samples collected from the Jackpile Mine in Laguna Pueblo, NM contained uranium (U) concentrations ranging from 35.3 to 772 μg L^{-1} (Blake et al., 2017); above the United States Environmental Protection Agency (USEPA) maximum contaminant levels (MCL) of 30 μg L^{-1} of U for drinking water (*National*

Primary Drinking Water Regulations | Ground Water and Drinking Water | US EPA, n.d.). Freshwater systems of isolated communities, such as Laguna Pueblo, NM, are contaminated by recreational activities, solid waste littering, wastewater effluents (Carr et al., 2016; Jingyi Li et al., 2018; Wong et al., 2020). Freshwater contaminated with microplastics and heavy metals can promote the interaction between these contaminants, enhance toxic effects, and shift the fate and transport of these contaminants through the environment (Zou et al., 2020).

1.2 Research Gaps. The gathered information about microplastic contamination in freshwater systems is still limited compared to marine environments. As of 2018, less than 4% of published research articles focused on the abundance of microplastics in freshwater systems compared to seawater (Harrison et al., 2018). Yao et al. (2020) identified that most studies focus on rivers and lakes, suggesting a lack of knowledge about microplastics occurring in other freshwater sources such as ponds, groundwater, and reservoirs. Likewise, more documentation is needed regarding microplastic pollution in freshwater systems located in isolated communities, sites previously contaminated with other contaminants, or remote places facilities. Moreover, the negative impacts of microplastics on the aquatic environment, organisms, human health and the association and interaction of microplastics with other contaminants need to be further researched.

Microplastics can associate with several types of metals. For instance, Verla et al. (2019) stated that experimental studies are still required to understand how aqueous anionic metals like arsenic (As), selenium (Se), chromium VI [Cr (VI)], molybdenum (Mo), and boron (B) binds on the surface of plastics. A better understanding of the relationship and behavior of metals and microplastics would provide valuable information about the transport of contaminants sorbed onto microplastics and potential toxicity synergies.

1.3 Research Objective. The overall objective of this study is to assess the reactivity of microplastics with heavy metals. This research is divided into two sub-objectives: (1) identify the occurrence of microplastics in freshwater systems in New Mexico containing elevated concentrations of heavy metals; and (2) evaluate the interaction of microplastics and heavy metals in laboratory-controlled conditions. This study provides information about microplastics occurring in freshwater systems in New Mexico and the potential adsorption of heavy metals onto them. Microplastics can act as carriers of various toxic heavy metals in waters through sorption and can accumulate in aquatic ecosystems (Tourinho et al., 2019; Zou et al., 2020). The association of heavy metals with microplastics may increase potential toxicity to several organisms at various trophic levels and enable the transport of these contaminants through the environment.

1.4 Research Overview. This thesis document is divided into four chapters, an appendix, and a reference section. Chapter 2 consists of literature review of previous and current research on microplastics, microplastics in freshwater systems, toxicity of heavy metals, and coexistence of microplastics and heavy metals. It discusses the prevalence of microplastics and heavy metals in freshwater systems and how they negatively affect the environment and human health. Chapter 3 and 4 are the main parts of the thesis. These sections are outlined as a research journal article which will be proposed and submitted to peer-reviewed journals. Chapter 3 is focused on the occurrence of microplastics and heavy metals in field sites of freshwater systems in New Mexico. It describes the sample treatment and analyses performed to detect microplastics and to quantify arsenic (As) and uranium (U) concentrations from the field samples. Chapter 3 also demonstrates the result of the occurrence of microplastics in freshwater systems in New Mexico containing elevated concentrations of heavy metals. Chapter 4 is focused on the interfacial reactions of microplastics and heavy metals. Chapter 4 describes the methodologies used and the results from kinetic and

adsorption isotherm experiments using various aqueous phase and spectroscopy analysis. Appendices A and B contain supplementary data collected from the study in Chapter 3 and 4.

Chapter 2: Literature Review

2.1 Microplastics

2.1.1 History of Plastic Production. Plastic production commercially started in the 1950s and has increased dramatically since then. The global annual plastic production in 2015 exceeds 300 million metric tons (Geyer et al., 2017; Lee et al., 2021; Rodrigues et al., 2018; Wong et al., 2020). Plastics are used worldwide due to their lightweight, durability, versatility, and low-cost production among other features (Adamcová et al., 2017; Veerappapillai & Muthukumar, 2015). The most widely used types of plastics are polyethylene (PE), polypropylene (PP), polyvinylchloride (PVC), polyethylene terephthalate (PET), and polystyrene (PS) (Andrady & Neal, 2009; Carr et al., 2016). Polystyrene is used as packaging materials, production of disposable cups, and many other uses (Veerappapillai & Muthukumar, 2015). Meanwhile, PE is the "largest volume polymer produced globally" (Demirors, 2011). It is used to produce carrier bags, bottles, containers, and other commercial and industrial products (Cheremisinoff, 1989). Poly (methyl methacrylate) also has a wide range of applications in nanotechnology, biomedical, pharmaceutical, and used as a substitute for glass products like aircraft canopies, windows, and aquariums (Ali et al., 2015). Unfortunately, plastics have been polluting aquatic ecosystems due to improper waste disposal and the extensive use of plastics worldwide (Barnes et al., 2009). As of 2015, Geyer et al. (2017) estimated that approximately 6300 million metric tons of plastic waste had been generated globally, and only 9% had been recycled, 12% was incinerated, and 79% ended up in landfills or was discarded in the natural environment. Plastics resist biodegradation and are prone to fragmentation which could reduce the size of plastic particles in the environment (Adamcová et al., 2017; Naqash et al., 2020). These small plastic particles, known as microplastics,

have raised much concern because of its ability to accumulate and interact with the aquatic ecosystems and other pollutants.

2.1.2 General Information of Microplastics. Microplastics are classified as solid polymer particles with an upper size limit of 5 mm and without a specified lower limit (Jingyi Li et al., 2018), while nanoplastics (NPs) are defined as plastic materials with <0.1 μm in size; both are considered as major sources in aquatic environments (Ateia et al., 2022). The diversity of microplastics depends on size, color, shape, chemical composition, density, and other characteristics (Duis & Coors, 2016). Microplastics are classified as primary and secondary microplastics (Jingyi Li et al., 2018). Primary microplastics are purposely made with a size smaller than 5 mm for cosmetic, pharmaceutical, industrial, or other products (Browne & Browne, 2015). On the contrary, the secondary microplastics are fragments of large plastics that are broken down by processes such as intense weathering, exposure to ultraviolent radiation, mechanical forces, photo-degradation, and other processes (Horton et al., 2017). Some of the contributing sources are plastic bags, bottles, fishing nets, straws, discarded plastic debris, and consumer products (Eerkes-Medrano et al., 2015).

2.1.3 Sources of Microplastics. Microplastics can derive from terrestrial and ocean-based sources (Jingyi Li et al., 2018). Studies have shown that 80% of microplastic contamination generates from terrestrial sources; they include different origins such as personal care products, improperly disposed plastics, and extensive use of plastics, and the 20% generates from ocean-based sources such as commercial fishing, vessels, littering of larger plastics pieces, and other activities in beaches, shores, and far offshore (Andrady, 2011; Cole et al., 2011). Additionally, the prominent microplastic contamination is classified as secondary microplastics. Most found secondary microplastics are fragments from consumer products and household items and fibers

from washing clothes which are mainly made of polyester, acrylic, and polyamide (Eerkes-Medrano et al., 2015).

2.1.4 Microplastic Contamination in Aquatic Environments. Microplastics pollution is a major issue in the marine environment. However, fewer efforts have been made to study the prevalence, fate, and impacts of microplastics in freshwater systems. Only less than 4% of microplastics-related studies are reportedly associated with freshwaters (Harrison et al., 2018). It has been estimated the amount of microplastic in surface water range from 10^{-8} to 100 pieces L^{-1} compared to 40 to 400 pieces L^{-1} in the ocean and beach sediments (Jingyi Li et al., 2018), indicating that microplastics affect freshwater and marine environments. Microplastics have been detected across the world; previous studies have found microplastics in the surface water of inland rivers of different continents (Z. Fu & Wang, 2019; Kataoka et al., 2019; Naqash et al., 2020; Zhang et al., 2018), glaciers (Horton & Barnes, 2020), sediments of remote lakes around the world (Sruthy & Ramasamy, 2017; Triebskorn et al., 2019; Yuan et al., 2019), or remote marine environment atmosphere (Trainic et al., 2020) among other sites. The abundance of microplastics also depends on spatial, temporal, and seasonal variability (Naqash et al., 2020; Wong et al., 2020). A study found that microplastic contamination has increased in surface waters after rainfall (Naqash et al., 2020). In open freshwater systems like rivers connected to the ocean, microplastics would be transported to the marine environment, while in isolated or static freshwater systems, microplastics would retain and accumulate (Eerkes-Medrano et al., 2015; Wong et al., 2020).

2.1.5 Microplastics in Freshwater Systems. Previous studies have identified microplastic contamination in freshwater systems. Su et. al (2016) found fibers ranging from 3.4 to 25.8 particles L^{-1} in Lake Taihu in China. The most common polymer type identified were cellophane (CP), polyethylene terephthalate (PET), polyester (PES), polypropylene (PP), and polyamide (PA)

with 100 to 1000 μm in size. Fibrous and fragmented microplastics were found along the middle and lower reaches of the Yangtze River Basin with concentrations varying from 0.24 particles L^{-1} to 1.8 particles L^{-1} (L. Li et al., 2019) and 0.5 to 3.1 particles L^{-1} (Su et al., 2018). Li et. al (2019) identified mainly polypropylene (PP), polyethylene (PE), and polycarbonate (PC). Meanwhile, Su. et al (2018) found that the most dominant polymers were polyester (33%), polypropylene (19%), and polyethylene (9%). Both studies found that microfibers with size < 1 mm were dominant (L. Li et al., 2019; Su et al., 2018). Luo et. al (2019) found microplastics with a range from 1.8 to 2.4 particles L^{-1} in Suzhou River, Huangpu River, and the urban creeks of Shanghai. The dominant polymer was fibrous polyester with 96% composition match, followed by rayon with 81% match. The microplastics showed trends of increasing abundance near the city center and estuary; indicating that domestic pollution is the contributing factor to microfiber abundance (Luo et al., 2019). Once terrestrial microplastics are exposed to natural water systems, they would likely be transported to oceans by rivers or reside in freshwater systems. The prevalence of microplastics in the freshwater ecosystems is closely related to anthropogenic activities and were more likely to be found in areas with high population density or proximity to urban centers (Wong et al., 2020; Yonkos et al., 2014). The results suggest that microplastic pollution in small and remote freshwater bodies is more serious than in estuarine and coastal waters (Luo et al., 2019). The prevalence and abundance of microplastics in freshwater systems are yet to be studied comprehensively as well as the environmental and health impacts.

2.1.6 Environmental Effects. The environmental effects of microplastics can be categorized into physical, chemical, and biological impacts (Jingyi Li et al., 2018). Although most of the initial studied focused on microplastic pollution in seawater, evidence suggests that freshwater systems may share similarities to marine systems in the prevalence of microplastics and

potential impacts (Eerkes-Medrano et al., 2015). The physical impact of microplastics on marine wildlife is entanglement and ingestion. Entanglement could cause drowning, suffocating, strangulating or starving to aquatic species (Allsopp et al., 2006). Microplastics with a diameter <150 μm are of particular concern given their small size and their potential to be ingested (Cox et al., 2019; *Microplastics in Drinking-Water*, 2019). Various organisms could perceive microplastics as food (Naqash et al., 2020). Organisms that ingest microplastics can suffer from punctured, impacted, or blocked digestive systems (Zhang et al., 2018), oxidative stress, endocrine disruption, immune response and ultimately reduced growth and survival (Choi et al., 2018; Espinosa et al., 2017; Greven et al., 2016; Lei et al., 2018; Lu et al., 2016; Luís et al., 2015). Chemical and biological impacts happen after ingestion where the toxicity of microplastics effects humans and living organisms (Jingyi Li et al., 2018). Microplastics could act as a medium to concentrate and release chemicals, pesticides, and other pollutants into the tissues of various organisms and into ecosystems' food chain (Verla et al., 2019). These chemicals come from the environment (e.g., polychlorinated biphenyls, PCBs or Dichlorodiphenyldichloroethylene, DDEs) or from plastic additives (e.g., plasticizers) during production (Eerkes-Medrano et al., 2015). Microplastics pose a threat to the environment through unintentional or intentional ingestion and its corresponding toxic chemicals. Microplastics pollution has an essential role in what is occurring in our environment because of its environmental effects, health effects, and its ability to act as a carrier for harmful and toxic chemicals such as metals, oils, and additives.

2.1.7 Human Health Effects. Although the knowledge on the impact of microplastics on aquatic ecosystems and human health is still limited, there is a concern about the translocation of microplastics to organisms and humans (Triebskorn et al., 2019). Airborne is an exposure route of microplastics to humans and its possible source are textile, landfills, plastic wastes incinerators,

and degraded plastic wastes (Wong et al., 2020). These airborne microplastics are transported into the terrestrial ecosystem by windblown mechanism and enter human through inhalation (Wong et al., 2020). Inhalation of plastics particles will either enter the digestive system via mucociliary clearing or remain trapped in the lungs (Cox et al., 2019); resulting in asthma, allergic alveolitis, pneumonia and bronchitis (Lwanga et al., 2017). Human could also get exposed to microplastics through consumption of freshwater organisms. For instance, consumption of fish or shellfish infected by microplastics and pollutants (Wong et al., 2020; Wright & Kelly, 2017). Microplastics have the potential to translocate into human tissues, trigger a localized immune response, and release constituent monomers, additives, and pollutants absorbed from the environment such as heavy metals and organic pollutants (Wright & Kelly, 2017). A previous study showed that the presence of plastic additives has been reported in urine and blood samples of human (Hauser et al., 2005). This exposure leads to physiological harm ranging from oxidative stress to carcinogenic behavior (Fen Wang et al., 2018).

2.2 Heavy Metals

2.2.1 General Information about Heavy Metals. Heavy metals are derived from two types of sources, natural and anthropogenic sources. Natural sources include the weathering of metal bearing rocks, volcanic eruptions, soil erosion, or dragging by rainwater (e.g., agricultural runoff) (Godoy et al., 2019). On the other hand, anthropogenic sources include industrial and urban wastewater, sewage effluents, open dumping and burning of solid wastes, and mining (J. Wang et al., 2017). Metals in the aquatic systems pose environmental and health problems due to their toxicity (Febrianto et al., 2009). Humans getting exposed to elevated concentrations of heavy metals can also suffer serious hazards. Arsenic is a toxic metal element classified as a Class I clear carcinogen by the International Agency for Research on Cancer (Dong et al., 2020). Arsenic can

affect fetal development, the central nervous system, and the circulatory system (Blake et al., 2015). Uranium is classified as kidney toxicant and has been linked to adverse developmental outcomes in animals (Blake et al., 2015). Cadmium (II) has also been shown to cause kidney damage, and copper (II) and nickel(II) ions could cause liver damage and dermatitis or chronic asthma (Febrianto et al., 2009). The toxicity of metals poses a hazardous threat in the environment and human health.

2.2.2 Mining. A century ago, mining was one of the most fast-growing industrial activities in the United States, which consequently left a legacy of >160,000 abandoned mines in the Western USA located near Native American communities (Lewis et al., 2017). Metal pollution is still evident in the environment close to abandoned mine sites. For example, high concentrations of uranium (U) were found in surface water adjacent to the abandoned Jackpile Mine in Laguna Pueblo, NM (35.3 to 772 μg L^{-1}) and in abandoned mine wastes in a Native American community in northeastern Arizona (67 - 169 μg L^{-1}) which are both above the USEPA maximum contaminant limit of 30 μg L^{-1} in drinking water (Blake et al., 2015). Elevated Arsenic (As) concentrations were also detected in sediments and mine waste solids (Blake et al., 2015). Recent studies show that Native Americans located near abandoned uranium mines have an increased likelihood for kidney disease and hypertension, and an increased likelihood of developing multiple chronic diseases (Blake et al., 2015, 2017). Previous studies performed biomonitoring and confirmed high exposure to uranium and associated metals in the waste in adults, neonates, and children in these communities (Lewis et al., 2017). These findings indicate that abandoned mine sites play a significant role as a potential anthropogenic source that can be transferred and exposed to the environment and the community.

2.3 Mechanism of Microplastics and Heavy Metals Adsorption

2.3.1 Influence of Physicochemical Properties of Microplastics on Adsorption. The adsorption of organic and inorganic contaminants on microplastics is highly dependent on the physicochemical properties of microplastics such as polymer types, specific surface area, polarity, particle size, morphology, surface charge, degree of crystallinity, and pore size distribution (Ateia et al., 2022; Naqash et al., 2020; Tourinho et al., 2019). For example, microplastics with high surface area would likely have high adsorption capacity to chemicals (Tourinho et al., 2019). It is important to note that the abundance of crystalline domains, molecular chain arrays, and rubbery-based microplastics has greatly influenced the adsorption of contaminants (Ateia et al., 2022).

The crystalline polymer requires higher energy for destabilizing ordered polymer chains, while amorphous polymer has greater sorption capacity due to the presence of randomly oriented polymer chains (Naqash et al., 2020). The carbon chain in rubbery polymer could move freely compared to glassy polymer where movement is restricted. Therefore, there is higher sorption of contaminants observed in rubbery polymers (Tourinho et al., 2019). Additionally, the molecular structures and various monomeric compositions of microplastics could influence different molecular interactions with contaminants. Most microplastics have hydrophobic surfaces and abundant functional groups. Pristine and aged microplastics can carry metals; aged and weathered microplastics undergo degradation, including photo-degradation, biodegradation, thermo-degradation, and hydrolysis (Tourinho et al., 2019). Photo-oxidation is the primary degradation process of polymers resulting in additional of oxygen-containing functional groups such as aldehydes, ketones, alcohol, carboxylic acids and hydroperoxides, which increase the polarity and charge of the surface (Ateia et al., 2022; Tourinho et al., 2019; Turner & Holmes, 2015). Aged microplastics show higher sorption capacity due to its increased surface area, porosity, roughness,

and hydrophilicity (Naqash et al., 2020; Tourinho et al., 2019). Among all commercial microplastics, PS, PE, and PVC were widely studied for the adsorption of organic and inorganic contaminants due to their high prevalence in the environment (Ateia et al., 2022). Meanwhile, PMMA has been widely used as a substitute for glass products like aircraft canopies, windows, and aquariums (Ali et al., 2015).

2.3.2 Influence of Heavy Metals Characteristics on Adsorption. Concentration, pH, redox conditions can influence the chemical speciation of metals such as U and As in the environment. In oxidized source waters, U(VI) and As(V) are the predominant oxidation states. Pentavalent arsenate (H_3AsO_4) is a weak-acid oxyanion with pKa values of 2.24 ($H_2AsO_4^-$), 6.76 ($HAsO_4^{2-}$) and 11.60 (AsO_4^{3-}) and uranyl (UO_2^{2+}) ion is a weak-acid oxycation; both are common in oxidizing waters (Benjamin, 2015). Recent research has shown that U and As can complex and co-precipitate in acidic environments (Gonzalez-Estrella et al., 2020). Environmentally relevant constituents such as calcium (Ca^{2+}), iron (Fe^{2+}), sodium (Na^+), and carbonate (CO_3^{2-}) or phosphate (PO_4^{3-}) can influence various complexation precipitation and dissolution reactions (Smedley & Kinniburgh, 2002). The concentrations of U in the solution can be influenced by the occurrence of solid uranyl phases such as compreignacite ($K_2(UO_2)_6O_4(OH)_6(H_2O)_8$), becquerelite ($Ca(UO_2)_6O_4(OH)_6 \cdot 8(H_2O)$), schoepite ($(UO_2)_8O_2(OH)_{12} \cdot 12(H_2O)$, Na-compreignacite ($Na_2(UO_2)_6O_4(OH)_6(H_2O)_8$), and clarkeite ($Na(UO_2)O(OH)$); the environmental fate of U under oxidizing conditions is controlled by the formation of these minerals and their respective solubilities (Gorman-Lewis, Burns, et al., 2008; Gorman-Lewis, Fein, et al., 2008). Sorption and oxidative dissolution processes of these secondary minerals can release U and As into water (Gonzalez-Estrella et al., 2020).

2.3.3 Influence of Aqueous Media Characteristics on Adsorption. The physicochemical properties of both the microplastics and the toxic heavy metals as well as environmental characteristics drive the interaction of heavy metals and the microplastics (Ateia et al., 2022; Naqash et al., 2020; Tourinho et al., 2019). In terms of the characteristics of contaminants, pKa, hydrophobicity, planarity, chain, ring structure, and functional groups affects the adsorption of contaminants on microplastics. The physicochemical properties and chemical compositions of microplastics could also be altered by abrasion, biofouling, degradation, and surface modification due to the complexity of the aquatic environment (Ateia et al., 2022). It is important to examine the effect of aqueous media characteristics on the adsorption behavior of different contaminants on microplastics. Various factors of medium affect the adsorption on microplastics such as pH, organic matters, ionic strength, salinity, contact time, and temperature (Naqash et al., 2020). For instance, cationic metals (e.g., Cd^{2+}, Co^{2+}, Ni^{2+}, Pb^{2+}) show higher sorption capacities with increasing pH > 7 (Turner & Holmes, 2015). Other studies also indicated that increasing pH results to high adsorption (Holmes et al., 2014; Fayuan Wang et al., 2019; Q. Wang et al., 2020; Zou et al., 2020). The influence of pH is critical to the adsorption mechanism. When the pH decreased, H^+ could compete with the metals for the adsorption sites of microplastics. When the pH increased, the functional groups of the microplastic surface were deprotonated which results to increasing the electronegativity and sorption sites of the microplastic surface (Zou et al., 2020). Salinity also plays an important role in the adsorption of contaminants onto the microplastic surface. The increase in salinity results to decrease in sorption due to the competition between ions for sorption sites and electrostatic forces (Jia Li et al., 2018; Liu et al., 2018). Previous studies proved that sorption of cationic pollutants on microplastics was dependent on NaCl concentration as the presence of sodium, magnesium, and calcium ions competed with the heavy metals during sorption

process, decreasing the activity of the charged pollutants. Additionally, a large amount of the anion (e.g. Cl^-) promoted the formation of complexes (Gao et al., 2021). An increase in salinity could also result to aggregation of microplastics as it compresses the electrical double layer and reduces repulsive forces which caused the "stacking effects" and the reduced surface area (Gao et al., 2021; Fayuan Wang et al., 2019). The presence of multivalent cations like Ca^{2+} is better than monovalent cations like Na^+ because monovalent cations could strongly compete for cationic exchange sites (i.e., carboxyl groups) on the MP surfaces during sorption process (Ateia et al., 2022). However, salinity could also increase sorption depending on the chemical contaminant (e.g., electrostatic nature, molecular configuration, and activity coefficient) and microplastic properties (Ateia et al., 2022; Godoy et al., 2019; Tourinho et al., 2019).

2.3.4 Sorption Mechanism of Microplastics and Heavy Metals. Hydrophobic and electrostatic interaction are the two predominant mechanisms for the sorption of contaminants on microplastics (Tourinho et al., 2019). Hydrophobic interactions involve the attraction of non-polar or slightly polar molecules to the non-polar microplastics surface. On the other hand, electrostatic interactions are driven by the attraction of oppositely charged molecules or repulsion of same charged molecules. Microplastics surfaces are usually negatively net charged due to the pH of point of zero charge (pH_{pzc}) being lower than most environmental pH, and because of the deprotonation of carboxyl and hydroxyl groups (Ateia et al., 2022; Jia Li et al., 2018). Hence, the negative surface charges of microplastics are likely to attract positively charged species (Tourinho et al., 2019). Regarding anionic species, repulsion by the microplastic surfaces could occur and reduce sorption (Naqash et al., 2020; Tourinho et al., 2019). Other mechanisms such as hydrogen bonds, van der Waals and pi-pi interactions could promote sorption of contaminants. Hydrogen bonds are weak electrostatic interactions, involving proton donors and proton acceptors. Van der

Waals forces are also weak interactions between molecules not involving covalent or ionic bonding, while pi-pi interactions are attraction forces between aromatic molecules. Therefore, aliphatic polymers like PE and PVC could undergo van der Waals interactions, while aromatic polymers like PS could undergo pi-pi interactions (Tourinho et al., 2019).

2.3.5 Interaction of Microplastics with Contaminants. Microplastics contamination has raised much concern because of their potential to accumulate and interact other pollutants in aquatic ecosystems (Holmes et al., 2014; Z. Wang et al., 2019; Zou et al., 2020). For instance, pollutants such as polycyclic aromatic hydrocarbons (PAH) and polychlorinated biphenyls (PCBs) are capable of sorbing to the plastic surface and become bioavailable to animals upon ingestion (Brennecke et al., 2016). Microplastics can transport plastic additives like phthalates, nonylphenol, and brominated flame retardants (Naqash et al., 2020). Phthalates were found in human urine and blood samples (Hauser et al., 2005). Inorganic contaminants like heavy metals could potentially interact with microplastics in aquatic systems. Previous studies have shown that microplastics have high affinity towards metals by the anionic sites of microplastic surface becoming activated and available for adsorption of cationic metals known as electrostatic interaction (Mao et al., 2020; Fayuan Wang et al., 2019).

2.3.6 Microplastics in Metal-Contaminated Aquatic Ecosystems. Microplastics can interact with heavy metals in aquatic systems with naturally elevated background concentrations of metals or affected by anthropogenic activities. With the limited number of studies on the abundance of microplastics in heavy metal-contaminated freshwater systems, previous studies have shown the interaction of metals and microplastics in various aquatic environments. The accumulation of metals such as aluminum (Al), chromium (Cr), manganese (Mn), iron (Fe), cobalt (Co), nickel (Ni), zinc (Zn), cadmium (Cd) and lead (Pb) to polyethylene terephthalate (PET),

high-density polyethylene (HDPE), polyvinyl chloride (PVC), low-density polyethylene (LDPE), and polypropylene (PP) were detected in San Diego Bay (Rochman et al., 2014). They also found that concentrations of all metals increased throughout the 12-month study period; suggesting that microplastics could accumulate greater metal concentrations the longer it remains at sea (Rochman et al., 2014). These findings were like Munier & Bendell et. al (2018) where they found PVC, HDPE, and LDPE adsorbing trace metals of copper (Cu), Zn, Cd, and Pb in nine urban intertidal regions in Burrard Inlet, Vancouver, British Columbia, Canada. The greatest concentrations measured were 698,000, 6,667, 930, and 188 $\mu g\ g^{-1}$ of lead, zinc, cadmium, and copper respectively from an unidentified particle made of PVC (Munier & Bendell, 2018). Holmes et. al (2012) also found polyethylene pellets from beaches of southwest England containing variable concentrations of Cr (44 – 751 ng g^{-1}), Co (17.7 – 107 ng g^{-1}), Ni (40 – 131 ng g^{-1}), Cu (0.064 – 1.32 $\mu g\ g^{-1}$), Zn (0.299 – 23.3 $\mu g\ g^{-1}$), Cd (1.09 – 76.7 ng g^{-1}) and Pb (0.149 – 1.64 $\mu g\ g^{-1}$). Brennecke et al. (2016) found a significant interaction between aged polyvinyl chloride (PVC) fragments and copper (Cu) and zinc (Zn) in seawater. The adsorption of Cu was greater in PVC fragments than in PS which could be due to higher surface area and polarity of PVC (Brennecke et al., 2016). Holmes et. al (2014) studied the interaction of trace metals (Cd, Co, Cr, Cu, Ni, Pb) to both virgin and aged polyethylene pellets under estuarine conditions. With increasing pH in river water, the adsorption of Cd, Co, Ni, and Pb onto the microplastics increased while adsorption of Cr decreased and adsorption of Cu remained the same (Holmes et al., 2014). These studies suggest that microplastics potentially interact and accumulate heavy metals highlighting the importance to survey freshwater systems that have been affected by metal contamination and exposed to plastic pollution as well.

2.3.7 Studies on Microplastics and Metals in Laboratory-Controlled Conditions. Other studies have reported that metal cations can adsorb onto the microplastic surfaces. For instance, the adsorption of divalent cation such as Cd^{2+}, Cu^{2+}, Pb^{2+}, Zn^{2+}, and Ni^{2+} has been reported onto microplastic materials such as HDPE, LDPE, PVC, PE, and PS at acidic and circumneutral pH (Ahechti et al., 2020; Brennecke et al., 2016; Godoy et al., 2019; Holmes et al., 2012, 2014; Mao et al., 2020; Turner & Holmes, 2015; Fayuan Wang et al., 2019; Zou et al., 2020). Another study showed that heavy metals have higher adsorption affinity to aged PS microplastics compared to pristine microplastics (Mao et al., 2020). The adsorption of arsenic (III) onto polytetrafluoroethylene and polystyrene microplastics at pH ranging from 3 to 7 has also been reported (Dong et al., 2019, 2020).

Chapter 3

Potential interactions of microplastics with uranium and arsenic in heavy metal-contaminated freshwater systems

*Jasmine Quiambao[1], Kendra Hess[2], Sloane Johnston[2], Kerry J. Howe[1], José M. Cerrato[1], and Jorge Gonzalez-Estrella[*2]*

*Corresponding author email address: jorgego@okstate.edu;

[1]Department of Civil Engineering, MSC01 1070, University of New Mexico, Albuquerque, New Mexico 87131, USA

[2]School of Civil & Environmental Engineering, 248 Engineering North, Oklahoma State University, Stillwater, Oklahoma 74078

ABSTRACT: This study detected microplastics in heavy metal contaminated freshwater systems located nearby Jackpile Mine, Laguna Pueblo, NM. Compared to the marine environment more information is needed to understand the degree of contamination of freshwater systems. The status of microplastic contamination in freshwater systems located in isolated communities, sites previously contaminated with other contaminants, or remote places needs further documentation. Contaminants binding onto microplastics potentially modifies toxicity effects and their fate and mobility through the environment. This study analyzed the occurrence of microplastics in six freshwater bodies located near the Jackpile Mine, Laguna Pueblo, NM contaminated with uranium (U) and arsenic (As). Samples were also taken in freshwater bodies of Albuquerque, NM (Rio Grande and Tingley Beach) to compare microplastic contamination of a rural community and an urban center. Samples were filtered, digested, and then analyzed with a stereo microscope for visual detection, Fourier Transform Infrared Spectroscopy – Attenuated Total Reflection (FTIR-ATR) for microplastic quantification and characterization, and Inductively Coupled Plasma Mass Spectrometry (ICP-MS) to quantify heavy metals. The Rio Grande samples showed the highest

concentration of microplastics (~ 20 – 114 pieces L^{-1}) in co-occurrence with U (~ 1 to 1.5 μg L^{-1}) and As (~ 2 to 3 μg L^{-1}), followed by samples taken from Tingley Beach (~ 48 – 82 pieces L^{-1}) in co-occurrence with U (~ 2.2 to 2.4 μg L^{-1}) and As (~ 10 to 11 μg L^{-1}), and samples taken from Laguna Pueblo freshwater (~ 4 – 18 pieces L^{-1}) in co-occurrence with U (~30 to 37 µg L^{-1}) and As (~ 0.5 to 1 μg L^{-1}). Our findings indicate that heavy metal contaminated freshwater systems of isolated locations can contain microplastics as well, increasing the likelihood of interaction between these contaminants. This study opens possibilities for further research needed to understand sorption of toxic heavy metals onto commonly occurring microplastics. Assessing potential interactions of toxic heavy metals and microplastics is crucial to understand compounding toxicity, reactivity, fate, and mobility through the environment.

3.1 Introduction

Microplastics are broadly defined as plastic materials with a diameter <5 mm (Carr et al., 2016; Jingyi Li et al., 2018; Zhao et al., 2014; Zou et al., 2020), while nanoplastics (NPs) are defined as plastic materials with <0.1 µm in size; both are considered as major sources in aquatic environments (Ateia et al., 2022). The word microplastics used in the whole document represent MPs with <5 mm and NPs with <0.1 µm unless specified for methodology uses. Several studies have determined that microplastics commonly occur in the marine environment (Eerkes-Medrano et al., 2015; Nuelle et al., 2014; O'Brine & Thompson, 2010; Song et al., 2015b); however, more information is needed to understand the degree of contamination of freshwater and terrestrial ecosystems (Blettler et al., 2018; Carbery et al., 2018; Gao et al., 2021; C. Li et al., 2020; Zhu et al., 2020). Studies have shown that 80% of microplastic contamination is generated from terrestrial sources such as personal care products, improperly disposed plastics, and extensive use of plastics

and the 20% generates from ocean-based sources due to commercial fishing, vessels, littering of larger plastics pieces, and other activities in beaches, shores, and far offshore (Andrady, 2011; Cole et al., 2011).

Once terrestrial microplastics are exposed to natural water systems, they would likely be transported to oceans by rivers or reside in freshwater systems. It has been estimated that the amount of microplastics in surface water range from vary from 10^{-5} to 10^{5} pieces m^{-3} compared to 40 to 400 pieces L^{-1} in the ocean and beach sediments (Jingyi Li et al., 2018). The prevalence of microplastics in the freshwater ecosystems is closely related to anthropogenic activities and were more likely to be found in areas with high population density or proximity to urban centers (Wong et al., 2020; Yonkos et al., 2014). Seasonal changes and flooding also showed a prominent increase of microplastic pollution (Naqash et al., 2020).

Microplastic contamination has raised much concern because of their potential to accumulate and interact other pollutants in aquatic ecosystems (Holmes et al., 2014; Z. Wang et al., 2019; Zou et al., 2020). For instance, microplastics can interact with heavy metals in aquatic systems with naturally elevated background concentrations of metals or affected by anthropogenic activities. Natural sources include the weathering of metal bearing rocks, volcanic eruptions, soil erosion, or dragging by rainwater (Godoy et al., 2019). On the other hand, anthropogenic sources include industrial and urban wastewater, sewage effluents, open dumping and burning of solid wastes, and mining (J. Wang et al., 2017).

Previous studies have shown the interaction of heavy metals and microplastics in various aquatic environments. Brennecke et al. (2016) found a significant interaction between aged polyvinyl chloride (PVC) fragments and copper (Cu) and zinc (Zn) in seawater. Holmes et. al (2014) studied the interaction of trace metals like cadmium (Cd), cobalt (Co), chromium (Cr),

copper (Cu), nickel (Ni), and lead (Pb) to both virgin and aged polyethylene pellets under estuarine conditions. The adsorption of Cd, Co, Ni, and Pb onto the microplastics increased with increasing pH in river water (Holmes et al., 2014). Heavy metals such as Zn, Cu, Pb, As, and other metals were also present at various points along the coast of China and in the Mediterranean Sea (Wang et al., 2012, 2018; Zhao et al., 2018). These studies suggest that microplastics potentially interact and accumulate other contaminants, specifically heavy metals, highlighting the importance to survey freshwater systems that have been affected by metal contamination and exposed to plastic pollution as well.

The objective of this study is to identify the occurrence of microplastics in freshwater systems with known uranium (U) and arsenic (As) contamination. This study analyzed the occurrence of microplastics in six freshwater bodies located near the Jackpile Mine of Laguna Pueblo, NM contaminated with U and As. Samples were also taken in freshwater bodies of Albuquerque, NM (Rio Grande and Tingley Beach) to compare microplastic contamination of a rural community and urban center. The findings from this study provide new insights about the occurrence of microplastics in freshwater systems in New Mexico containing elevated concentrations of heavy metals.

3.2 Experimental Methods

3.2.1 Procedures to avoid plastic contamination in field and laboratory experiments. To avoid plastic background contamination, the use of plastic materials was reduced as much as possible, all experimental apparatus and glassware was sonicated for 30 min in the same ultrasonic bath with ultra-pure water (18 MΩ) and covered with aluminum foil before use, all benchtops were carefully cleaned, and all laboratory procedures were conducted in a fume hood. Field controls

were included to monitor any airborne contamination. In laboratory procedures, a control containing only ultra-high purity water during filtering and digestion were included to account for any microplastic interference.

3.2.2 Sampling Methodology. Three one (1) L samples were collected from six locations along Paguate River and freshwater reservoirs near the Jackpile mine of Laguna Pueblo NM, and three locations on the Rio Grande, and Tingley Beach in Albuquerque, NM (Table A1). Samples were taken in freshwater bodies of Albuquerque, NM to compare microplastic contamination of a rural community and urban center.

3.2.3 Sampling Treatment for Detection of Microplastics and Heavy Metals. Samples were treated to extract microplastics. To extract microplastics and assure the quality of visual assessment and polymer identification, we followed Koelmans et. al (2019) recommendations. Water samples were vacuum filtered with a glass frit filter unit and 0.5 μm borosilicate glass microfiber filter. The filtrate was stored at 4°C for metal quantification. The original sample bottle was rinsed three times with ultra-pure water (18 MΩ) and vacuum filtered to maximize the microplastic extraction from the samples. Particles retained on the filter were washed with 100 mL of 30% (v/v) H_2O_2 into a serum bottle for digestion. Digestion was carried out in an oscillation incubator at 50°C and 80 rpm for 48 h. The initial filter before digestion was placed in a petri dish at 4°C. After digestion, the H_2O_2 solution was vacuum filtered through 25 mm 0.2 μm Al_2O_3 filter (Whatman Andodisc 25) and glass frit filter unit. Lastly, the filter with the possible microplastic particles was rinsed slowly with ultra-pure water (18 MΩ) to remove excess H_2O_2 solution and stored in a petri dish at 4°C for subsequent observation and identification of microplastics. The filtrate recovered from the microplastic extraction procedure was analyzed with Inductively Coupled Plasma-Mass Spectrometry (ICP-MS) to quantify the soluble U and As.

3.2.4 Characterization of Microplastics from Freshwater Systems.

The extracted particles were examined and imaged using a stereomicroscope (AmScope 7X-180X Trinocular Zoom Stereo Microscope) as initial visual identification**.** Then, two representative filters were selected from each sampling location and analyzed using a FTIR spectrometer (micro-FTIR, Thermo Nicolet iN10 MX). Particles were detected using OMNIC Picta® software, a full mosaic image was taken for each Al_2O_3 filter, and from that image suspected plastic particles were marked and counted. From these marked particles, 10% of the particles or at least five (which ever was greater) were randomly analyzed with ATR-FTIR. Each measurement was taken using a 51 sec detection time with 256 scans, a spectral range of 4000-675 cm^{-1} and a resolution of 8 cm^{-1}. Aperture size was adapted to fit each particle. The resulting spectra were searched against the HR Polymer Additives and Plasticizers, Hummel Polymer Sample Library, Polymer Laminate Films, and Synthetic Fibers by Microscope libraries.

3.3 Results and Discussion

Microplastics in Freshwater Systems Contaminated with U and As and in Albuquerque Metropolitan Area. A range from 4 to 18 pieces L^{-1} were detected in the samples taken from three different locations at Laguna Pueblo, New Mexico, US (Table A1). Particles randomly selected from those filters indicated composition matches of 29% to 72% (Table 3.1). The most common polymer found in these samples were cellophane (CP) with 33 - 44% matches followed by poly(styrene:vinylidene chloride) with 38 – 48% matches and rayon with 50 - 72% matches (Table 3.1). Representative images of the analyses are shown in Figure 3.1A. In these locations, the concentration of U ranged from ~ 30 to 37 $\mu g\ L^{-1}$ while the concentration of As ranged from ~ 0.5 to 1 $\mu g\ L^{-1}$ (Fig. 3.2A), indicating potential interaction between microplastics and these toxic metals. We must note that additional samples of those sites analyzed by our research group have

shown that the concentration of U ranged from ~ 1 to 333 μg L^{-1} and concentration of As ranged from ~ 1 to 6 μg L^{-1} (Table A2).

On the other hand, a range of 48 to 82 pieces L^{-1} were detected in the samples taken from two different locations at Tingley Beach, New Mexico, US (Table A1). Particles randomly selected from those filters indicated matches from 23% to 73% (Table A1). The most common polymers found in these samples were cellophane with 51- 64% matches followed by polyester (PES) with 73% match and rayon with 63 - 67% match (Table 3.1). Representative images of the analyses are shown in Figure 3.1B. In these locations, the concentration of U ranged from ~ 2.2 to 2.4 μg L^{-1} while the concentration of As ranged from ~ 10 to 11 μg L^{-1} (Fig. 3.2B). A range from 20 - 114 pieces L^{-1}were detected in samples taken from two different Rio Grande locations. Particles randomly selected from those filters indicated matches from 28% to 73% (Table 3.1). The most common polymer found in these samples were cellophane with 38 - 72% matches followed by poly(styrene:vinylidene chloride) with 37 - 41% matches and polyamide 6 + Polyamide 6,6 with 73% match (Table 3.1). Representative images of the analyses are shown in Figure 3.1C. In these locations, the concentration of U ranged from ~ 1 to 1.5 μg L^{-1} while the concentration of As ranged from ~ 2 to 3 μg L^{-1} (Fig. 3.2B). These findings indicate that urban center like Albuquerque freshwater systems have higher microplastic contamination compared to a rural community like Laguna Pueblo, New Mexico.

If we follow the procedure of Yang et al. (2015) in which a spectrum with a match greater than 70% was automatically identified as microplastics, our findings indicate that the polymers found were polyester (73%), polyamide 6 + polyamide 6,6 (73%), rayon (72%), and cellophane (72%) matches (Table 3.1). Other polymers detected with matches between 23-67% were rejected as microplastics (Table 3.1).

Studies about microplastic contamination of freshwater systems. Previous studies have identified microplastic contamination in freshwater systems. Su et. al (2016) found a range from 3.4 to 25.8 particles L^{-1} in Lake Taihu in China. The most common polymer type identified were CP, polyethylene terephthalate (PET), PES, polypropylene (PP), polyamide (PA). Fibrous and fragmented microplastics were found along the middle and lower reaches of the Yangtze River Basin with concentrations varying from 0.24 particles L^{-1} to 1.8 particles L^{-1} (L. Li et al., 2019) an 0.5 to 3.1 particles L^{-1} (Su et al., 2018). Li et. al (2019) identified mainly PP, polyethylene (PE), and polycarbonate (PC). Meanwhile, Su. et al (2018) found that the most dominant polymers were PES (33%), PP (19%), and PE (9%). Luo et. al (2019) found microplastics with a range from 0.9 to 2.4 particles L^{-1} in Suzhou River, Huangpu River, and the urban creeks of Shanghai. The dominant polymer was fibrous PES with 96% match, followed by rayon with 81% match (Luo et al., 2019). These previous findings coincide with our study as we found similar polymer type such as PES, PA, rayon, and CP in freshwater bodies in New Mexico (Table 3.1).

With the limited number of studies on the abundance of microplastics in heavy metal-contaminated freshwater systems, previous studies have shown the interaction of metals and microplastics in marine environments. The accumulation of metals such as aluminum (Al), manganese (Mn), iron (Fe), Cr, Co, Ni, Zn, Cd and Pb to PET, high-density polyethylene (HDPE), low-density polyethylene (LDPE), PVC, and PP were detected in San Diego Bay (Rochman et al., 2014). They also found that concentrations of all metals increased throughout the 12-month study period; suggesting that microplastics could accumulate greater metal concentrations the longer it remains at sea (Rochman et al., 2014). These findings were like Munier & Bendell et. al (2018) where they found PVC, HDPE, and LDPE adsorbing trace metals of Cu, Zn, Cd, and Pb in nine urban intertidal regions in Burrard Inlet, Vancouver, British Columbia, Canada. Holmes et. al

(2012) also found polyethylene pellets from beaches of southwest England containing variable concentrations of trace metals (Cr, Co, Ni, Cu, Zn, Cd and Pb). These previous findings are comparable to our results where we found microplastics such as PES, PA, rayon, and CP in metal-contaminated (i.e., U and As) freshwater systems in New Mexico. Therefore, it is important to observe the possibility of microplastic and metal interactions in freshwater systems.

Environmental Implications. Our findings indicate that heavy metal contaminated freshwater systems of isolated locations can be affected by microplastic pollution, which may increase the likelihood of the interaction between these contaminants. The prevalence of microplastics in freshwater systems potentially enables their interaction with several contaminants. Such interactions are of concern due to potential enhancement of toxic effects and transport of contaminants through the environment. These findings have implications for assessing potential interactions of toxic heavy metals and microplastics to understand compounding toxic effects and their reactivity, fate, and mobility through the environment. Future research should evaluate the interaction of microplastics and heavy metals in laboratory-controlled conditions.

3.5 Conclusions

The Rio Grande samples showed the highest concentration of microplastics (~ 20 – 114 pieces L^{-1}) in co-occurrence with U (~ 1 to 1.5 μg L^{-1}) and As (~ 2 to 3 μg L^{-1}), followed by samples taken from Tingley Beach (~ 48 – 82 pieces L^{-1}) in co-occurrence with U (~ 2.2 to 2.4 μg L^{-1}) and As (~ 10 to 11 μg L^{-1}), and samples taken from Laguna Pueblo freshwater (~ 4 – 18 pieces L^{-1}) in co-occurrence with U (~30 to 37 μg L^{-1}) and As (~ 0.5 to 1 μg L^{-1}). Our findings indicate that heavy metal contaminated freshwater systems of isolated locations can be also affected by microplastic pollution, which may increase the likelihood of the interaction between these contaminants. Further studies are needed to understand sorption of heavy metals onto

commonly occurring microplastics. Assessing potential interactions of toxic heavy metals and microplastics is crucial to understand compounding toxic effects and their reactivity, fate, and mobility through the environment.

3.6 Acknowledgments

Funding for this work has been provided by the Center for Water and the Environment, funded by the National Science Foundation (CREST Grant Number 1914490), NIEHS Superfund Research Program (Award 1 P42 ES025589), the National Institute on Minority Health and Health Disparities of the National Institutes of Health under Award Number P50MD015706, and the New Mexico Water Resources Research Institute, the NM State Legislature (NMWRRI-SG-2020). The content, opinions, findings, conclusions, and recommendations are those of the authors do not necessarily represent the official views of the New Mexico Water Resources Research Institute, NIEHS Superfund Research Program, NIMHD, National Science Foundation, or the National Institutes of Health.

Table 3.1. Number of particles detected and analyzed with micro-FT-IR including the polymer type and their percentage matches in Laguna Pueblo, Tingley Beach, and the Rio Grande, New Mexico.

Site	No. of Particles Detected	No. of Particles Analyzed	Name of Particle	Polymer Type	% Match
Site L3	5	5	L3-1	Poly(styrene:vinylidene Chloride)	44
			L3-2	Cellophane	44
			L3-3	Cellophane	43
			L3-4	Cellophane	40
			L3-5	Cellophane	34
Site L4	18	5	L4-1	Rayon	50
			L4-2	Styrene Derived Plasticizer	42
			L4-3	Poly(styrene:vinylidene Chloride)	42
			L4-4	Poly(styrene:vinylidene Chloride)	38
			L4-5	Propylene Glycol Dibenzonate #1	29
Site L5	18	5	L5-1	Rayon	72
			L5-2	Poly(styrene:vinylidene chloride)	48
			L5-3	Acrylonitrile Butadiene Styrene Terpolymer #6	46
			L5-4	Cellophane	33
			L5-5	Cellophane	33
Site T1	88	9	T1-1	Rayon	67
			T1-2	Cellophane	64
			T1-3	Cellophane	63
			T1-4	Cellophane	51
			T1-5	ABS/PVC Blend	40
			T1-6	Acrylonitrile Butadiene Styrene Terpolymer #6	39
			T1-7	ABS/PVC Blend	30
			T1-8	Benzyl Alcohol	29
			T1-9	Calcium Zinc Molybdate #1	23
Site T2	51	5	T2-1	Polyester	73
			T2-2	Polyester	73
			T2-3	Rayon	63
			T2-4	Cellophane	53
			T2-5	2-Amino-2-Methyl-1-Propanol #1	47
Site R1	18	5	R1-1	Poly(styrene:vinylidene Chloride)	41
			R1-2	Cellophane	38
			R1-3	Endothermic Foaming Agent #2	33
			R1-4	5-Phenyltetrazole, Calcium Salt	31
			R1-5	N,N-Diphenyl-P-Phenylenediamine	28
Site R3	112	11	R3-1	Polyamide 6 + Polyamide 6,6	73
			R3-2	Cellophane	72
			R3-3	Polytetrafluoroethylene #4	58
			R3-4	Cellophane	53
			R3-5	Zinc Molybdate on TALC	46
			R3-6	Basic Lead Carbonate	45
			R3-7	Rayon	41
			R3-8	Polystyrene #1	38
			R3-9	Poly(styrene:vinylidene Chloride)	37
			R3-10	Poly(styrene:4-vinylpyridine)	36
			R3-11	Benzyl Alcohol	32

*MicroFTIR analyses are available in supplmentary information

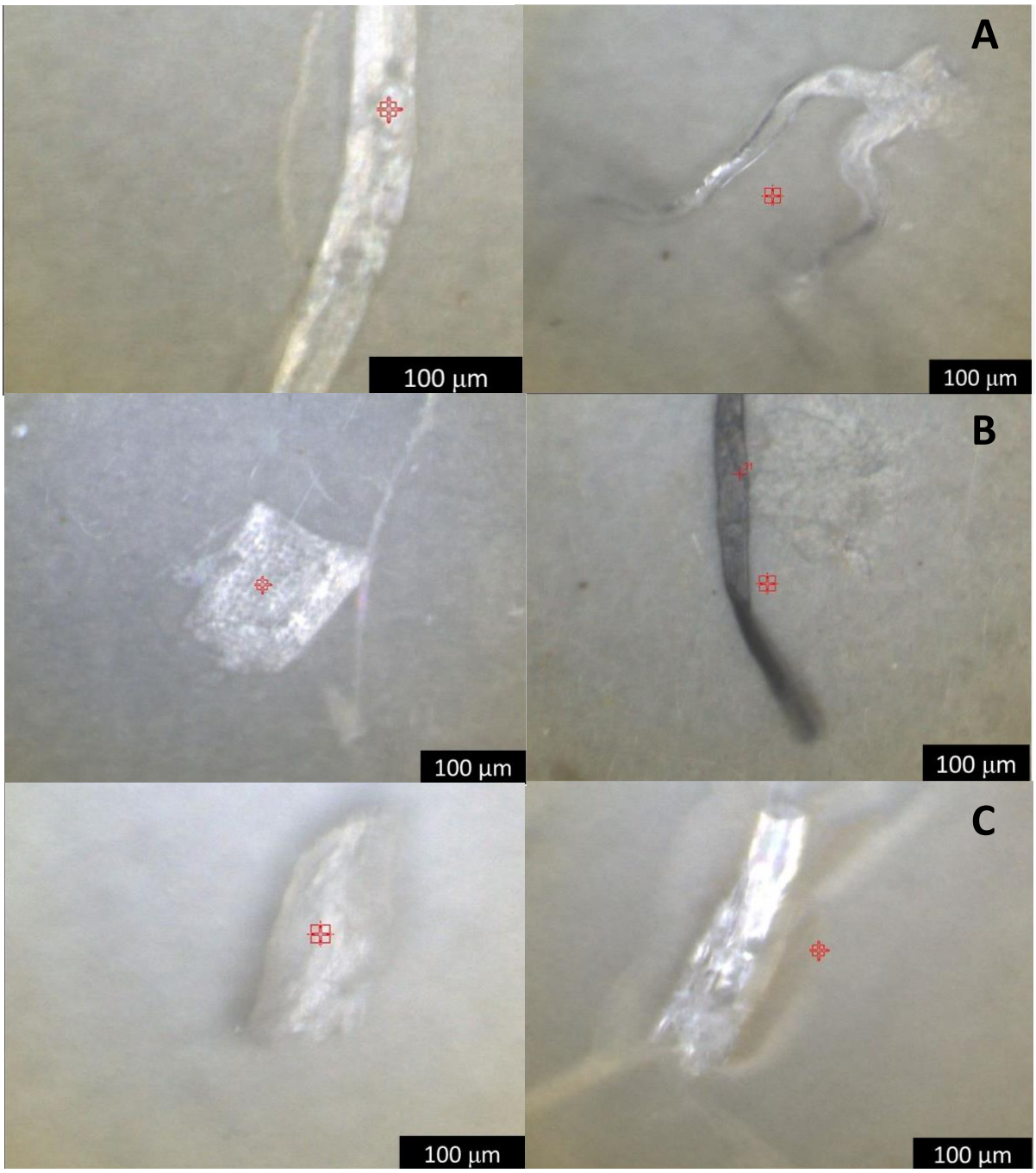

Figure 3.1. Representative images of plastic-like particles found in (A) Laguna Pueblo, New Mexico (Site L5), (B) Tingley Beach, Albuquerque, New Mexico (Site T1 & T2), and (C) the Rio Grande, Albuquerque, New Mexico (Site R1 & R3).

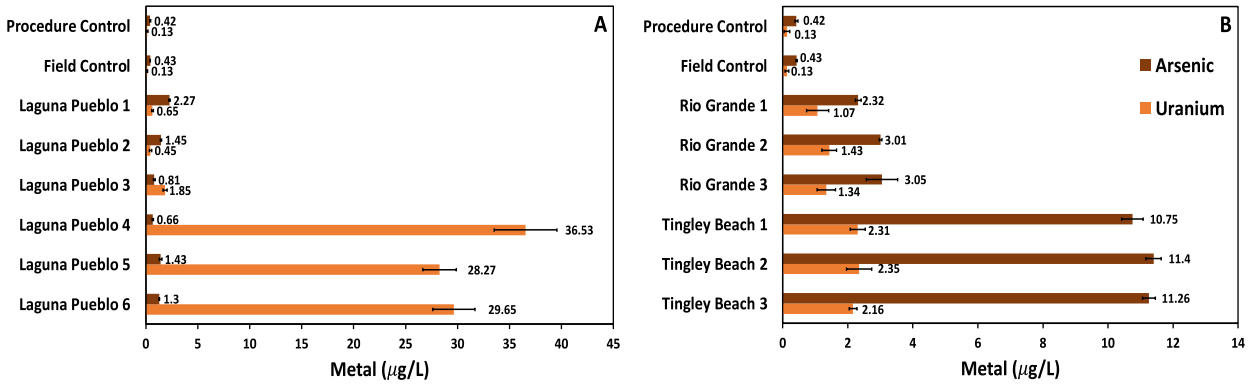

Figure 3.2. Elemental analysis for uranium (U) and arsenic (As) in (A) Laguna Pueblo, New Mexico and (B) the Rio Grande and Tingley Beach in Albuquerque, New Mexico.

Chapter 4

Interfacial Interactions of U, As, and Microplastics: Influence of Precipitation Reactions

*Jasmine Quiambao[*1], Kendra Hess[4], Sloane Johnston[4], Achraf Noureddine[2], Michael Spilde[3], Adrian Brearley[3], José M. Cerrato[1], Kerry J. Howe[1], and Jorge Gonzalez-Estrella[*4]*

*Corresponding email addresses: jorgego@okstate.edu; jannequiambao@unm.edu

[1] Department of Civil Engineering, MSC01 1070, University of New Mexico, Albuquerque, New Mexico 87131, USA

[2] Department of Chemical & Biological Engineering, MSC01 1120, 1 University of New Mexico Albuquerque, NM 87131, USA

[3] Department of Earth and Planetary Sciences, MSC03 2040, University of New Mexico, Albuquerque, New Mexico 87131, USA

[4] School of Civil & Environmental Engineering, 248 Engineering North, Oklahoma State University, Stillwater, Oklahoma 74078

ABSTRACT: This study evaluated the interfacial interactions of arsenic (As) and uranium (U) with commercial microplastics in acidic and neutral pH in laboratory-controlled conditions. Microplastics likely interact with heavy metals in aquatic ecosystems affected by anthropogenic activities or with naturally high metal concentrations. Such conditions likely enable accumulation of metals onto microplastics. Therefore, more documentation is needed to better understand the interfacial interactions of microplastic and heavy metals. We conducted experiments with pristine commercial poly(methyl-methacrylate, polyethylene, and polystyrene microplastics, and exposed to 0.02 – 0.2 mM of As or U solutions. Transmission Electron Microscopy, Scanning Electron

Microscopy, and Energy Dispersive X-Ray Spectroscopy were used to evaluate microplastic morphology and metal accumulation. Inductively Coupled Plasma-Optical Emission Spectrometry was used to quantify soluble metal concentrations. Our findings indicate that As does not interact with any of the microplastics tested at pH 3 and pH 7, neither U with any microplastics at pH 3. Control experiments conducted without microplastics at pH 7 indicate that U underwent homogenous precipitation. Experiments supplied with U and microplastics at pH 7 indicated that microplastics potentially serve as substrate surface for the adsorption and nucleation of U precipitates. Chemical speciation modeling and TEM analyses suggest the U precipitates resemble sodium-compreignacite and schoepite. Our results importantly implicate that microplastics may enable transport of metals through the environment in understudied pathways.

Keywords: adsorption, heavy metals, spectroscopy, microscopy, uranium, arsenic, homogenous, heterogenous, precipitates

Synopsis:

Uranium can precipitate and accumulate on the microplastic surface at circumneutral pH conditions applicable to natural and anthropogenic environments.

4.1 Introduction

Microplastics represent an environmental concern to aquatic environments (Eerkes-Medrano et al., 2015; W. Fu et al., 2020; Triebskorn et al., 2019; Wong et al., 2020). Microplastics (MPs) are defined as plastic materials with a diameter <5 mm (Carr et al., 2016; Jingyi Li et al., 2018; Zhao et al., 2014; Zou et al., 2020), while nanoplastics (NPs) are defined as plastic materials with <0.1 μm in size (Ateia et al., 2022). The word microplastics used in the whole document represent MPs with <5 mm and NPs with <0.1 μm unless specified for methodology uses. Aquatic environments can contain U and As due to natural or anthropogenic processes (Dong et al., 2019,

2020; Godoy et al., 2019). Accumulation of heavy metals onto microplastics could increase toxicity effects and affect their fate and mobility through the environment. However, we have limited knowledge about chemical interactions (e.g., surface or interfacial interactions, sorption/desorption, or precipitation reactions) between microplastics and metals in environmentally relevant conditions (Ateia et al., 2022).

The adsorption of organic and inorganic contaminants on microplastics depends on the physicochemical properties of microplastics such as polymer chemistry, specific surface area, polarity, particle size, morphology, surface charge, degree of crystallinity, and pore size distribution (Ateia et al., 2022; Naqash et al., 2020; Tourinho et al., 2019). For example, microplastics with high surface area would likely have high adsorption capacity to chemicals (Tourinho et al., 2019); or the abundance of crystalline domains, molecular chain arrays, and rubbery-based microplastics influence the adsorption of contaminants as well (Ateia et al., 2022).

Crystalline polymers require higher energy for destabilizing ordered polymer chains, while amorphous polymers have greater sorption capacity due to the presence of randomly oriented polymer chains (Naqash et al., 2020). The carbon chain in rubbery polymers may move more freely compared to glassy polymers; therefore, rubbery polymers show higher sorption capacity (Tourinho et al., 2019). Additionally, the molecular structures and various monomeric compositions of microplastics could influence different molecular interactions with contaminants (Ateia et al., 2022). Most microplastics have hydrophobic surfaces and abundant functional groups (T. Wang et al., 2020). Weathering could affect the adsorption of metals onto aged microplastics by increasing the surface area and creating additional oxygen functional groups on the microplastics (Brennecke et al., 2016). Among all commercial microplastics, PS, PE, and polyvinyl chloride (PVC) have been widely studied for the adsorption of organic and inorganic

contaminants due to their high prevalence in the environment (Ateia et al., 2022). Meanwhile, PMMA has been widely used as a substitute for glass products like aircraft canopies, windows, and aquariums (Ali et al., 2015).

Concentration, pH, and redox conditions can influence the chemical speciation of metals such as U and As in the environment. In oxidized source waters, U(VI) and As(V) are the predominant oxidation states. Pentavalent arsenate (H_3AsO_4) is a weak-acid oxyanion with pKa values of 2.24 ($H_2AsO_4^-$), 6.76 ($HAsO_4^{2-}$)and 11.60 (AsO_4^{3-}) and uranyl (UO_2^{2+}) ion is a weak-acid oxycation; both are common in oxidizing waters (Benjamin, 2015). Recent research has shown that U and As can complex and co-precipitate in acidic environments (Gonzalez-Estrella et al., 2020). Environmentally relevant constituents such as calcium (Ca^{2+}), iron (Fe^{2+} and Fe^{3+}), sodium (Na^+), and carbonate (CO_3^{2-}) or phosphate (PO_4^{3-}) can influence various complexation precipitation and dissolution reactions (Smedley & Kinniburgh, 2002). The concentrations of U in the solution can be influenced by the occurrence of solid uranyl phases such as compreignacite ($K_2(UO_2)_6O_4(OH)_6(H_2O)_8$), becquerelite ($Ca\text{-}(UO_2)_6O_4(OH)_6{\cdot}8(H_2O)$), schoepite $(UO_2)_8O_2(OH)_{12}{\cdot}12(H_2O)$, Na-compreignacite ($Na_2(UO_2)_6O_4(OH)_6(H_2O)_8$), and clarkeite ($Na(UO_2)O(OH)$); the environmental fate of U under oxidizing conditions is controlled by the formation of these minerals and their respective solubilities (Gorman-Lewis, Burns, et al., 2008; Gorman-Lewis, Fein, et al., 2008). Sorption and oxidative dissolution processes of these secondary minerals can release U and As into water (Gonzalez-Estrella et al., 2020).

The interaction between microplastics and heavy metals is driven by physicochemical properties of microplastics, chemical characteristics of toxic heavy metals, and environmental conditions (Ateia et al., 2022; Naqash et al., 2020; Tourinho et al., 2019). Properties of contaminants such as pKa, hydrophobicity, planarity, chain, ring structure, and functional groups

affect the adsorption of contaminants on microplastics. For instance, cationic metals (e.g., Cd^{2+}, Co^{2+}, Ni^{2+}, Pb^{2+}) show higher sorption capacities with increasing pH. Parameters of the aqueous media such as pH, organic matter composition, ionic strength, salinity, contact time, and temperature affect the adsorption behavior of different contaminants on microplastics as well (Naqash et al., 2020). For example, an increase in salinity decreases sorption due to competition between ions for sorption sites and electrostatic forces (Jia Li et al., 2018; Liu et al., 2018); however, salinity could increase sorption as well depending on the chemical contaminant and microplastic properties (Godoy et al., 2019). Abrasion, biofouling, degradation, and a complex aqueous environment may affect the physicochemical properties and chemical composition of microplastics and affect sorption mechanisms (Ateia et al., 2022).

Previous studies have stated that hydrophobic and electrostatic interactions are two predominant mechanisms for the sorption of contaminants on microplastics (Tourinho et al., 2019). Hydrophobic interactions involve the attraction of non-polar or slightly polar molecules to the non-polar microplastic surface. On the other hand, electrostatic interactions are driven by the attraction of oppositely charged molecules or repulsion of same-charged molecules. Microplastic surfaces are usually negatively charged because the pH of point of zero charge (pH_{pzc}) is lower than most environmental pH, and because of the deprotonation of carboxyl and hydroxyl groups (Ateia et al., 2022; Jia Li et al., 2018). Hence, the negative surface charges of microplastics are likely to attract positively charged species (Tourinho et al., 2019). For anionic species, repulsion by the microplastic surface reduce sorption (Naqash et al., 2020; Tourinho et al., 2019). Other mechanisms such as hydrogen bonding, van der Waals and pi-pi interactions could promote sorption of contaminants. Hydrogen bonds are weak electrostatic interactions, involving proton donors and proton acceptors. Van der Waals forces are also weak interactions between molecules

not involving covalent or ionic bonding, while pi-pi interactions are attraction forces between aromatic molecules. Therefore, aliphatic polymers like PE and PVC could undergo van der Waals interactions, while aromatic polymers like PS could undergo pi-pi interactions (Tourinho et al., 2019).

The association and interaction of microplastics with heavy metals needs to be further researched. For instance, the binding of anionic metals and metalloids like As, selenium, chromium, molybdenum, and boron onto the surface of plastics needs to be better understood (Verla et al., 2019). Additionally, the role of precipitation reactions affecting the interaction of metals and microplastics remains unknown. A better understanding of the relationship and behavior of metals and microplastics would provide valuable information about the transport of contaminants sorbed onto microplastics and potential toxicity synergies.

The objective of this study was to determine the interfacial interactions of As and U with polyethylene (PE), polystyrene (PS), and polymethyl(meta)acrylate (PMMA) commercial microplastics for acidic and neutral pH in laboratory-controlled conditions. The novelty of this study is the integration of controlled laboratory experiments with aqueous chemistry, microscopy, and spectroscopy techniques that enables the identification of precipitation reactions between metals and microplastics that have been overlooked in the literature.

4.2 Materials and Methods

4.2.1 Materials

Arsenic and U were used in these experiments because elevated concentrations have been detected in freshwater systems in New Mexico closed to abandoned mine sites (Blake et al., 2017). Sodium arsenate dibasic heptahydrate, $Na_2HAsO_47H_2O$ reagent (≥98%) was purchased from Sigma Aldrich. Uranyl nitrate hexahydrate reagent, $UO_2(NO_3)_26(H_2O)$ (98-102%) was purchased

from IBI Labs. Three types of common, high-production-volume microplastics were used in these experiments; PE, PS, and PMMA. Polyethylene is considered the "largest volume polymer produced globally" (Demirors, 2011) while PMMA has a wide range of applications where it is used as a substitute for glass products like aircraft canopies, windows, and aquariums (Ali et al., 2015). Polyethylene (0.96 g/cc, 10 – 63 μm) and PMMA microspheres (1.2 g/cc, 1-45 μm) were purchased from Cospheric (California, USA). Polystyrene is used for packaging, disposable cups, and many other uses (Veerappapillai & Muthukumar, 2015). Polystyrene beads (200-300μm) were purchased from Polysciences. Glass microfiber filters (Advantec GC-50 borosilicate diameter, 47mm; Pore Size: 0.5 μm) were purchased from Cole-Parmer.

4.2.2 Methods

4.2.2.1 Adsorption Kinetic Experiment. Kinetic experiments were carried out to determine the equilibrium time for adsorption of metals onto PMMA, PE, and PS commercial microplastics. Experimental units were run in triplicate and prepared by rinsing all the glassware with 10% (v/v) HNO_3 and DI water, then sonicating for 30 min in a Cole-Parmer CPXH Series sonicator with ultra-pure water (18 MΩ). A mass of 0.1 g of PMMA, PE, and PS pristine commercial microplastics were added into each 100 mL serum bottle with 0.05 mM As or U at pH 3 and pH 7 separately, resulting in a plastic-water ratio of 1:1000. pH adjustments were conducted with 0.1 M HNO_3 or NaOH. The bottles were placed in an orbital shaker (VWR Advanced Orbital Shaker Model 15000) to agitate the samples at 150 rpm for 7 d at room temperature. Samples of 1mL were taken at 0, 0.25, 0.5, 1, 2, 6, 24, 50, 120, and 168 h using a syringe tip. Samples were filtered using Pall Laboratory Acrodisc 0.45 μm syringe filter and then diluted 12x using 2% nitric acid, HNO_3 for metal analyses. After 7 d, the remaining solutions were filtered using 0.5 μm glass microfiber

filter and glass frit filter units. The collected samples were analyzed with Inductively Coupled Plasma-Optical Emission Spectrometry (ICP-OES) to quantify the soluble U and As.

4.2.2.2 Adsorption Isotherm of Heavy Metals onto Microplastics. These series of experiments were performed to assess the adsorption of different concentrations of As and U onto PE, PS, and PMMA commercial microplastics at pH 3 and pH 7. Glassware was cleaned by rinsing with 10% (v/v) HNO_3 and DI water, then sonicating for 30 min in a Cole-Parmer CPXH Series Sonicator with ultra-pure water (18 MΩ). pH adjustments were made with 0.1 M HNO_3 or NaOH. Polyethylene, PS, and PMMA commercial microplastics were weighed into borosilicate glass vials. Isotherms were carried out for 48 h by separately exposing the three commercial microplastics to 0.05, 0.1, and 0.2 mM of U or As, resulting in a plastic-water ratio of 1:1000. An additional set of experiments were conducted to isolate the interactions between soluble U and microplastics at pH 7. Lower U concentrations were used (0.02, 0.04, and 0.06 mM), the U solutions were filtered prior to exposure to the microplastics to ensure that precipitates were not present, polypropylene centrifuge tubes were used instead of glass to ensure that the glass was not providing a surface for heterogenous precipitation, and a control with no microplastics was also included. All experimental conditions were run in triplicates in a VWR Advanced Orbital Shaker Model 15000 at 150 rpm at room temperature (25°C) for 48 h. After the adsorption process, the sample solutions were vacuum filtered through a 0.5 μm glass microfiber filter and glass frit filter unit. Each filter paper was slowly rinsed with ultra-pure water (18 MΩ) to avoid additional compounds precipitating as the remaining water evaporated from the filter surface. The filtered water samples were transferred into centrifuge tubes and the filters were placed in a petri dish and stored at 4°C. Metal adsorption was determined by quantifying the soluble concentration of U and As with ICP-OES.

4.2.2.3 Characterization of Commercial Microplastics. Polyethylene, PMMA, and PS microplastics were exposed to U and As were analyzed with various spectroscopy techniques to identify any precipitation reaction on the surface. Transmission Electron Microscopy (TEM), Scanning Electron Microscopy (SEM), and Energy Dispersive Spectroscopy (EDS) were used to examine the microplastics morphology and quantify heavy metals binding onto the surface. Fourier Transform Infrared (FTIR) Attenuated Total Reflectance (ATR) was used to examine the surface chemistry composition and binding of microplastics to U and As. Zeta potential ζ was used to measure the surface charge of microplastics at pH 3 and pH 7. Surface area was also calculated using the measured particle size of each commercial microplastic through the SEM.

The scanning electron microscopy (SEM) was conducted on a Tescan Vega3 XMU variable pressure SEM (Tescan Orsay Holding a.s., Brno, Czech Republic). Samples were coated with silver at first. However, this created a spectral overlap with uranium M-alpha lines, thus gold coating was used on later samples. Accelerating voltage was 15 kV initially but that was reduced to 10 kV to reduce damage and potential charging on the polymer bead samples. Sample current used ranged from 10 to 30 pA with a spot size <100 nm.

Samples were prepared for TEM analyses by brushing holey carbon TEM films on Cu grids gently across the filter papers. The spheres attached to the holey carbon film by electrostatic attraction. TEM was performed using a JEOL NEOARM 200CF aberration-corrected scanning transmission electron microscope operating at 200 kV in the Nanomaterials Characterization Facility at the University of New Mexico. A variety of electron microscopy techniques were used, including bright-field TEM (BF-TEM), bright-field scanning TEM (STEM), high-angle annular dark-field (HAADF) (STEM), SEM, selected area electron diffraction (SAED) and X-ray analysis in both spot and STEM mode. Bright-field TEM images and electron diffraction patterns were

acquired using a GATAN OneView 4k x 4K digital camera and processed using GATAN Microscopy Suite® (GMS) imaging software. Background corrected full spectral X-ray maps and quantitative EDS data were obtained using twin JEOL 100mm2 SDD EDS detectors and processed using Oxford AZtec X-ray analysis software. Quantification of EDS spectra was carried out using the Cliff-Lorimer thin film approximation using theoretical k-factors.

4.3 Results and Discussion

4.3.1 Lack of Interfacial Interaction of As & U with Commercial Pristine Microplastics. All experiments supplied with As and PE, PS, and PMMA microplastics at pH 3 and pH 7 remained close to the initial concentration (0.05 mM) after the 48 h of exposure (Figure 4.1A-C). The control showed no change in the concentration as well. Similarly, the soluble U concentration exposed to the three types of microplastics at pH 3 and the control without microplastics remained close to the initial concentration (0.05 mM) after the 48 h exposure (Figure 4.1D-F). At pH 3 and 7, As(V) is predominantly in the anionic forms $H_2AsO_4^-$ and $HAsO_4^{2-}$, since the pKa values for the first two dissociations of H_3AsO_4 are 2.24 and 6.76. At pH 3, neither As nor U interacts with the microplastics because surface charge is unstable, resulting in a lack of electrostatic attraction (Figure 4.2). At pH 7, microplastics are negatively charged, causing a charge repulsion with As (anionic metalloids). A paired-samples t-test was performed to evaluate whether the concentration is significantly different at t = 0 and t = 48 h; no significant difference was found ($p > 0.05$).

Other studies have reported metal cations adsorbed onto the microplastic. For instance, the adsorption of divalent cations such as Cd^{2+}, Cu^{2+}, Pb^{2+}, Zn^{2+}, and Ni^{2+} has been reported onto microplastic materials such as high density PE, low density PE, PVC, PE, and PS at acidic and circumneutral pH (Ahechti et al., 2020; Brennecke et al., 2016; Godoy et al., 2019; Holmes et al., 2012, 2014; Mao et al., 2020; Turner & Holmes, 2015; Fayuan Wang et al., 2019; Zou et al., 2020).

Previous findings indicated the importance of electrostatic interactions in the adsorption of microplastics with bivalent cations at pH > 7 (Fayuan Wang et al., 2019; Zou et al., 2020). With pH < 7, adsorption can decrease due to the electrostatic repulsion between the positively charged surface and the cationic ions (Godoy et al., 2019). At pH 3, we noted minimal interaction of U with microplastics. Our findings indicate that the uranyl ion (UO_2^{2+}) did not adsorb to the slightly positive or slightly negative charge of the microplastics used in this study at pH 3. It is important to note that our study involves uranyl ion (UO_2^{2+}) which is an oxycation and can complex with other ligands like carbonate and phosphate; resulting to adsorption inhibition with microplastics, whereas previous studies involve divalent cations such as Cd^{2+}, Cu^{2+}, Pb^{2+}, Zn^{2+}, and Ni^{2+}.

Although the adsorption of arsenic (III) onto polytetrafluoroethylene (PTFE) and PS microplastics at pH ranging from 3 to 7 has been reported (Dong et al., 2019, 2020), our results indicate that there is limited adsorption of arsenic (V) onto microplastics at these pH ranges. A possible explanation based on chemical equilibrium analyses indicate that arsenic (V) is predominantly negatively charged at this pH range, occurring as $H_2AsO_4^-$ and $HAsO_4^{2-}$, whereas arsenic (III) species are uncharged in this range (Benjamin, 2015). Therefore, these oxyanions species would repel with negatively surface charges at pH 7 (Figure 4.2). At pH 3, the charge of the surface could be slightly positive or slightly negative, which could indicate an unstable charge of the surface where it would have minimal interactions with negatively charged $H_2AsO_4^-$.

4.3.2 U Precipitation onto Microplastic Surface at pH 7. The soluble U concentration in assays supplied with PMMA and PE at pH 7 decreased significantly ($p < 0.05$) (Figure 4.1D-F). The U concentration decreased from 0.05 mM to ~0.003 mM after 48 h (Figure 4.1D-F). The U concentration also decreased in the control without microplastics. SAED TEM analysis confirmed the solid phase Na-compreignacite on the surface of PMMA (Figure 4.3A). SEM EDS analysis

also confirmed uranium precipitates on the surface of PMMA (Figure 4.3B). Chemical equilibrium analyses were conducted and indicated that the solution was supersaturated with respect to schoepite and Na-compreignacite; both uranyl oxide hydrates. Na-bearing U solids were the primary phases in our study because NaOH was used to adjust the pH resulting in the presence of Na in the solution. Therefore, it is likely that homogenous precipitation affected the decrease of U on the control without microplastics at pH 7 as the solution is supersaturated, while heterogenous precipitation took place with the presence of microplastics because they provided surface sites for U solids to deposit and precipitate heterogeneously. These results suggest that U homogenous and heterogenous precipitation processes are relevant mechanisms that may be observed in aquatic environments supersaturated with U.

Past studies have confirmed Na-compreignacite and schoepite precipitates form at pH 7 when U is at concentration comparable to those used in our study (Gorman-Lewis, Burns, et al., 2008; Gorman-Lewis, Fein, et al., 2008; Kanematsu et al., 2014). No U solids formed at pH 3 where all U minerals were predicted to be undersaturated by thermodynamic calculations. Meanwhile, potassium (K)-compreignacite was the primary phase formed at pH 7. The K-bearing U solids were dominant in all conditions due to the high K concentrations in the synthetic wastewaters and the KOH used to adjust the pH; precipitates formed at higher pH also showed smaller particles sizes. A previous study concluded that a variety of more-soluble uranyl oxide hydrate phases may form depending on pH, concentrations of base cations, and dissolved uranyl concentrations, and temperature (Kanematsu et al., 2014).

Evaluation of U Precipitation onto the Surface of PMMA microplastics. To further investigate the surface interaction mechanism of U and microplastics, three different U concentrations (0.05, 0.1, and 0.2 mM) were exposed to PMMA microplastics at pH 7 for 48 h.

PMMA microplastics were selected for these experiments because they have the smallest particle size (1-45 μm), largest surface area (0.86 ± 0.87 m^2/g), most negatively charged surface (-42.83 ± 5.17 mV) compared to PE and PS at pH 7 (Table 4.1) and exhibited a higher decreased in the U concentration in the sorption isotherm experiments. The soluble U concentration in assays supplied with and without PMMA microplastics (control) still decreased (Figure 4.4). The data showed reproducibility where U could still precipitate homogenously without the presence of microplastics in the solution, and U could precipitate heterogeneously and accumulate on the microplastic surfaces. A paired-samples t-test was also demonstrated that the decrease of U concentration is significantly different ($p < 0.05$). The overall findings show that homogenous and heterogenous precipitation of U onto the surface of the microplastics are key mechanism for U reactivity in the system studied.

Filtered U Solution & Microplastics. The additional experiments were run with U concentrations of 0.02, 0.04, and 0.06 mM that were prefiltered to ensure that U precipitates were not present. The data collected merely coincide with the data shown in Figure 4.1D-F at pH 3; indicating that U does not interact with microplastics at pH 3 (Figure 4.5A-D). This finding is also explained by the unstable surface charge of the microplastics at pH 3 (Figure 4.1). The filtered U solution exposed to the three microplastics and the control at pH 7 slightly decreased (Figure 4.6). The use of glass vials was eliminated in this section as it can influence precipitation reactions; polypropylene tubes was used instead. These findings imply that homogenous and heterogenous precipitation are still occurring in the system even with the substitution from glass to plastic and with the extra filtration step to remove U precipitate before microplastic exposure. Although U precipitated homogenously in the control without microplastics, the SEM analyses confirmed U mineral precipitated heterogeneously on the microplastics surface. The EDS analyses also showed

U and Na compositions and did not show any silica (Si) (Figure 4.7). A paired-samples t-test showed the decrease of U concentration is significantly different, $t(2) = 64.27$, $p = 0.0002$, ($p < 0.05$). These results demonstrate that the precipitation process drives the interaction between the microplastics and uranium, and not the soluble ions in the system.

Previous study found that crystalline or amorphous uranyl oxide hydrates, either compreignacite or meta-schoepite precipitated at pH 7 in the absence of Si. Meanwhile, in the presence of dissolved Si, amorphous phases dominated by compreignacite precipitated rapidly at pH 7 and followed by the formation of poorly crystalline boltwoodite. The thermodynamically stable uranyl silicate phase was slow even in the presence of Si (Kanematsu et al., 2014). These findings coincide with our study as we found similar U mineral, compreignacite and schoepite at pH 7 for both approaches, glass vials and polypropylene tubes as the container indicating that the role of silicates in the precipitation of U was low in our study.

4.4 Environmental Implications

Our findings indicate that can precipitate and accumulate on the microplastic surface at pH 7. These findings have implications to aquatic ecosystems affected by anthropogenic activities or with naturally high metal concentrations. The interaction of microplastics and U occurs in the typical pH and representative range of U concentrations detected in freshwater systems. However, real environmental conditions (e.g., pH, organic matter composition, ionic strength, salinity, contact time, and temperature) may affect the interaction as this study was strictly controlled-batch experiments involving ultra-pure water and pristine microplastics. Future research should observe the behavior of microplastics and U in different pH ranges, temperature, contact time, pristine and weathered microplastics, and exposing to various aqueous media like samples collected from freshwater and seawater.

4.5 Conclusion

The main finding is the formation of U precipitates on the surface of the microplastics at pH 7; indicating that microplastics can serve as a surface for U adsorption and nucleation. Chemical speciation modeling and TEM analyses also suggest that the U solids formed are sodium-compreignacite and schoepite. The lack of interfacial interaction of As and U with commercial microplastics (i.e., PMMA, PE, and PS) at pH 3 is explained by unstable surface charge of the microplastics. Also, no interaction of As was identified at pH 7 which could be due to the charge repulsion of As (anionic metalloids) and the negative surface of microplastics. Our study provides insights about the interfacial interaction of U and As with microplastics in laboratory-controlled condition and information about their fate, mobility, and potential synergies in the environment.

4.6 Acknowledgments

Funding for this work has been provided by the Center for Water and the Environment, funded by the National Science Foundation (CREST Grant Number 1914490), NIEHS Superfund Research Program (Award 1 P42 ES025589), the National Institute on Minority Health and Health Disparities (NIMHD) of the National Institutes of Health under Award Number P50MD015706, and the New Mexico Water Resources Research Institute, the NM State Legislature (NMWRRI-SG-2020). The content, opinions, findings, conclusions, and recommendations are those of the authors and do not necessarily represent the official views of the New Mexico Water Resources Research Institute, NIEHS Superfund Research Program, National Science Foundation, NIMHD, or the National Institutes of Health.

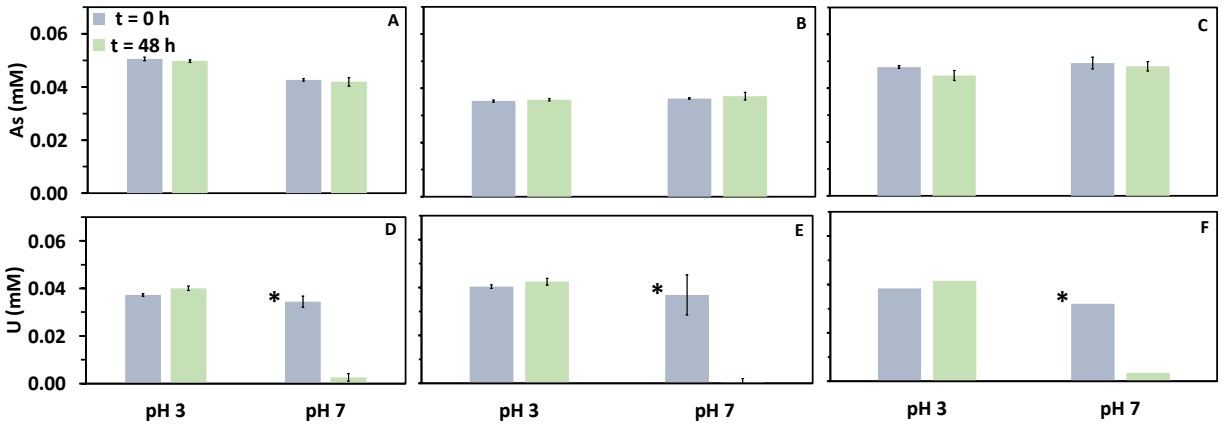

Figure 4.1. Soluble As concentration in batch experiments containing (A) PMMA, (B) PE, and (C) PS and soluble U concentration in batch experiments containing (D) PMMA, (E) PE, and (F) control without microplastics at pH 3 and pH 7 at 0 and 48 h exposure. Error bars indicate standard deviation obtained from duplicates. Asterisks represent the significant difference of soluble U concentration.

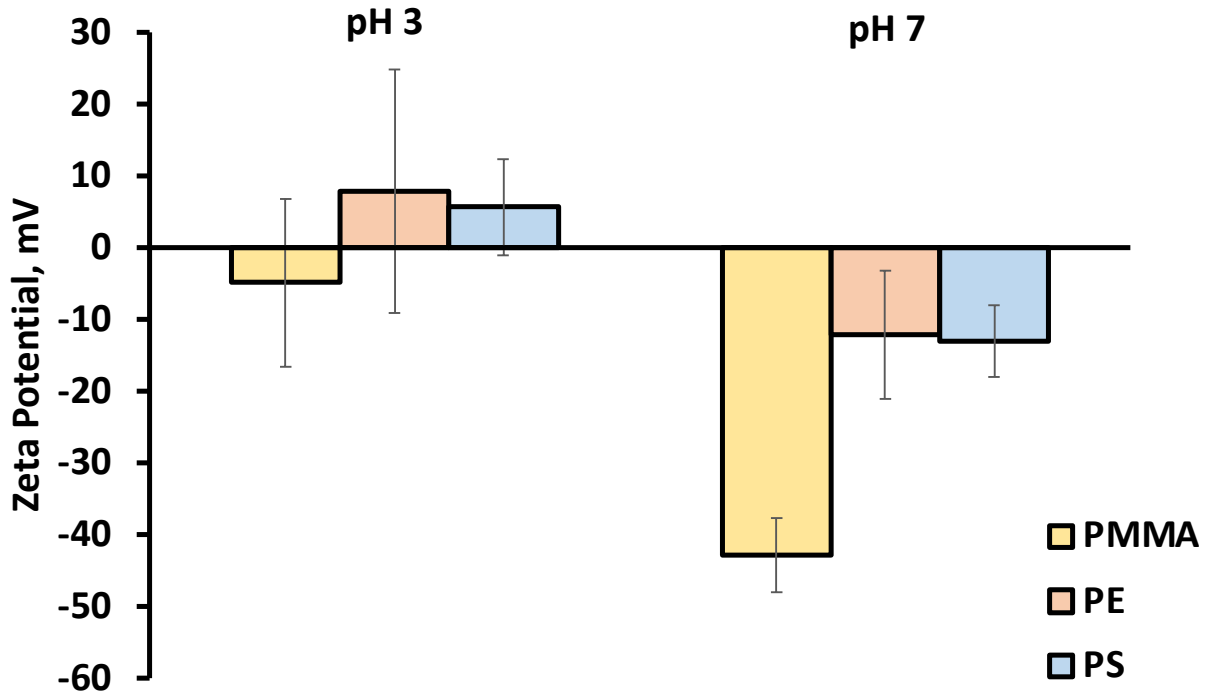

Figure 4.2. Zeta potential (mV) of the three commercial microplastics (PMMA, PE, and PS) at pH 3 and pH 7.

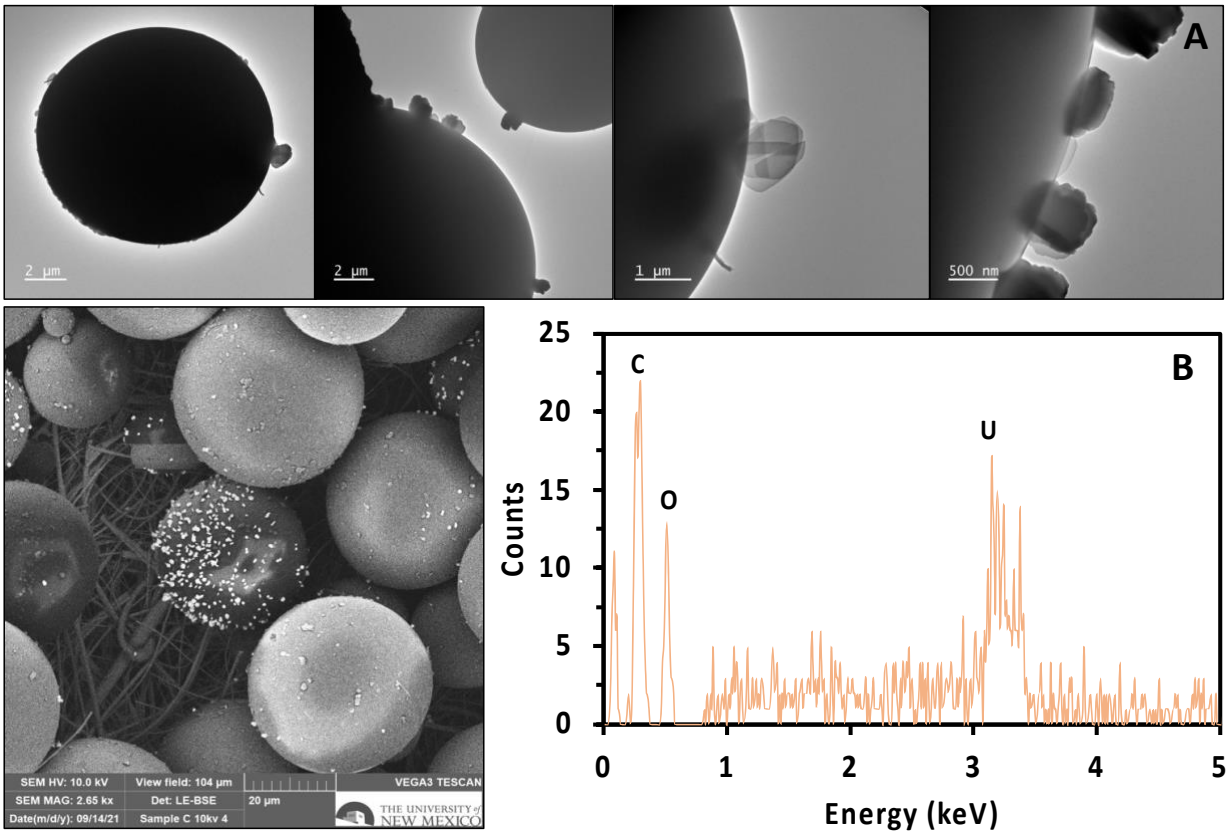

Figure 4.3. 0.06 mM of U exposed to PMMA at pH 7 for 48 h. (A) TEM images of precipitates onto the commercial PMMA microplastic surface (B) SEM/EDS analyses showing the presence of U on the microplastic surface.

Table 4.1. Microplastic properties of commercial poly (methyl methacrylate) (PMMA), clear polyethylene (PE), and polystyrene (PS) including density, particle size, surface area, and ZETA potential at pH 3 and pH 7.

Commercial Microplastics	**Density (g/c^3)**	**Particle Size (µm)**	**Surface Area (m^2/g)**	**Zeta Potential at pH 3 (mV)**	**Zeta Potential at pH 7 (mV)**
Poly (Methyl Methacrylate)	1.2	1-45	0.86 ± 0.87	-4.88 ± 11.74	-42.83 ± 5.17
Clear Polyethylene	0.96	10-63	0.21 ± 0.14	7.83 ± 16.95	-12.10 ± 8.92
Polystyrene	1.05	200-300	0.020 ± 0.0050	5.65 ± 6.64	-13.06 ± 4.94

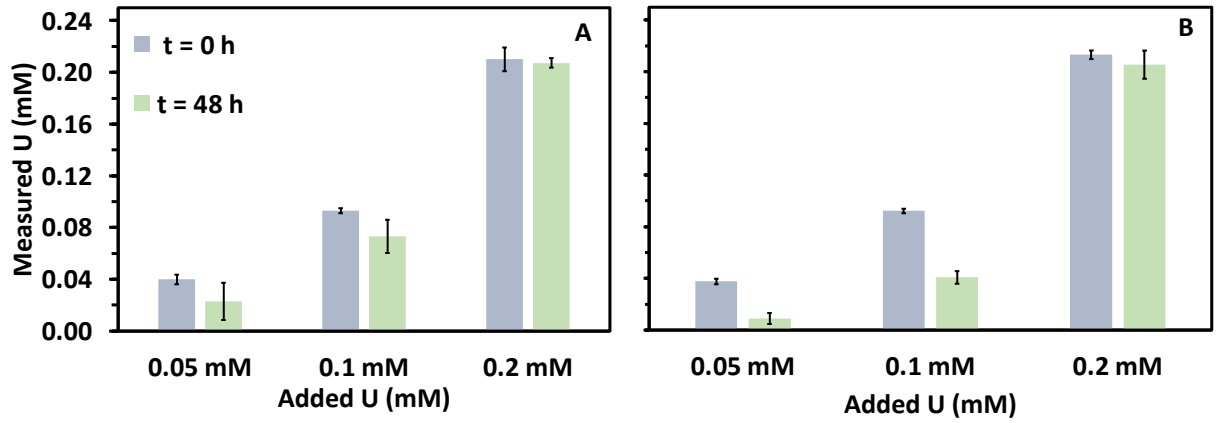

Figure 4.4. Soluble U concentration in batch experiments containing (A) PMMA and (B) control (no microplastics) at pH 7 at 0 and 48 h exposure. Error bars indicate standard deviation obtained from triplicates.

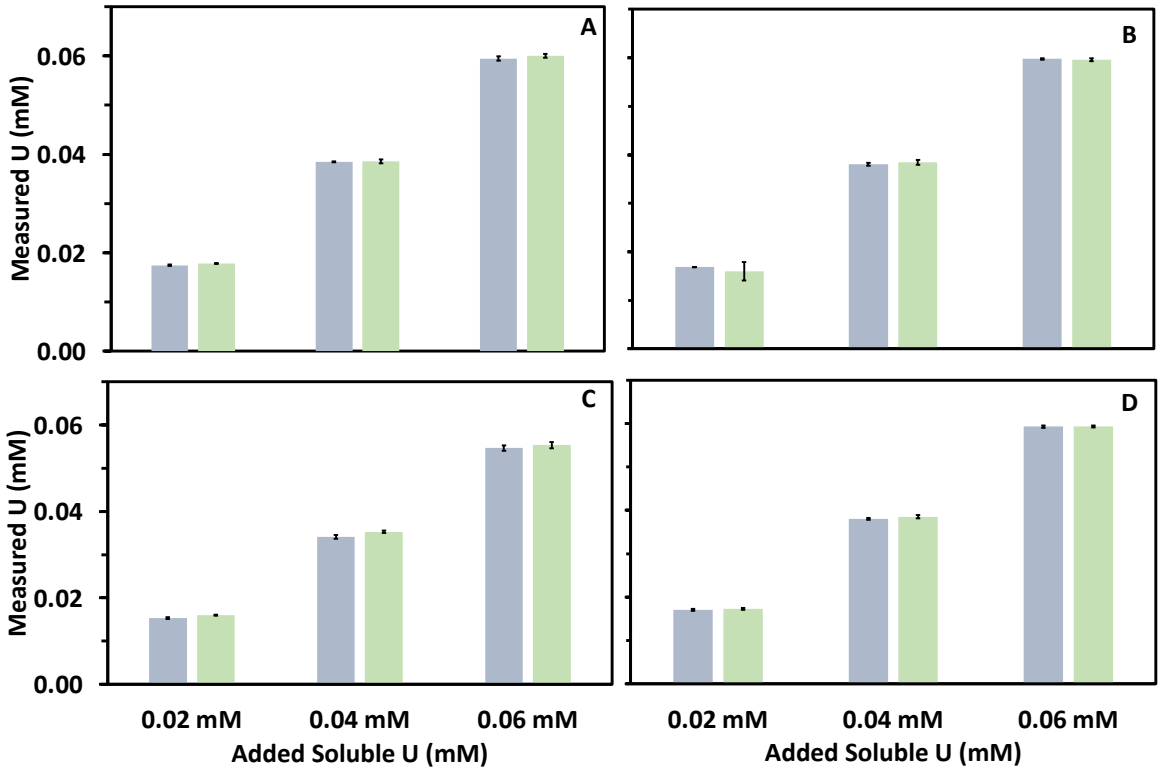

Figure 4.5. Soluble U concentration of filtered solution in batch experiments containing (A) PMMA, (B) PE, (C) PS, and (D) control (no microplastics) at pH 3 at 0 and 48 h. Error bars indicate standard deviation obtained from triplicates.

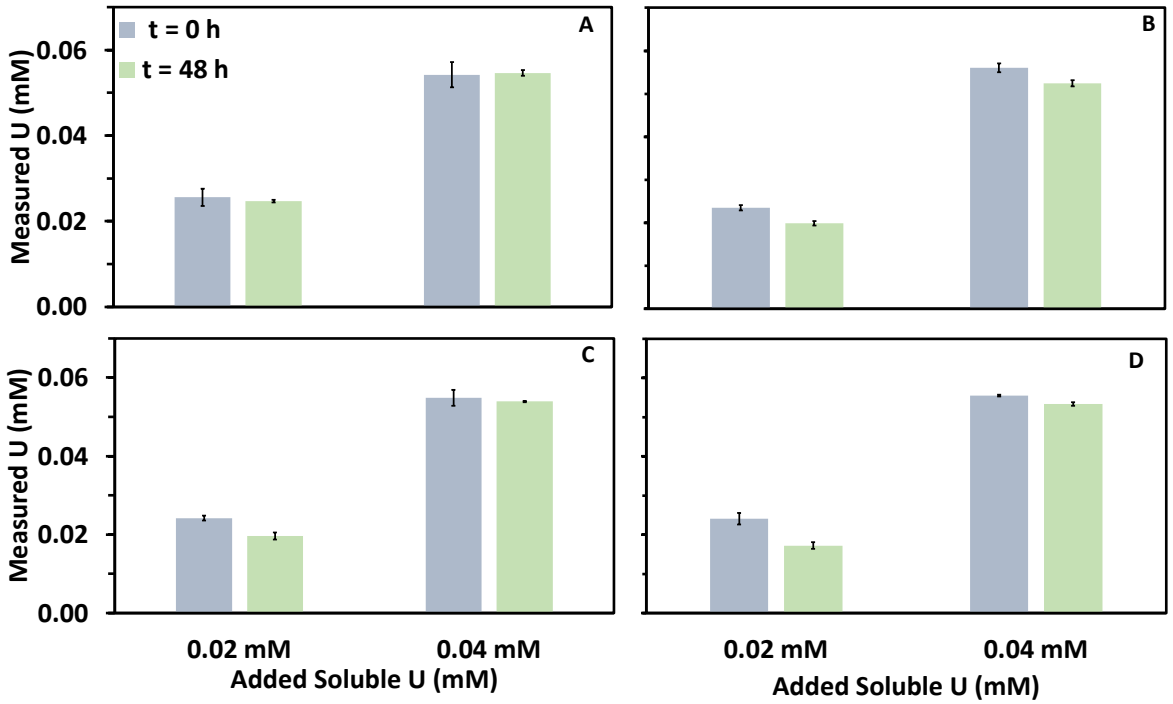

Figure 4.6. Soluble U concentration of filtered solutions in batch experiments containing (A) PMMA, (B) PE, (C) PS, and (D) control (no microplastics) at pH 7 at 0 and 48 h. Error bars indicate standard deviation obtained from triplicates.

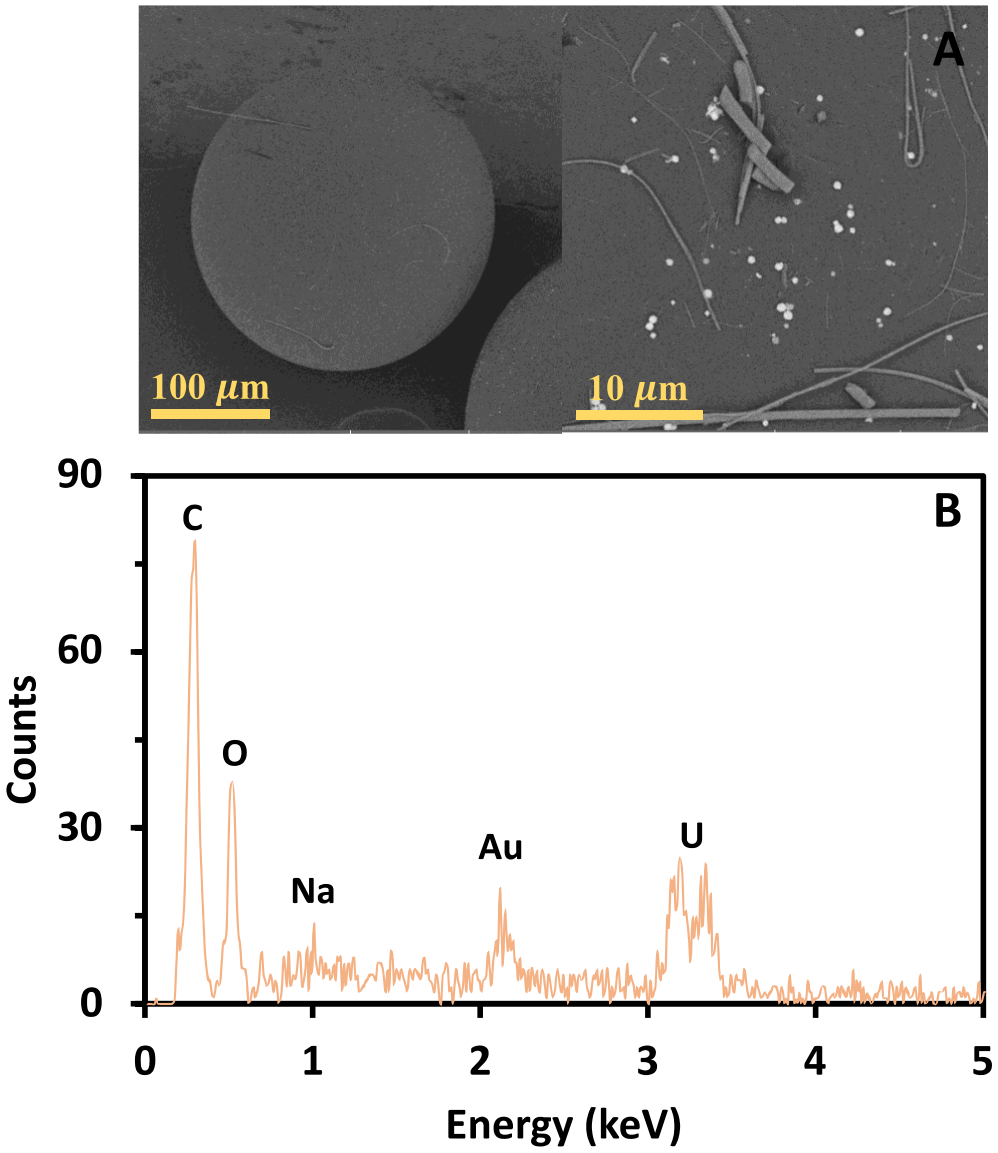

Figure 4.7. (A) SEM images and (B) EDS analyses of precipitates onto the commercial PS microplastic surface recovered from experiments initiated with 0.06 mM of U exposed to PS at pH 7; the one with additional filtration step before 48 h exposure.

Appendix A

Potential interactions of microplastics with uranium and arsenic in heavy metal-contaminated freshwater systems

*Jasmine Quiambao[1], Kendra Hess[2], Sloane Johnston[2], Kerry J. Howe[1], José M. Cerrato[1], and Jorge Gonzalez-Estrella[*2]*

*Corresponding email address: jorgego@okstate.edu;

[1]Department of Civil Engineering, MSC01 1070, University of New Mexico, Albuquerque, New Mexico 87131, USA

[2]School of Civil & Environmental Engineering, 248 Engineering North, Oklahoma State University, Stillwater, Oklahoma 74078

Summary of Supporting Information

Short Communication: Environmental Engineering Science

Table A1. Sampling name, date, site #, coordinates, and description of six freshwater bodies located nearby Jackpile Mine, Laguna Pueblo, NM and freshwater bodies of Albuquerque, NM (Rio Grande and Tingley Beach).

Sample Name	Sample Date	Site #	Coordinates	Description
Laguna Pueblo, New Mexico	2/23/20	Site L1	35°09'01.0"N 107°23'56.8"W	Fishing Pond, Laguna, NM
Laguna Pueblo, New Mexico	2/23/20	Site L2	35°09'14.9"N 107°24'18.6"W	Rio Paguate, Laguna, NM
Laguna Pueblo, New Mexico	2/23/20	Site L3	35°04'00.2"N 107°19'34.7"W	Wetland, Laguna, NM
Laguna Pueblo, New Mexico	2/23/20	Site L4	35°03'56.1"N 107°19'36.8"W	Wetland Creek, Laguna, NM
Laguna Pueblo, New Mexico	2/23/20	Site L5	35°07'24.0"N 107°20'10.3"W	Laguna, NM - Close to Jackpile Mine
Laguna Pueblo, New Mexico	2/23/20	Site L6	35°07'22.1"N 107°20'10.4"W	Laguna, NM - Close to Jackpile Mine
Tingley Beach, Albuquerque, New Mexico	7/9/20	Site T1	35°05'08.7"N 106°40'25.2"W	Tingley Beach, Albuquerque NM
Tingley Beach, Albuquerque, New Mexico	7/9/20	Site T2	35.084307, -106.671966	Tingley Beach, Albuquerque NM
Tingley Beach, Albuquerque, New Mexico	7/9/20	Site T3	35.083300, -106.671543	Tingley Beach, Albuquerque NM
Rio Grande, Albuquerque, New Mexico	7/9/20	Site R1	35°05'16.5"N 106°40'41.7"W	Rio Grande, Albuquerque NM
Rio Grande, Albuquerque, New Mexico	7/9/20	Site R2	35°05'26.3"N 106°41'04.2"W	Rio Grande, Albuquerque NM
Rio Grande, Albuquerque, New Mexico	7/9/20	Site R3	35.089566, -106.680866	Rio Grande, Albuquerque NM

Table A2. Elemental analysis for uranium (U) and arsenic (As) in Laguna Pueblo, New Mexico from August to September 2020.

Sampling Locations	As (μg/L)	U (μg/L)
Rio Paguate 1st Diversion	2.31	0.83
Rio Paguate 2nd Diversion	2.19	2.34
Rio Paguate Bridge in Jackpile Mine ("ford")	2.23	233.56
Rio Paguate Bridge in Jackpile Mine ("ford")	2.89	329.56
Rio Paguate Bridge in Jackpile Mine ("ford")	3.33	332.80
Rio San Jose Acequia Site 16	4.15	3.34
Rio San Jose Diversion to Field Site 17	4.52	3.66
Paguate Lake Outfall Site 9	0.00	0.00
Rio Paguate Bridge in Jackpile Mine (Stop 1) ("ford")	1.40	274.06
Rio Paguate Bridge in Jackpile Mine (Stop 1) ("ford")	1.75	296.56
Rio Paguate Bridge in Jackpile Mine (Stop 1) ("ford")	1.75	280.10
Rio Moquino in Jackpile Mine	5.54	40.38
Rio Moquino in Jackpile Mine	1.46	31.41
Rio Moquino in Jackpile Mine	1.92	28.78

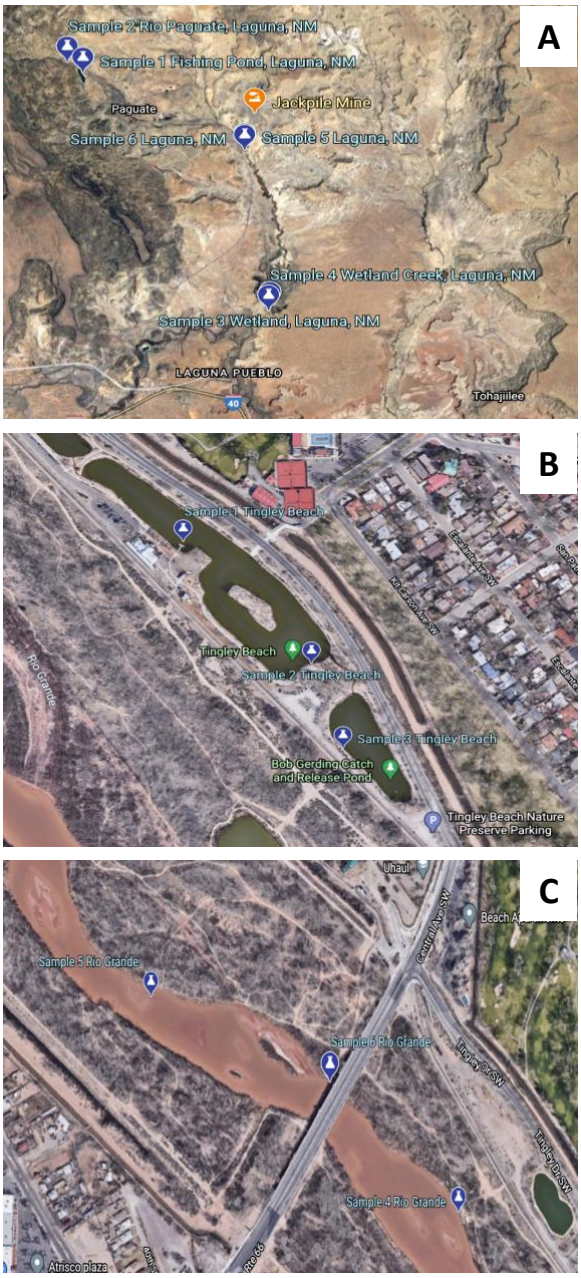

Figure A1. Sampling locations of freshwater systems at (A) Laguna Pueblo, New Mexico near the Jackpile Mine, (B) Tingley Beach, and (C) the Rio Grande in Albuquerque, New Mexico.

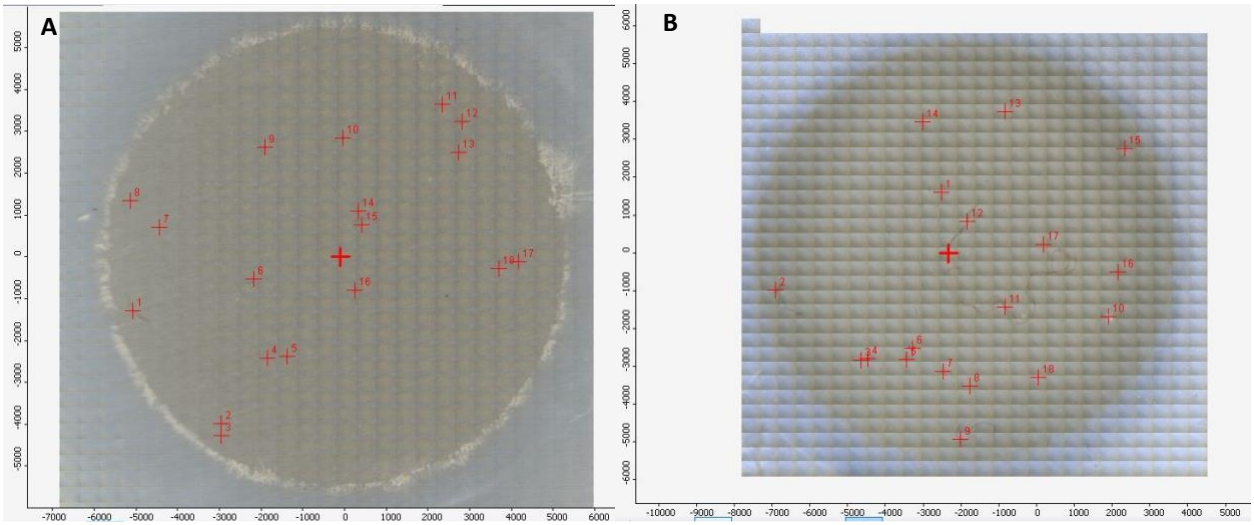

Figure A.2. A full mosaic image of the Al2O3 filter with particle count of (A) ~ 18 for Laguna Sample 4 (L4) and (B) ~ 18 for Laguna Sample 5 (L5).

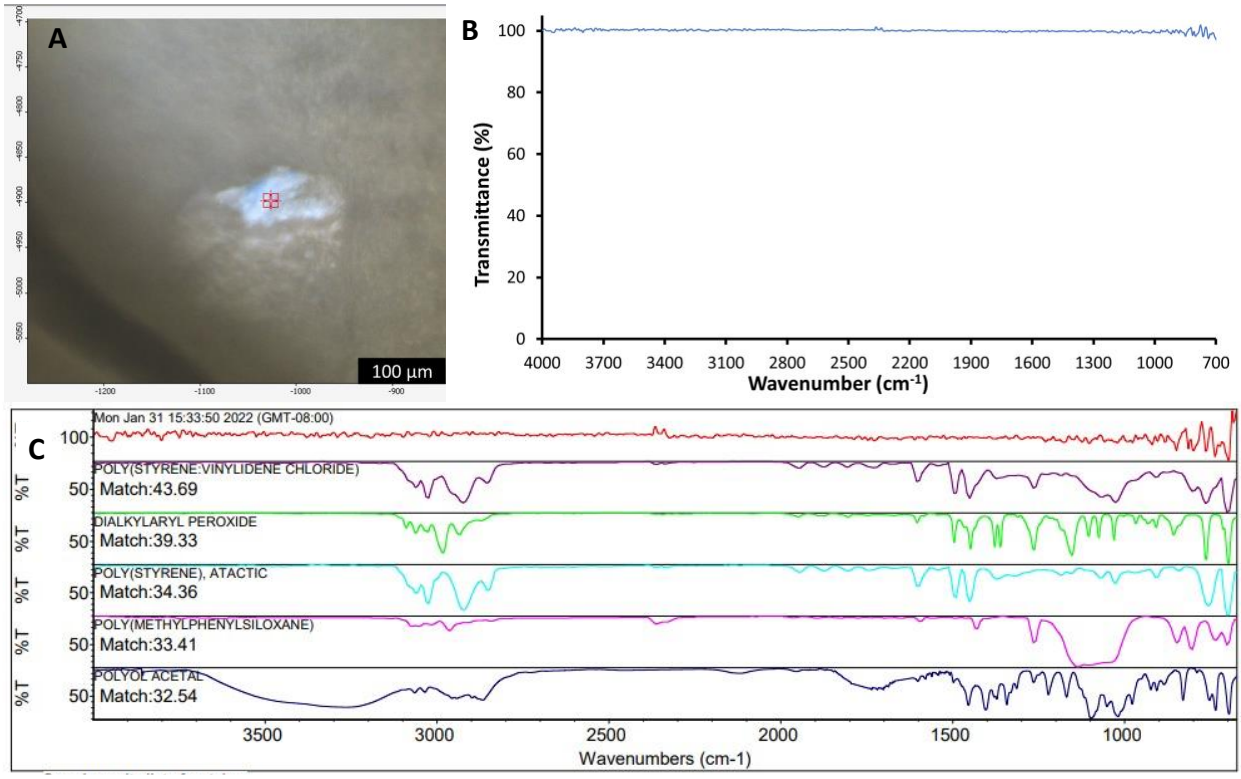

Figure A3. (A) An image of L3-1 particle found from Laguna Sample 3, (B) ATR-FTIR spectra of L3-1 particle, and (C) ATR-FTIR spectra of L3-1 particle with ~ 44% matched with poly(styrene:vinylidene Chloride).

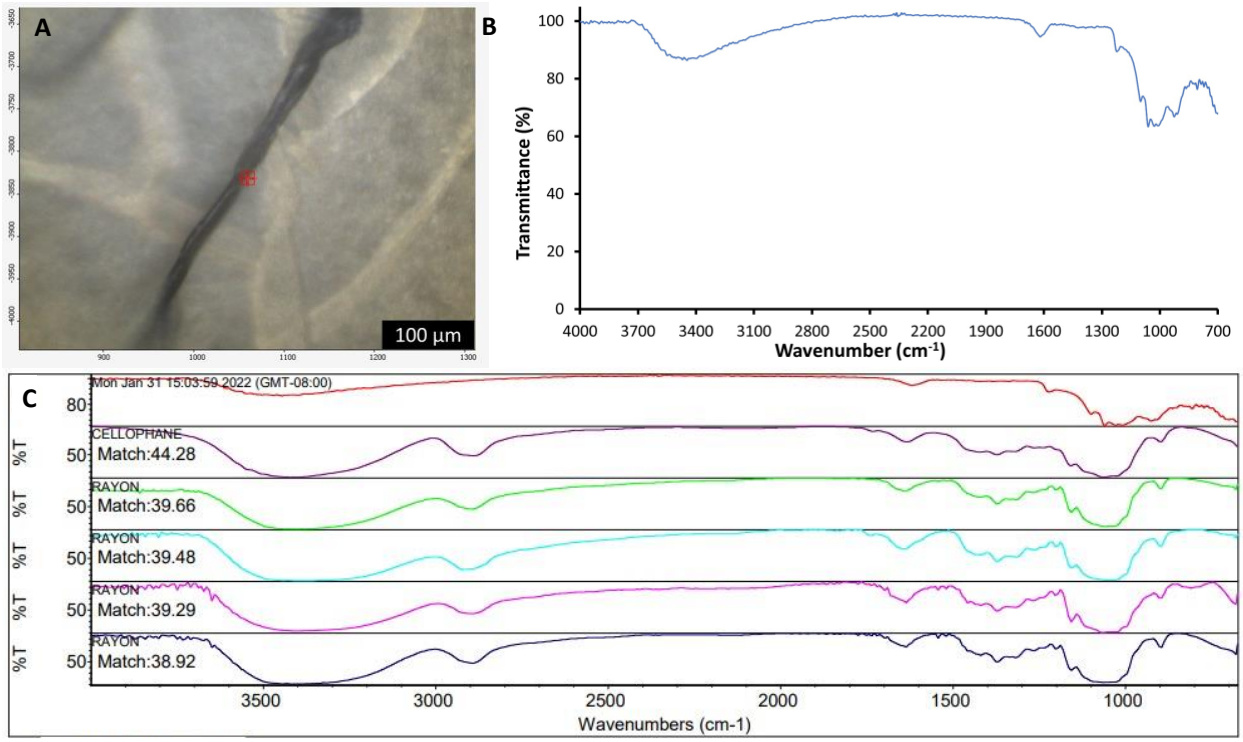

Figure A4. (A) An image of L3-2 particle found from Laguna Sample 3, (B) ATR-FTIR spectra of L3-2 particle, and (C) ATR-FTIR spectra of L3-2 particle with ~ 44% matched with cellophane.

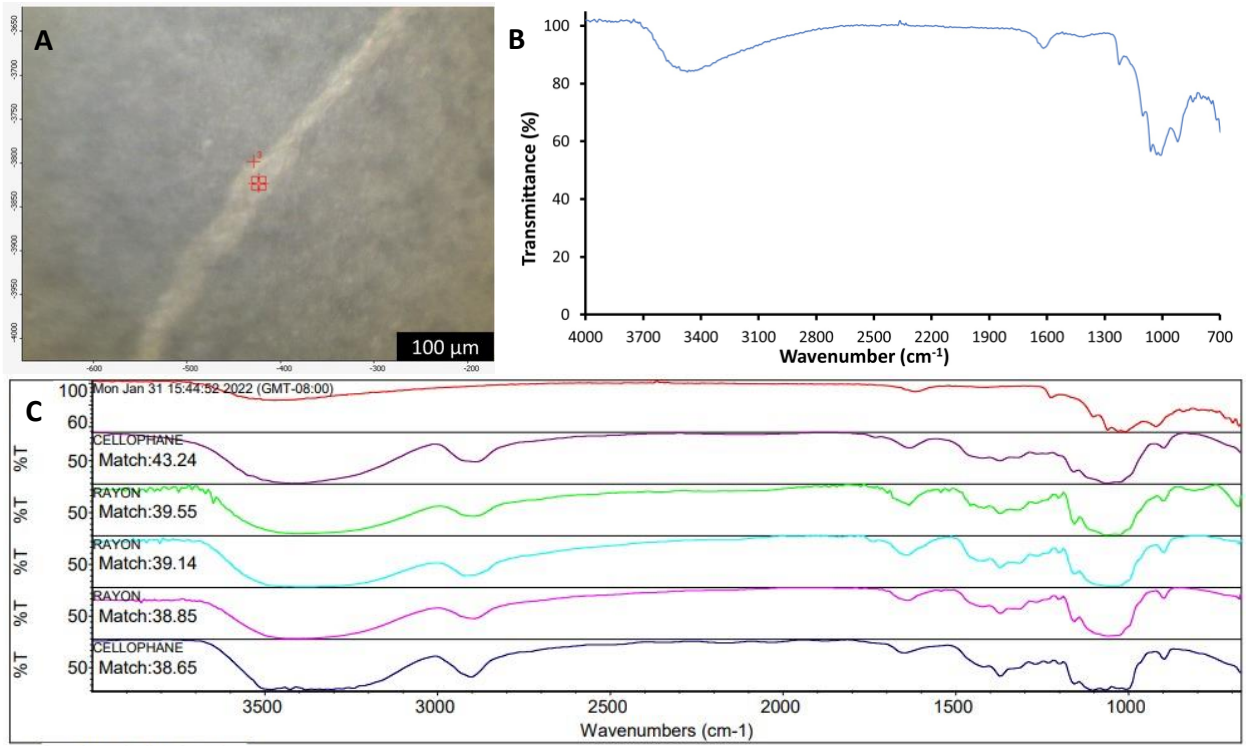

Figure A5. Figure A5. (A) An image of L3-3 particle found from Laguna Sample 3, (B) ATR-FTIR spectra of L3-3 particle, and (C) ATR-FTIR spectra of L3-3 particle with ~ 43% matched with cellophane.

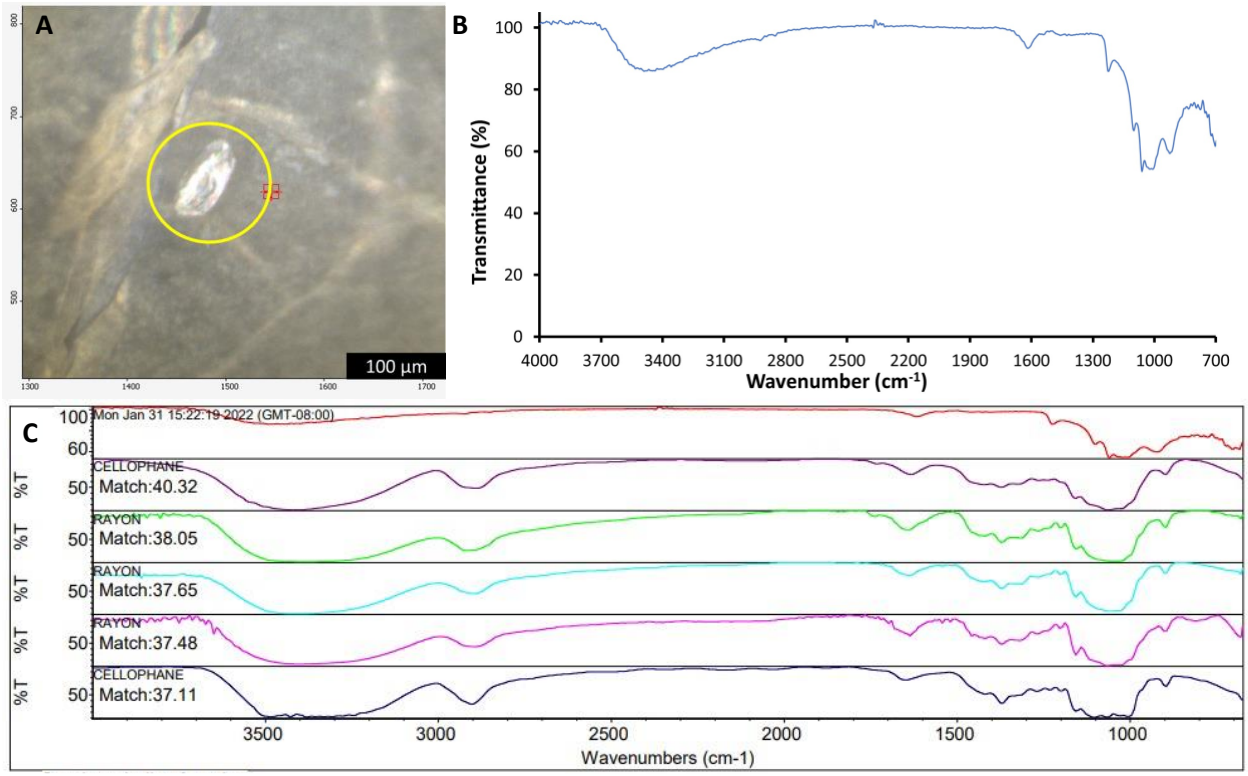

Figure A6. (A) An image of L3-4 particle found from Laguna Sample 3, (B) ATR-FTIR spectra of L3-4 particle, and (C) ATR-FTIR spectra of L3-4 particle with ~ 40% matched with cellophane.

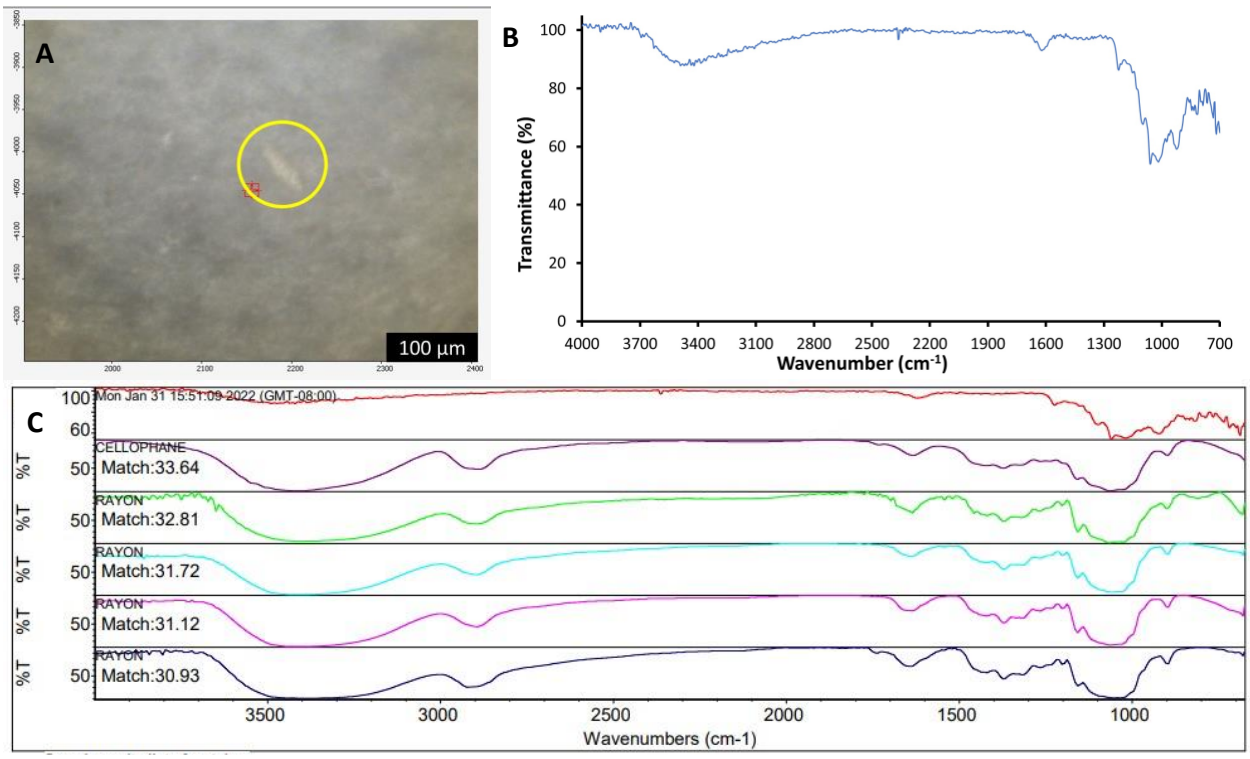

Figure A7. (A) An image of L3-5 particle found from Laguna Sample 3, (B) ATR-FTIR spectra of L3-5 particle, and (C) ATR-FTIR spectra of L3-5 particle with ~ 34% matched with cellophane.

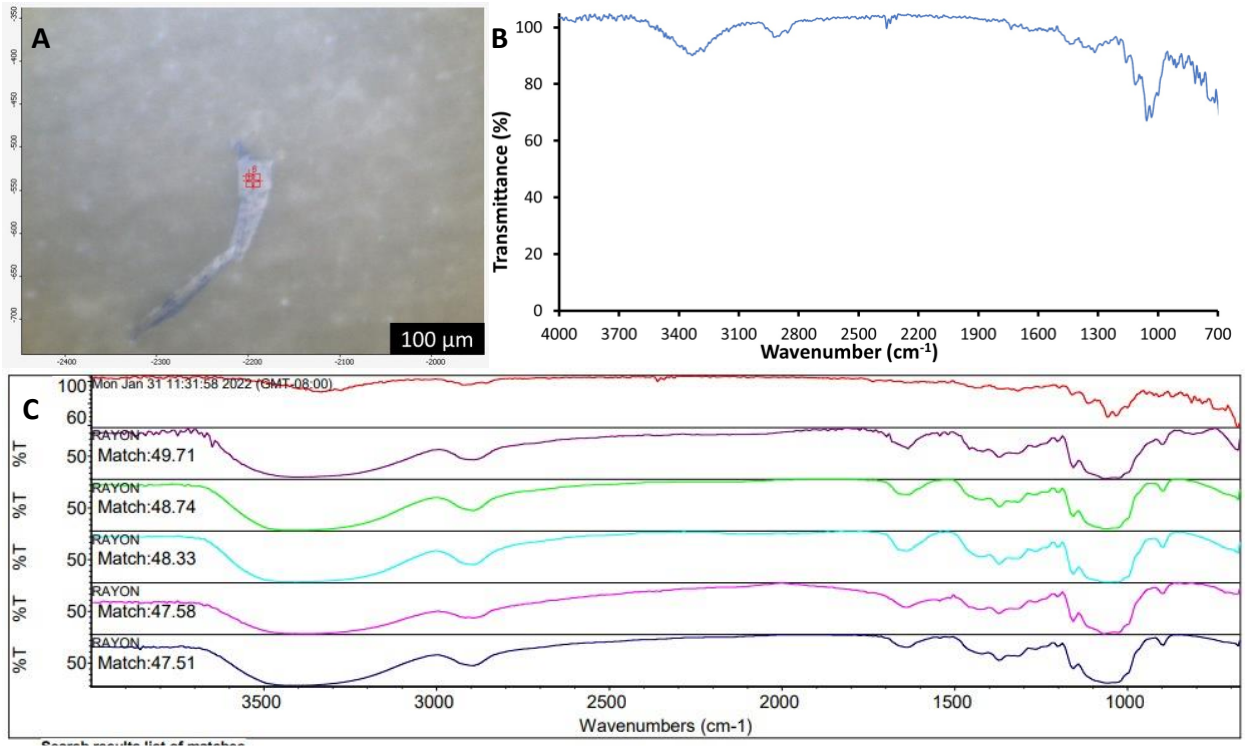

Figure A8. (A) An image of L4-1 particle found from Laguna Sample 4, (B) ATR-FTIR spectra of L4-1 particle, and (C) ATR-FTIR spectra of L4-1 particle with ~ 50% matched with rayon.

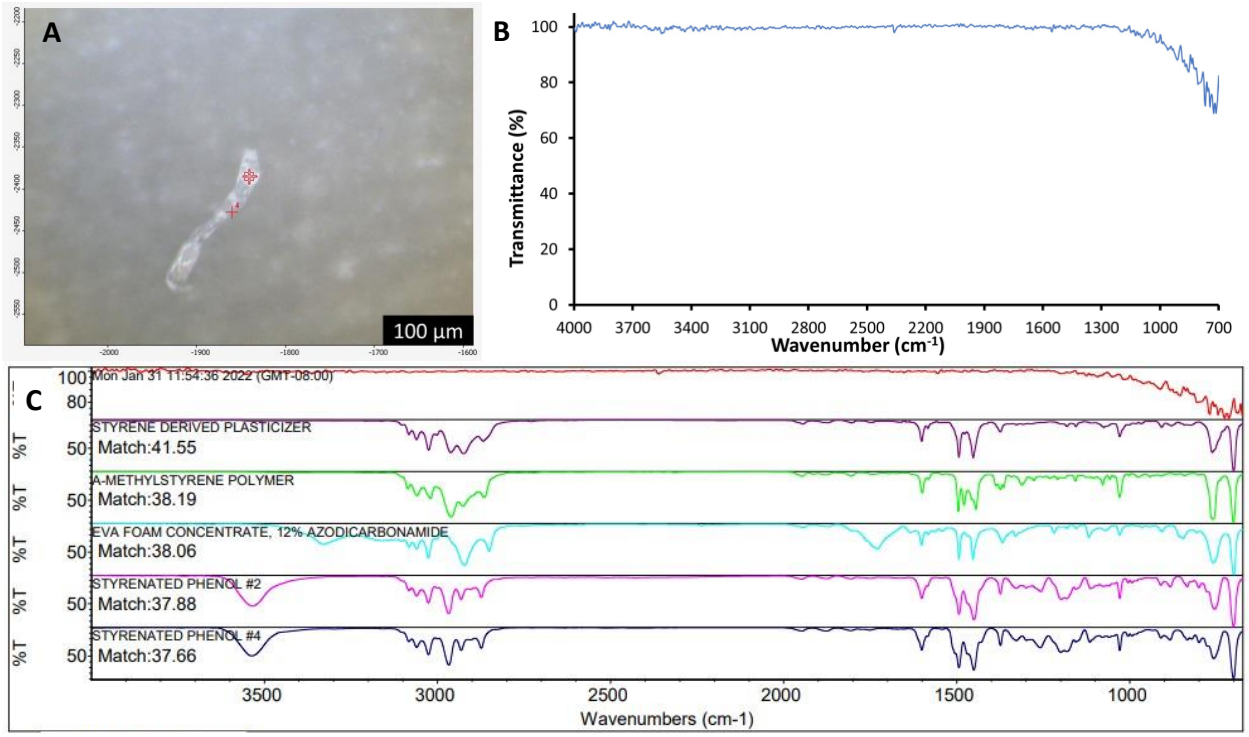

Figure A9. (A) An image of L4-2 particle found from Laguna Sample 4, (B) ATR-FTIR spectra of L4-2 particle, and (C) ATR-FTIR spectra of L4-2 particle with ~ 42% matched with styrene derived plasticizer.

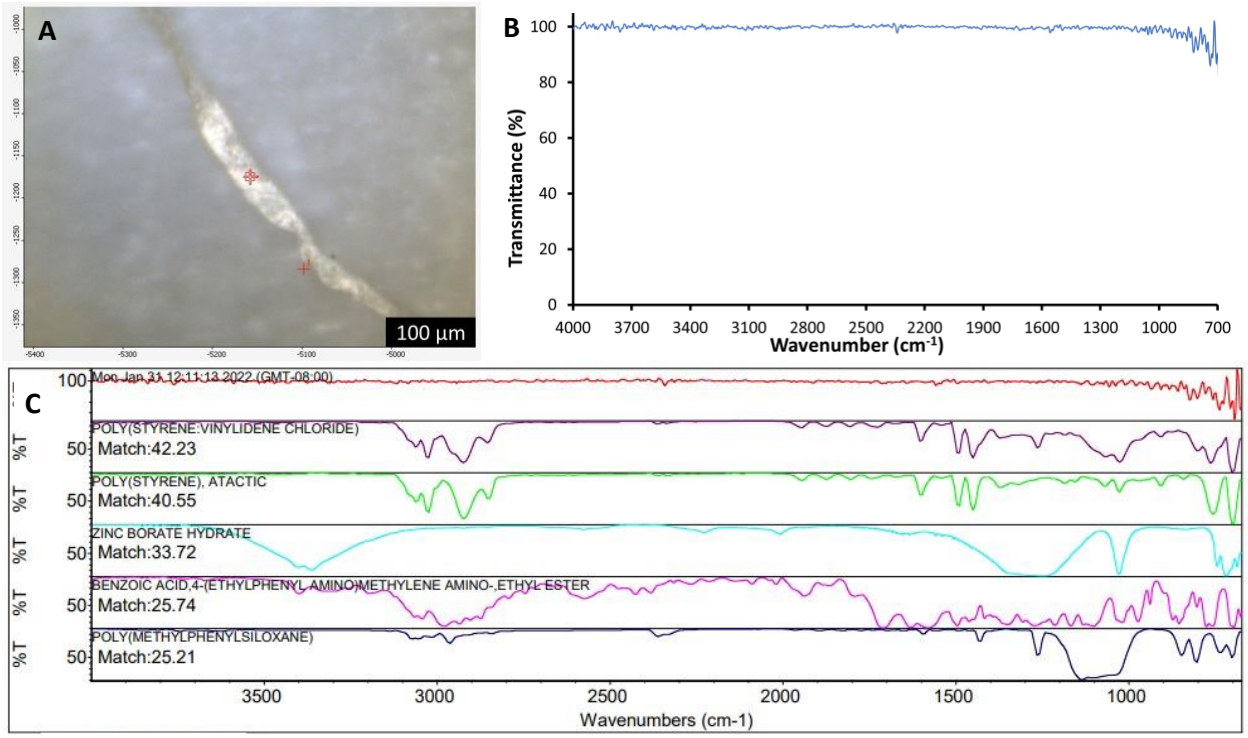

Figure A10. (A) An image of L4-3 particle found from Laguna Sample 4, (B) ATR-FTIR spectra of L4-3 particle, and (C) ATR-FTIR spectra of L4-3 particle with ~ 42% matched with poly(styrene:vinylidene chloride).

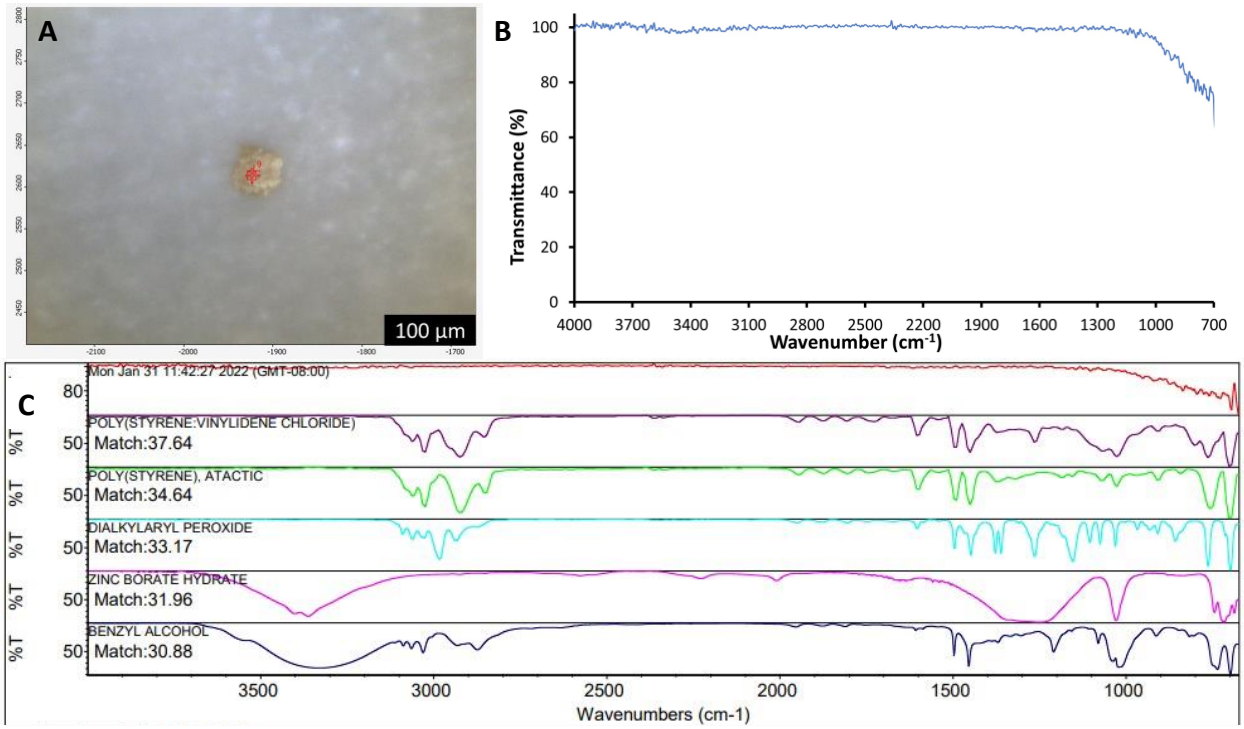

Figure A11. Figure A11. (A) An image of L4-4 particle found from Laguna Sample 4, (B) ATR-FTIR spectra of L4-4 particle, and (C) ATR-FTIR spectra of L4-4 particle with ~ 38% matched with poly(styrene:vinylidene chloride).

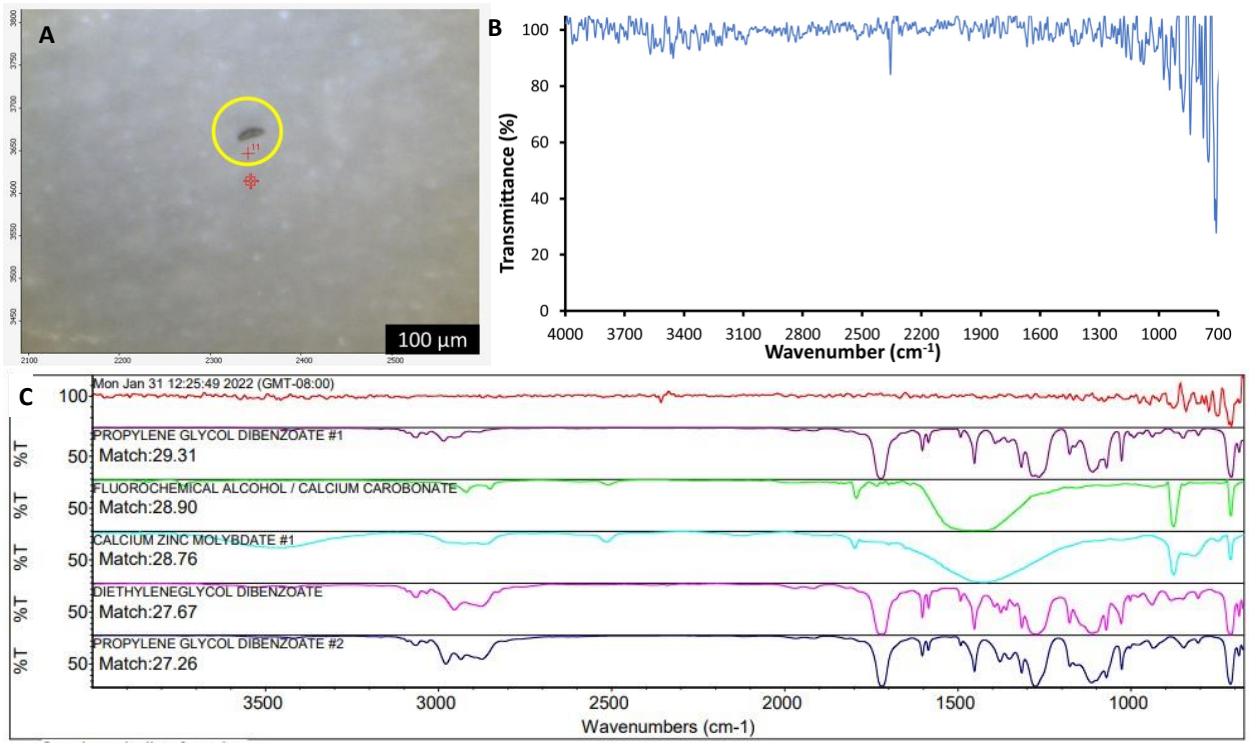

Figure A12. (A) An image of L4-5 particle found from Laguna Sample 4, (B) ATR-FTIR spectra of L4-5 particle, and (C) ATR-FTIR spectra of L4-5 particle with ~ 29% matched with propylene glycol dibenzonate #1.

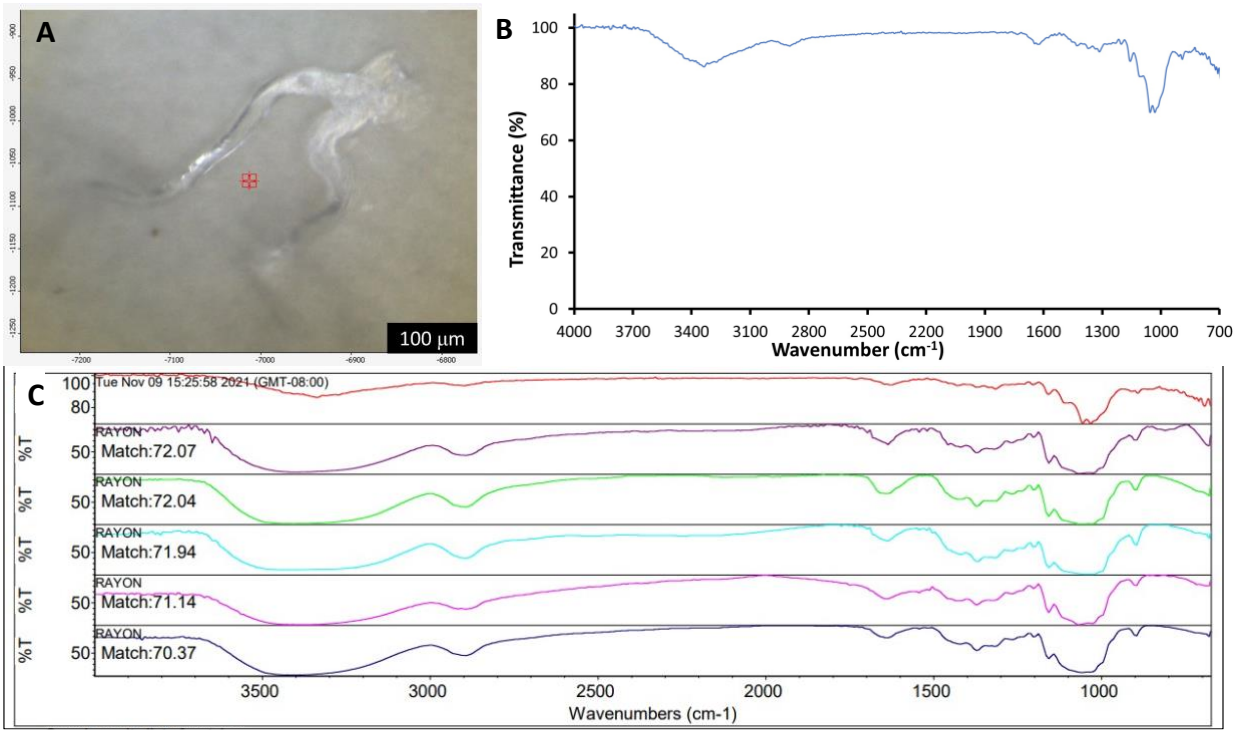

Figure A13. (A) An image of L5-1 particle found from Laguna Sample 5, (B) ATR-FTIR spectra of L5-1 particle, and (C) ATR-FTIR spectra of L5-1 particle with ~ 72% matched with rayon.

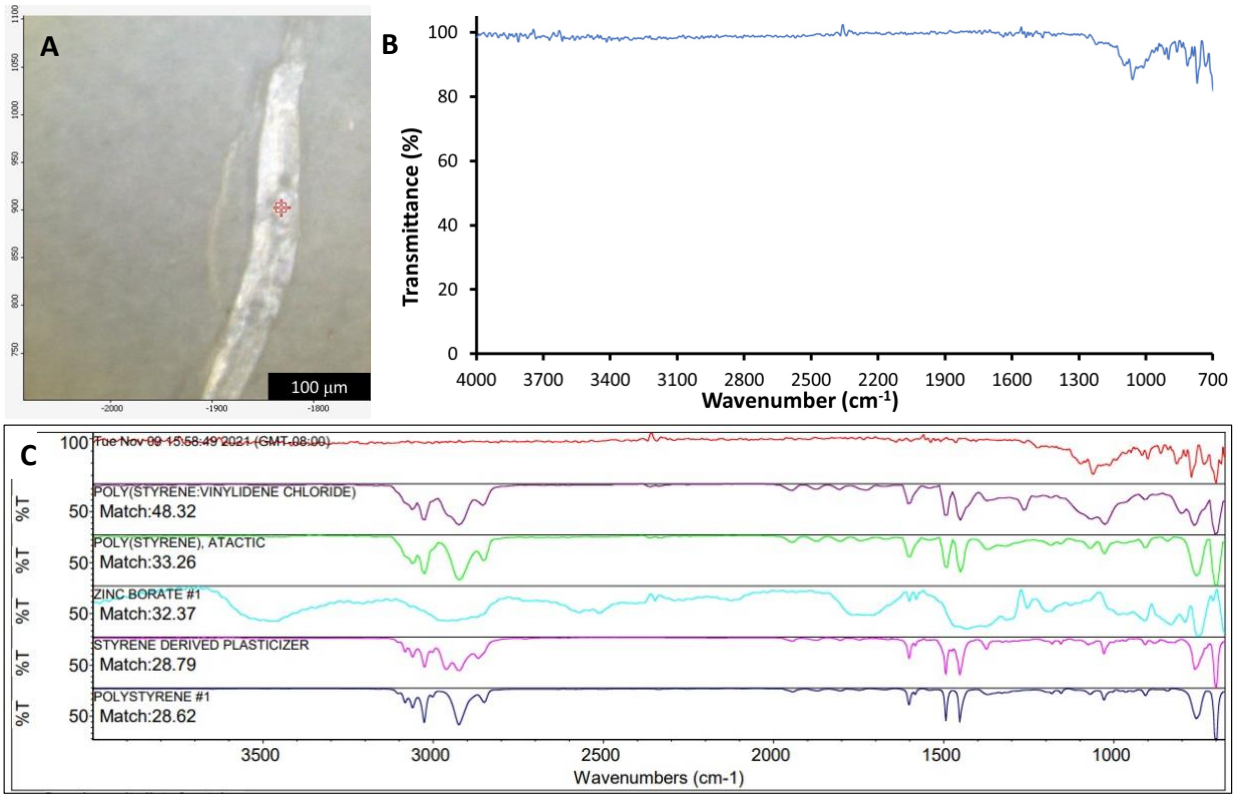

Figure A14. (A) An image of L5-2 particle found from Laguna Sample 5, (B) ATR-FTIR spectra of L5-2 particle, and (C) ATR-FTIR spectra of L5-2 particle with ~ 48% matched with poly(styrene:vinylidene chloride).

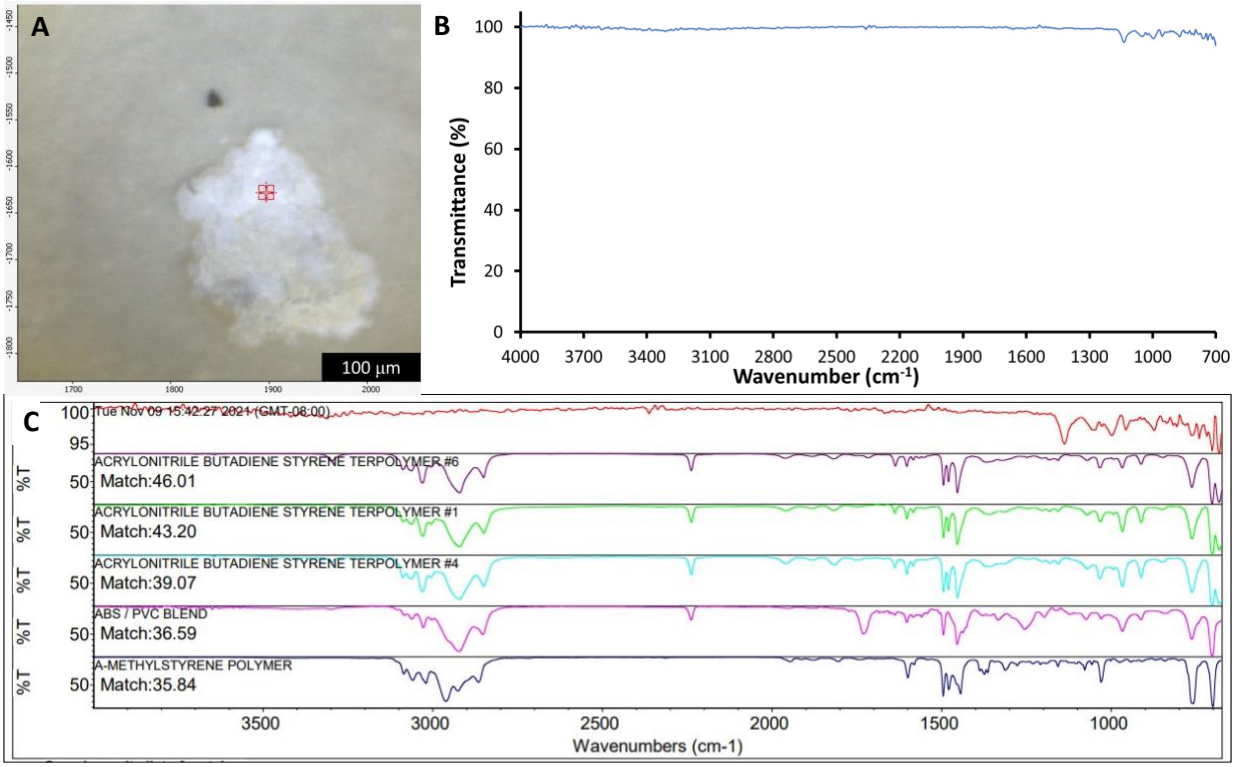

Figure A15. (A) An image of L5-3 particle found from Laguna Sample 5, (B) ATR-FTIR spectra of L5-3 particle, and (C) ATR-FTIR spectra of L5-3 particle with ~ 46% matched with acrylonitrile butadiene styrene terpolymer #6.

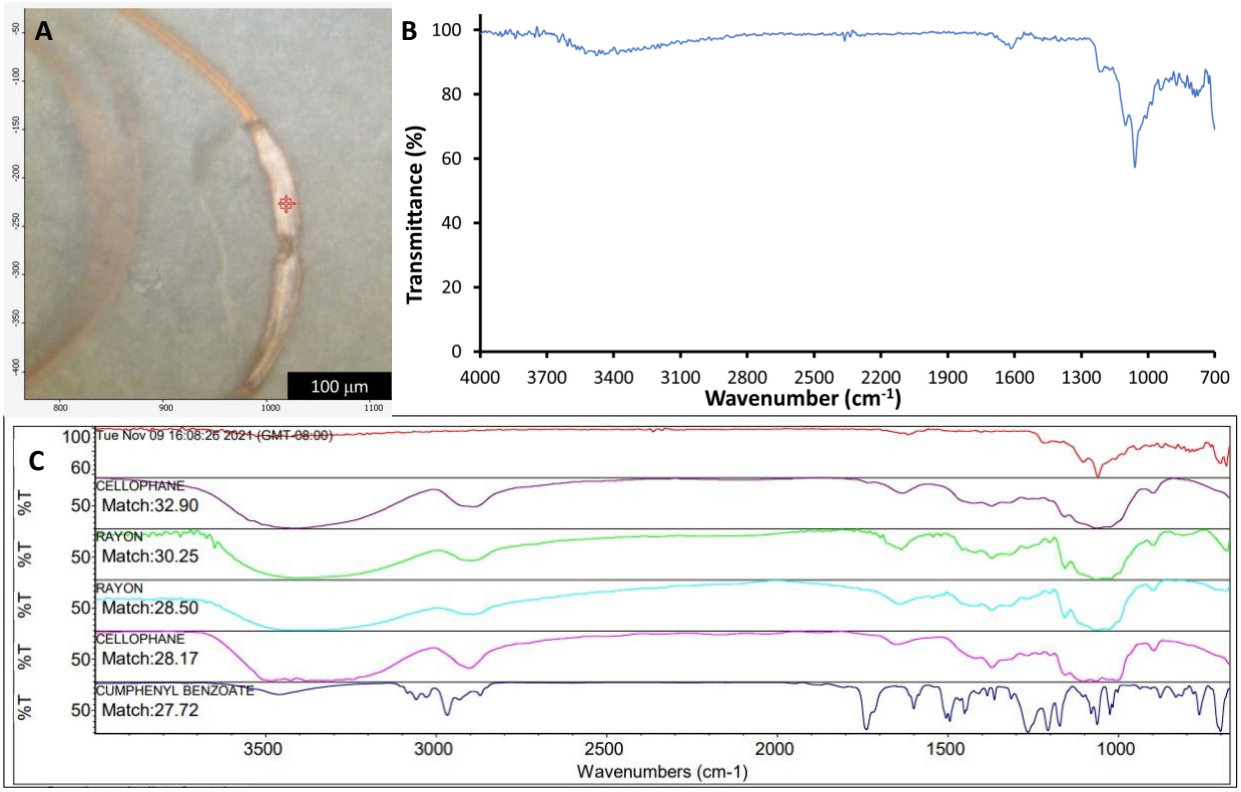

Figure A16. (A) An image of L5-4 particle found from Laguna Sample 5, (B) ATR-FTIR spectra of L5-4 particle, and (C) ATR-FTIR spectra of L5-4 particle with ~ 33% matched with cellophane.

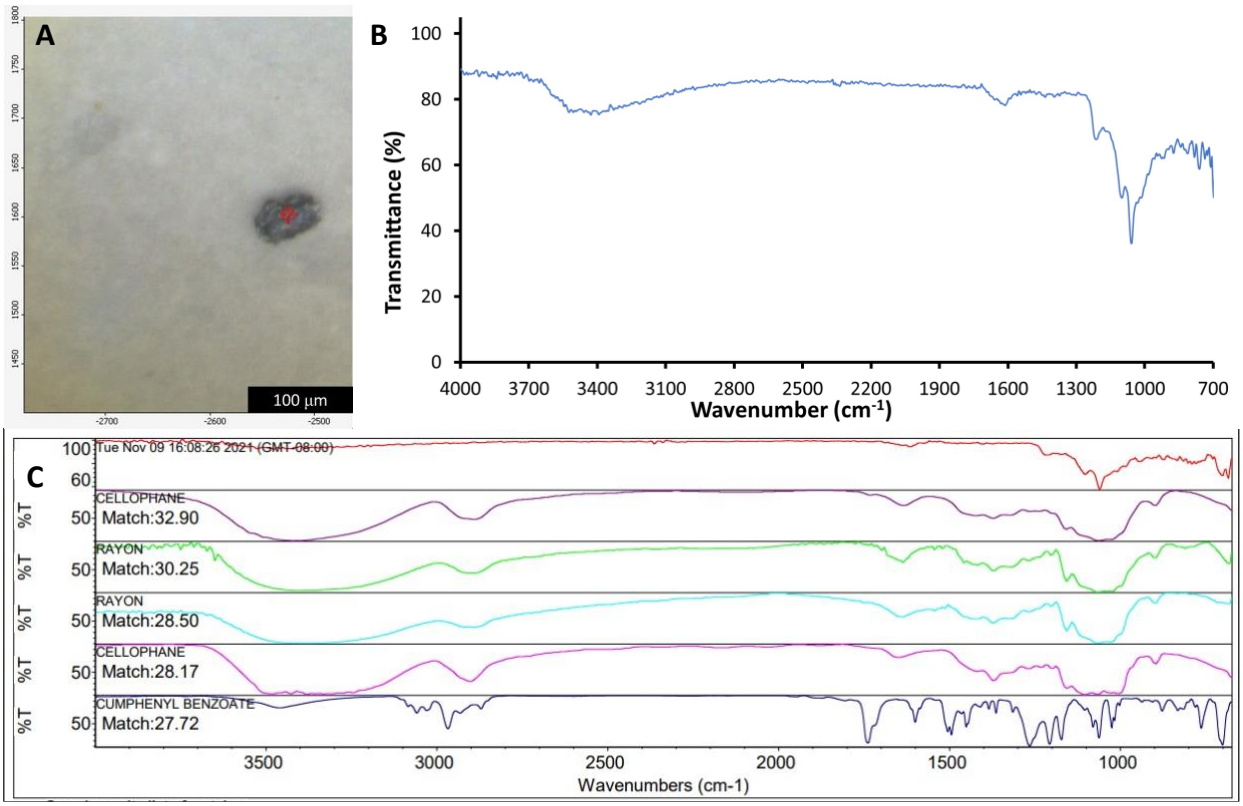

Figure A17. (A) An image of L5-5 particle found from Laguna Sample 5, (B) ATR-FTIR spectra of L5-5 particle, and (C) ATR-FTIR spectra of L5-5 particle with ~ 33% matched with cellophane.

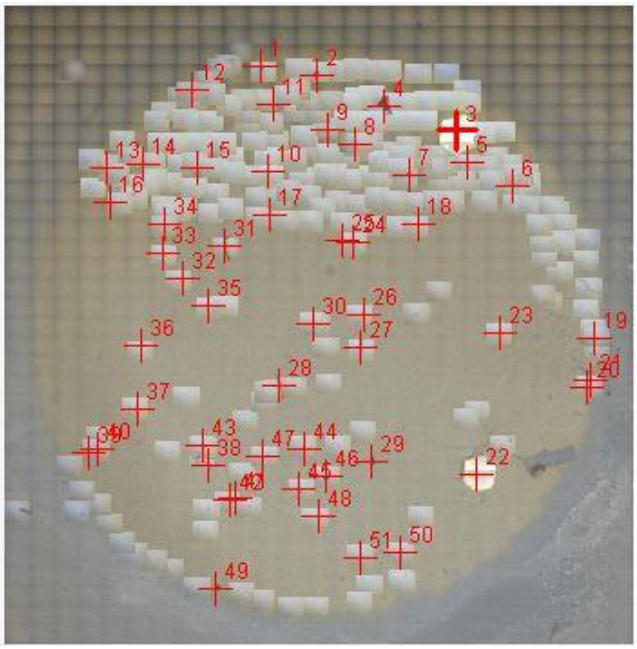

Figure A18. A full mosaic image of the Al2O3 filter of Tingley Beach Sample 2 (T2) with particle count ~ 51.

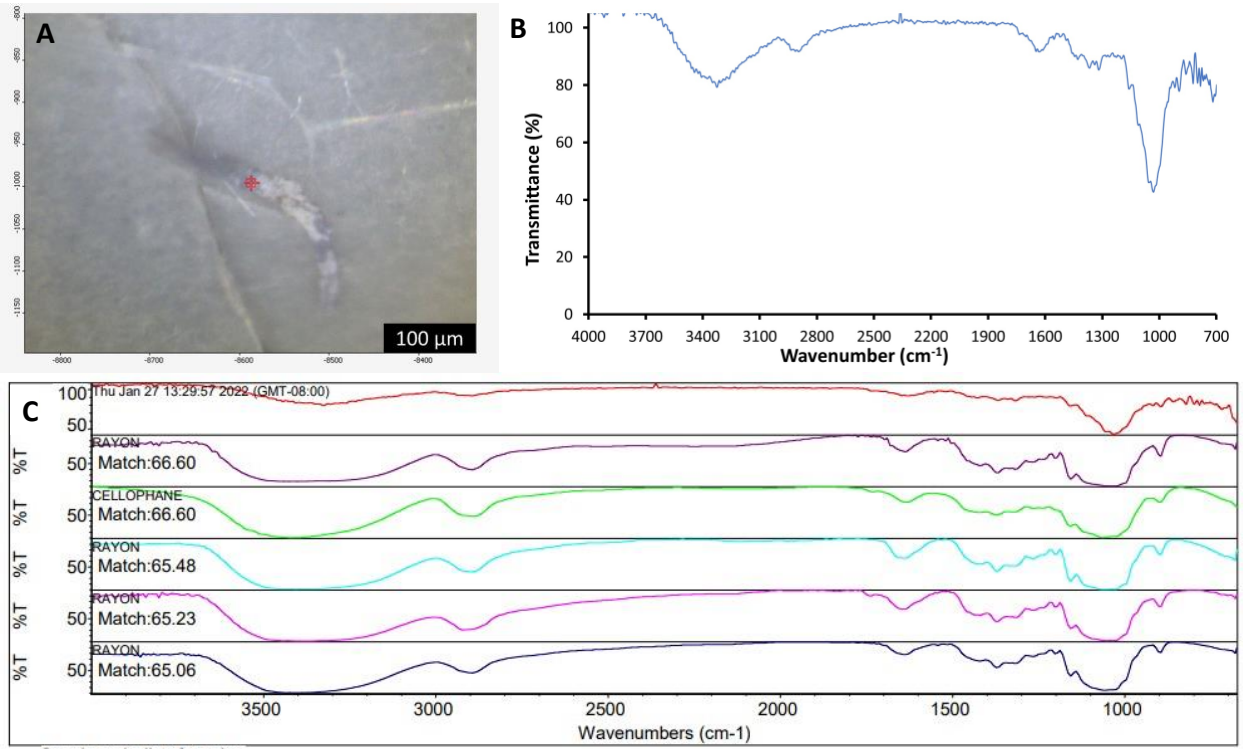

Figure A19. (A) An image of T1-1 particle found from Tingley Beach, New Mexico, (B) ATR-FTIR spectra of T1-1 particle, and (C) ATR-FTIR spectra of T1-1 particle with ~ 67% matched with rayon.

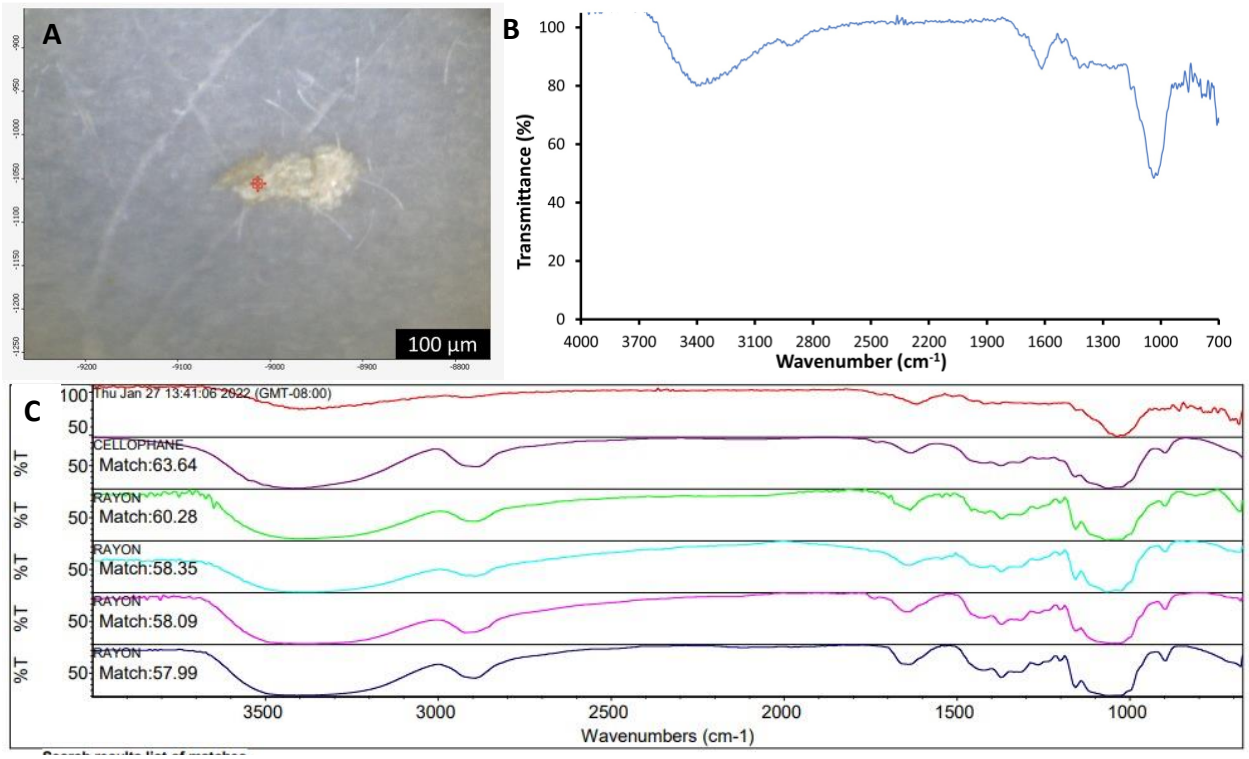

Figure A20. (A) An image of T1-2 particle found from Tingley Beach, New Mexico, (B) ATR-FTIR spectra of T1-2 particle, and (C) ATR-FTIR spectra of T1-2 particle with ~ 64% matched with cellophane.

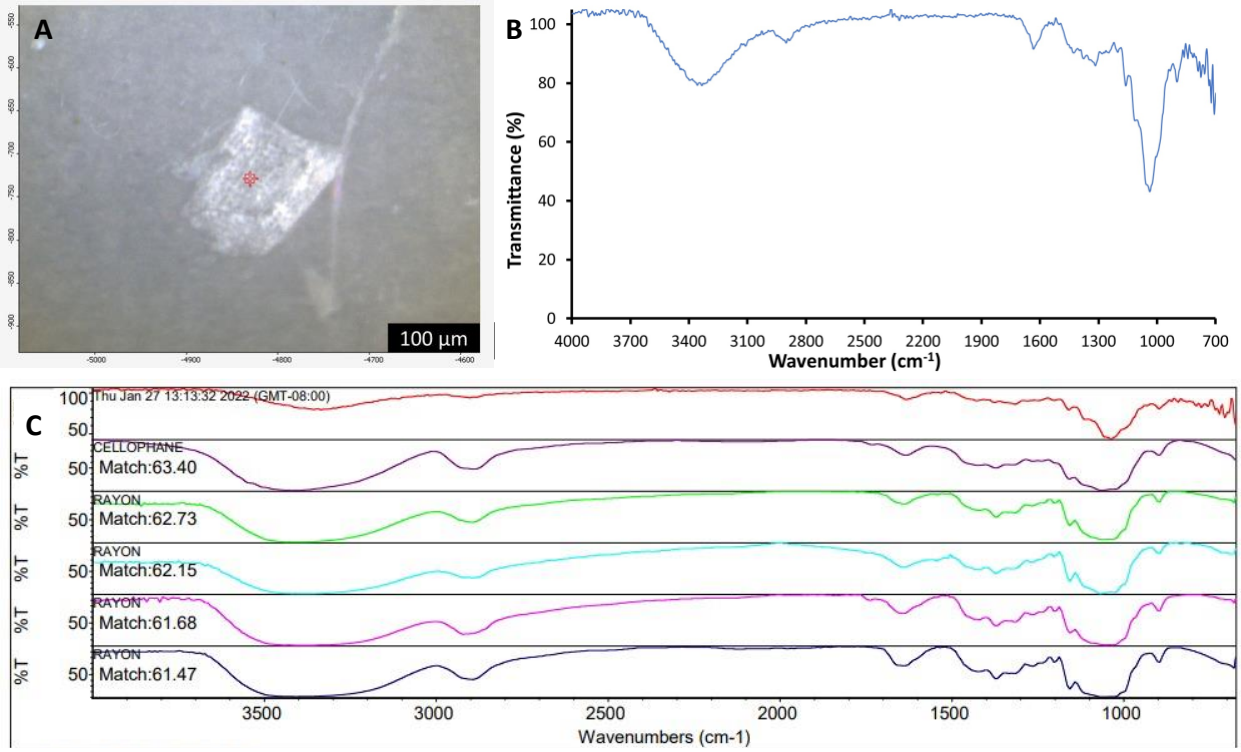

Figure A21. (A) An image of T1-3 particle found from Tingley Beach, New Mexico, (B) ATR-FTIR spectra of T1-3 particle, and (C) ATR-FTIR spectra of T1-3 particle with ~ 63% matched with cellophane.

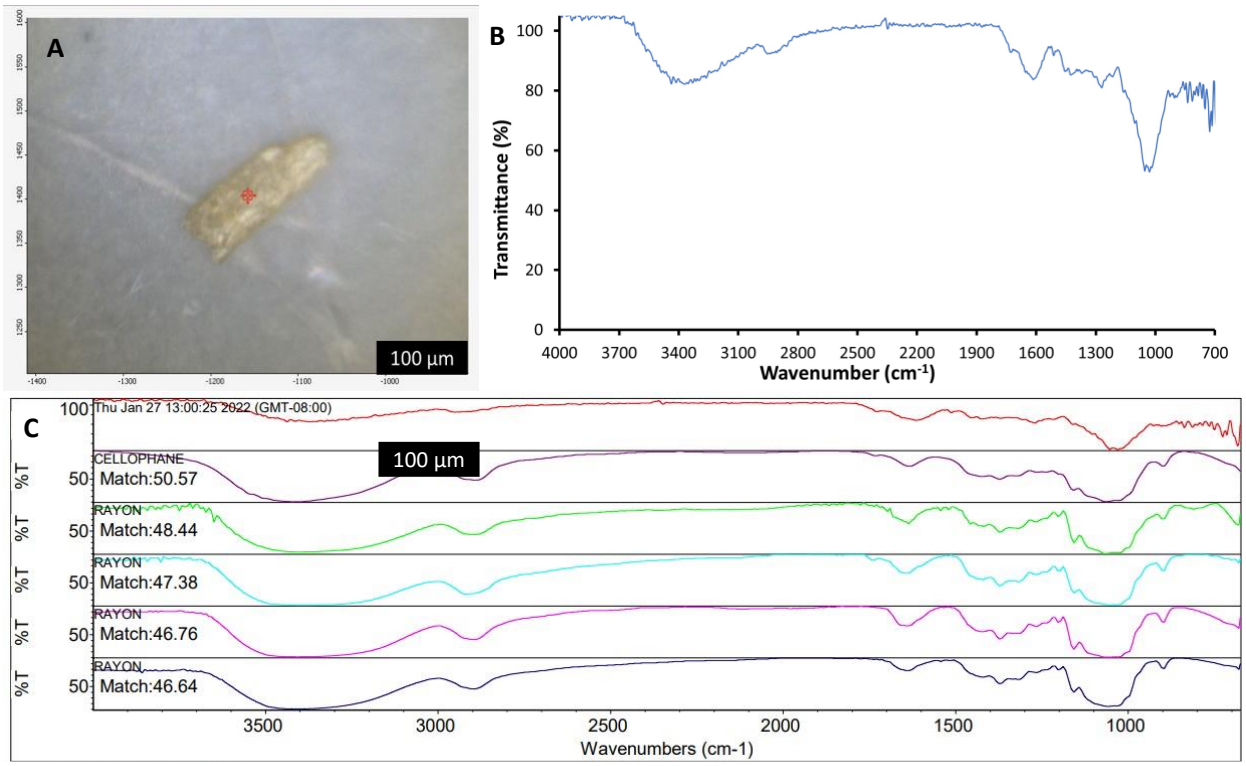

Figure A22. (A) An image of T1-4 particle found from Tingley Beach, New Mexico, (B) ATR-FTIR spectra of T1-4 particle, and (C) ATR-FTIR spectra of T1-4 particle with ~ 51% matched with cellophane.

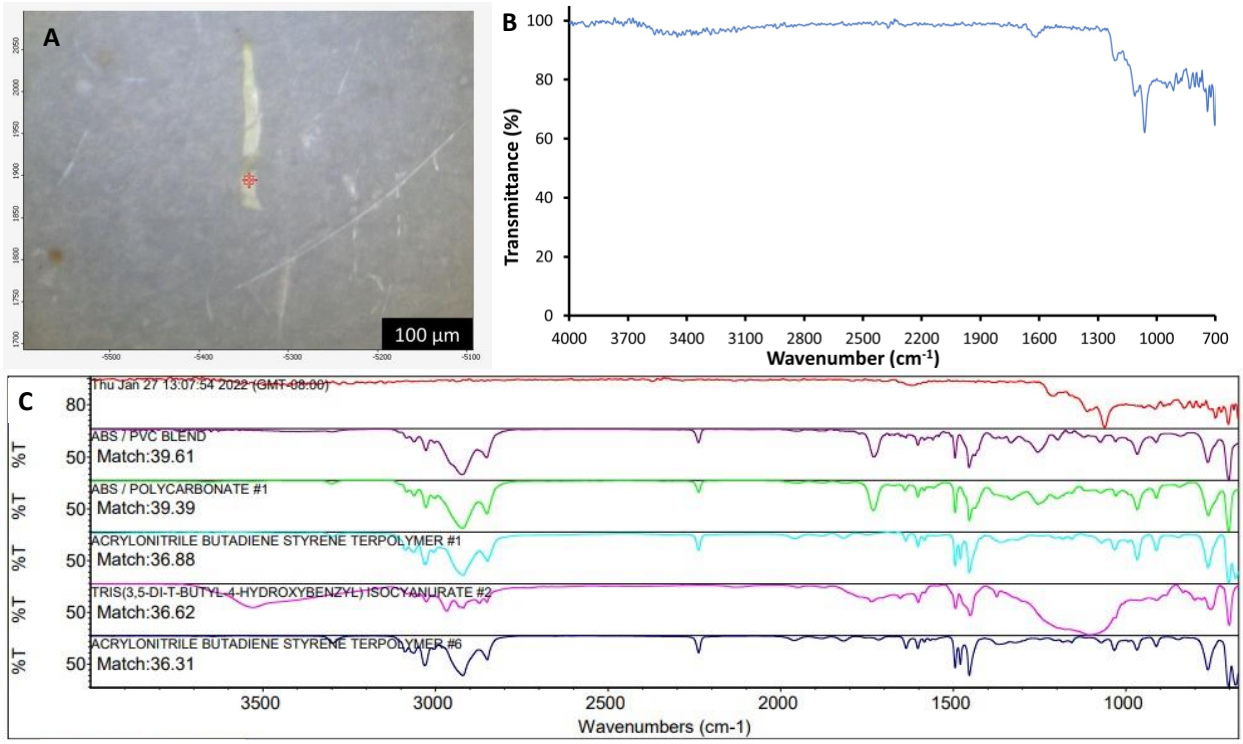

Figure A23. (A) An image of T1-5 particle found from Tingley Beach, New Mexico, (B) ATR-FTIR spectra of T1-5 particle, and (C) ATR-FTIR spectra of T1-5 particle with ~ 40% matched with ABS/PVC blend.

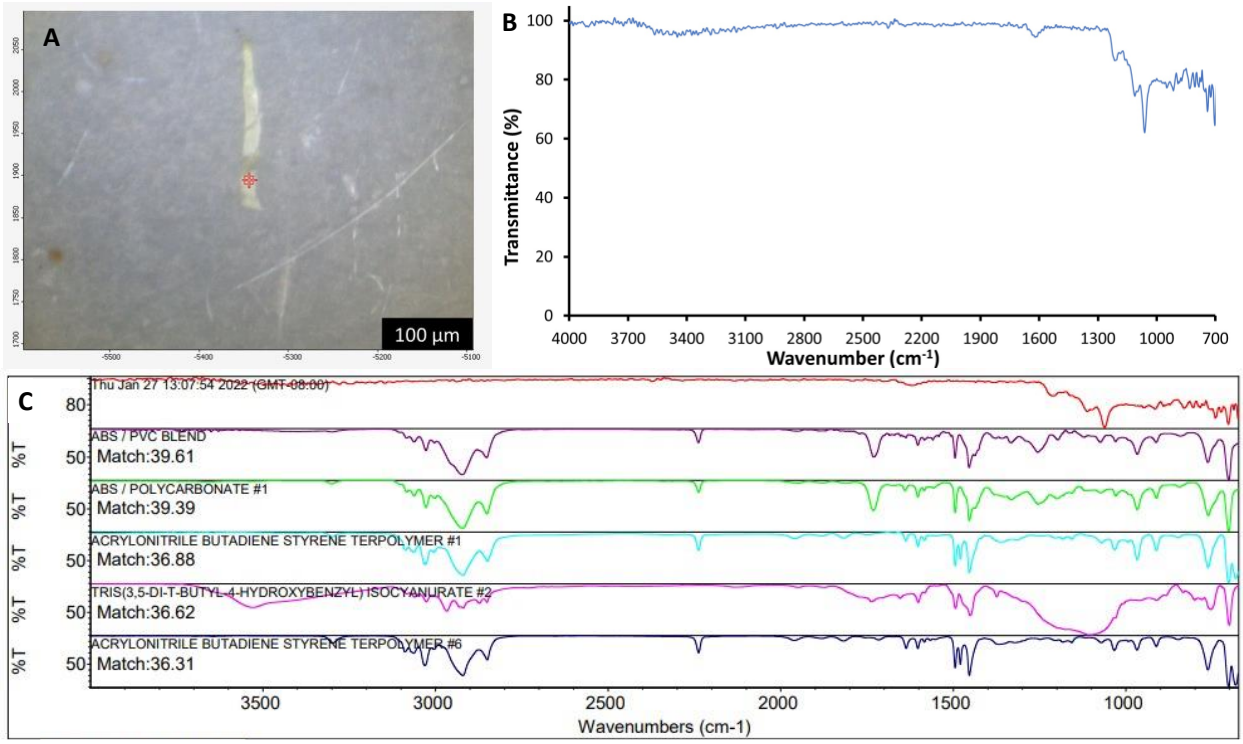

Figure A24. (A) An image of T1-6 particle found from Tingley Beach, New Mexico, (B) ATR-FTIR spectra of T1-6 particle, and (C) ATR-FTIR spectra of T1-6 particle with ~ 39% matched with acrylonitrile butadiene styrene terpolymer #6.

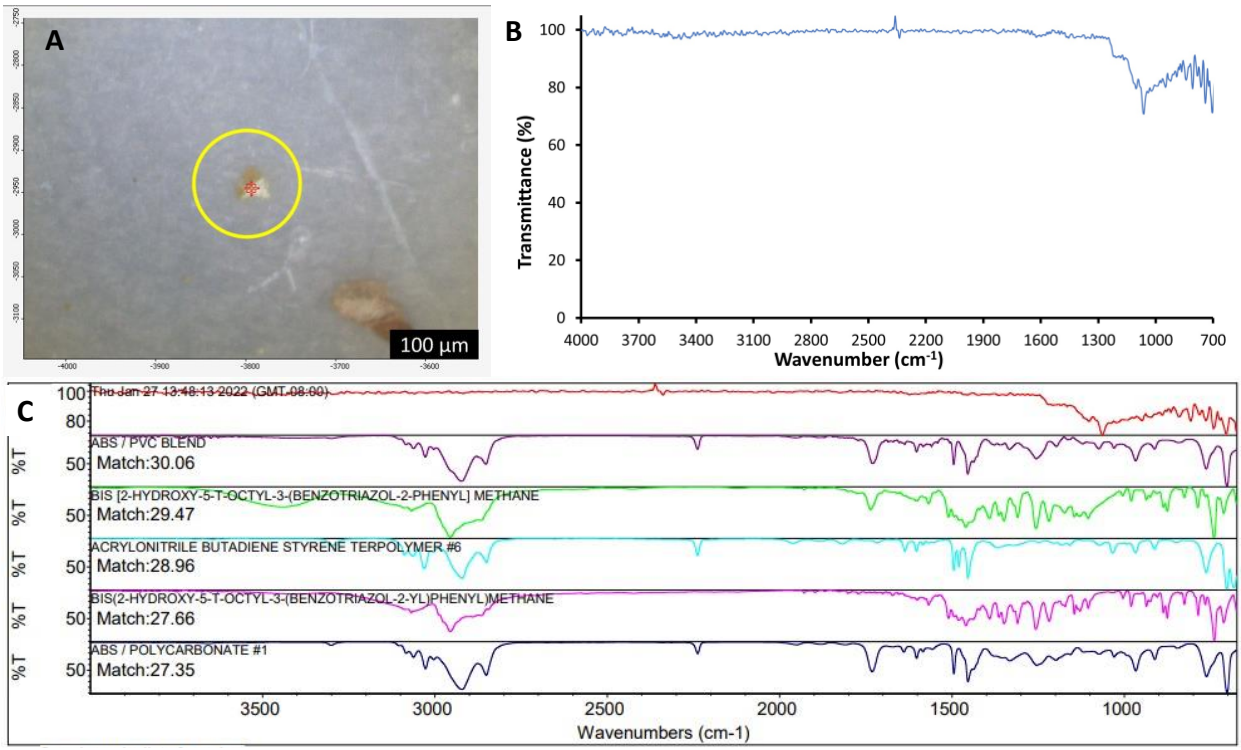

Figure A25. (A) An image of T1-7 particle found from Tingley Beach, New Mexico, (B) ATR-FTIR spectra of T1-7 particle, and (C) ATR-FTIR spectra of T1-7 particle with ~ 30% matched with ABS/PVC blend.

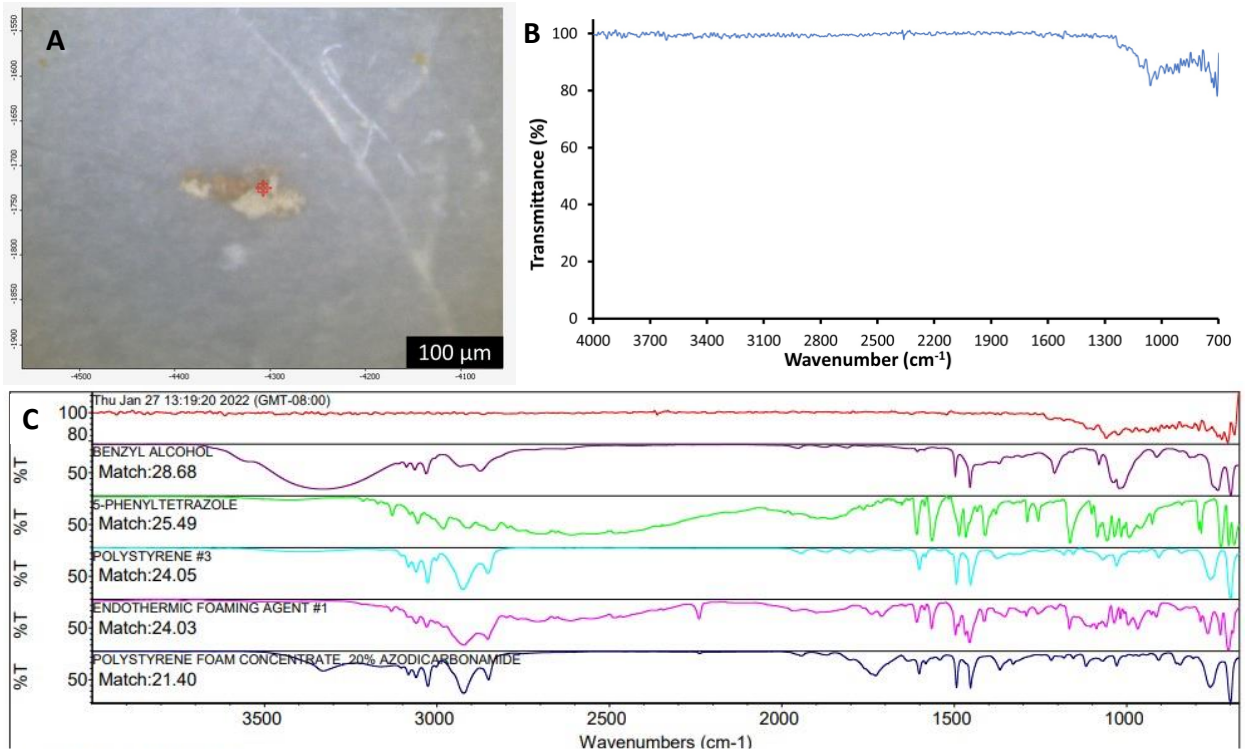

Figure A26. (A) An image of T1-8 particle found from Tingley Beach, New Mexico, (B) ATR-FTIR spectra of T1-8 particle, and (C) ATR-FTIR spectra of T1-8 particle with ~ 29% matched with benzyl alcohol.

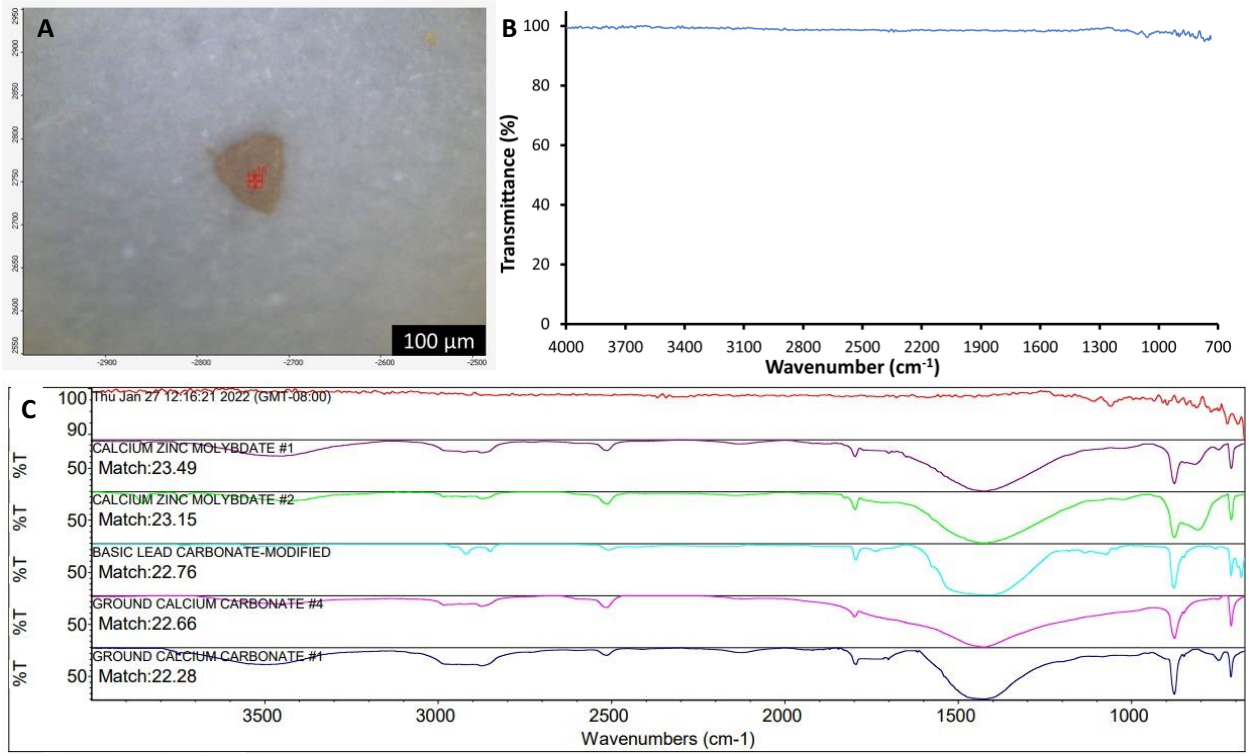

Figure A27. (A) An image of T1-9 particle found from Tingley Beach, New Mexico, (B) ATR-FTIR spectra of T1-9 particle, and (C) ATR-FTIR spectra of T1-9 particle with ~ 23% matched with matched with calcium zinc molybdate #1.

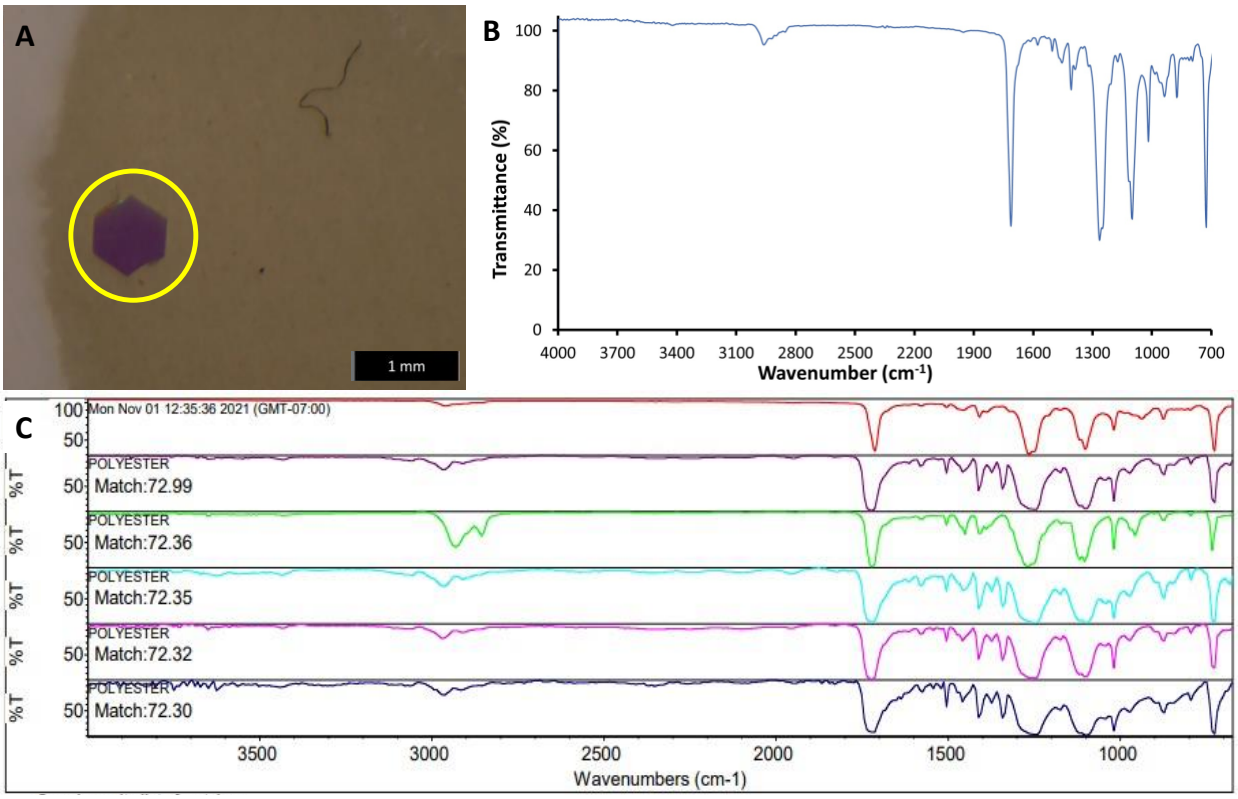

Figure A28. (A) An image of T2-1 particle found from Tingley Beach, New Mexico, (B) ATR-FTIR spectra of T2-1 particle, and (C) ATR-FTIR spectra of T2-1 particle with ~ 73% matched with polyester.

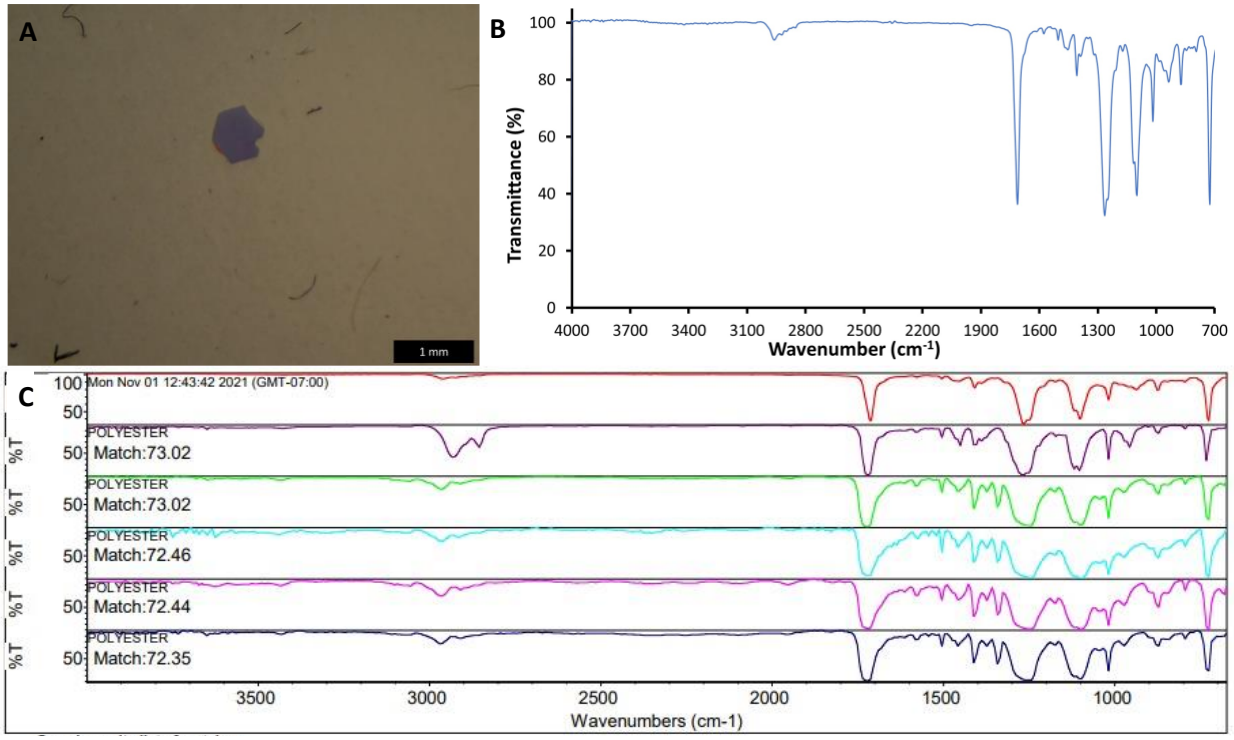

Figure A29. (A) An image of T2-2 particle found from Tingley Beach, New Mexico, (B) ATR-FTIR spectra of T2-2 particle, and (C) ATR-FTIR spectra of T2-2 particle with ~ 73% matched with polyester.

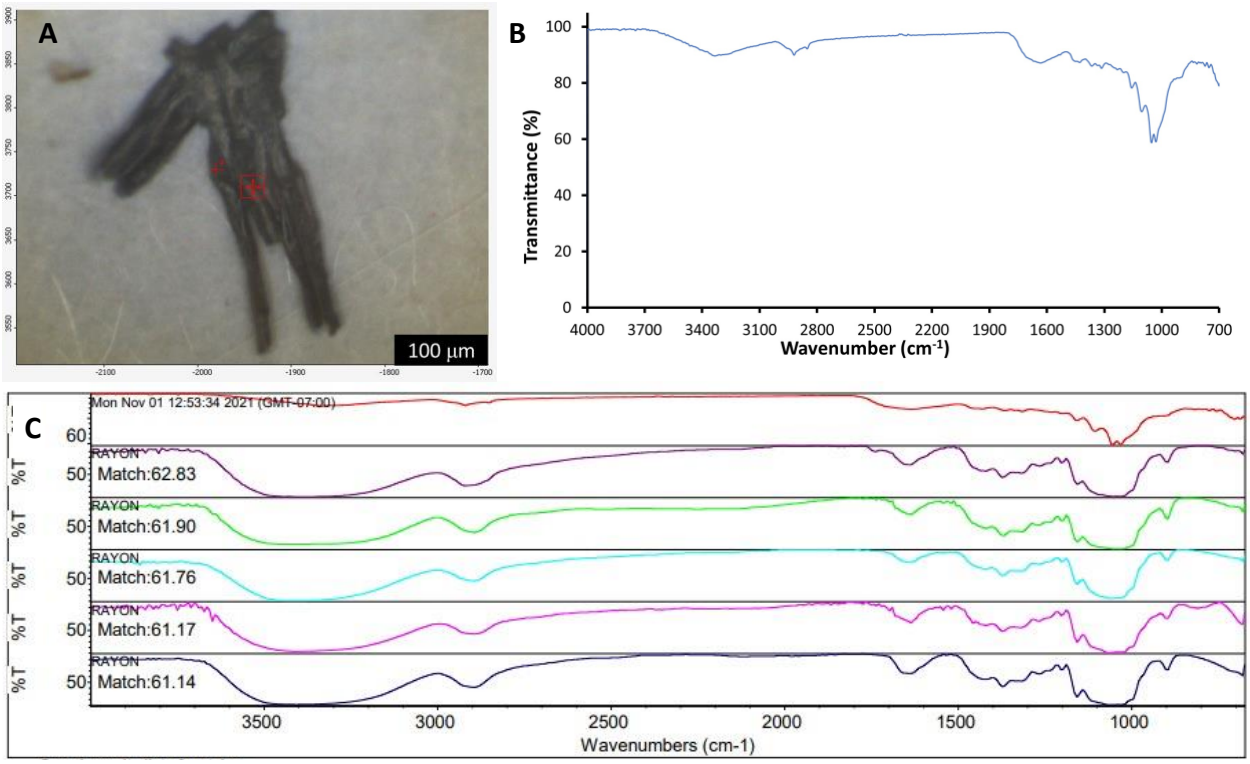

Figure A30. (A) An image of T2-3 particle found from Tingley Beach, New Mexico, (B) ATR-FTIR spectra of T2-3 particle, and (C) ATR-FTIR spectra of T2-3 particle with ~ 63% matched with rayon.

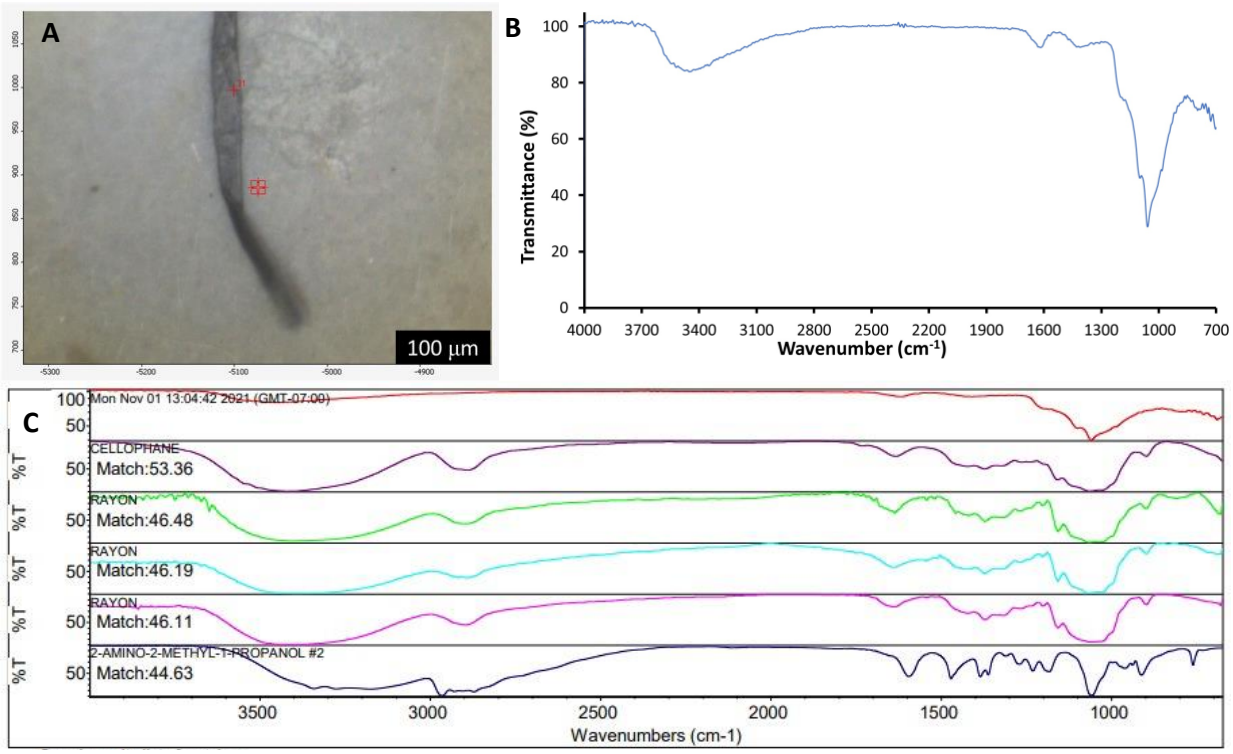

Figure A31. (A) An image of T2-4 particle found from Tingley Beach, New Mexico, (B) ATR-FTIR spectra of T2-4 particle, and (C) ATR-FTIR spectra of T2-4 particle with ~ 53% matched with cellophane.

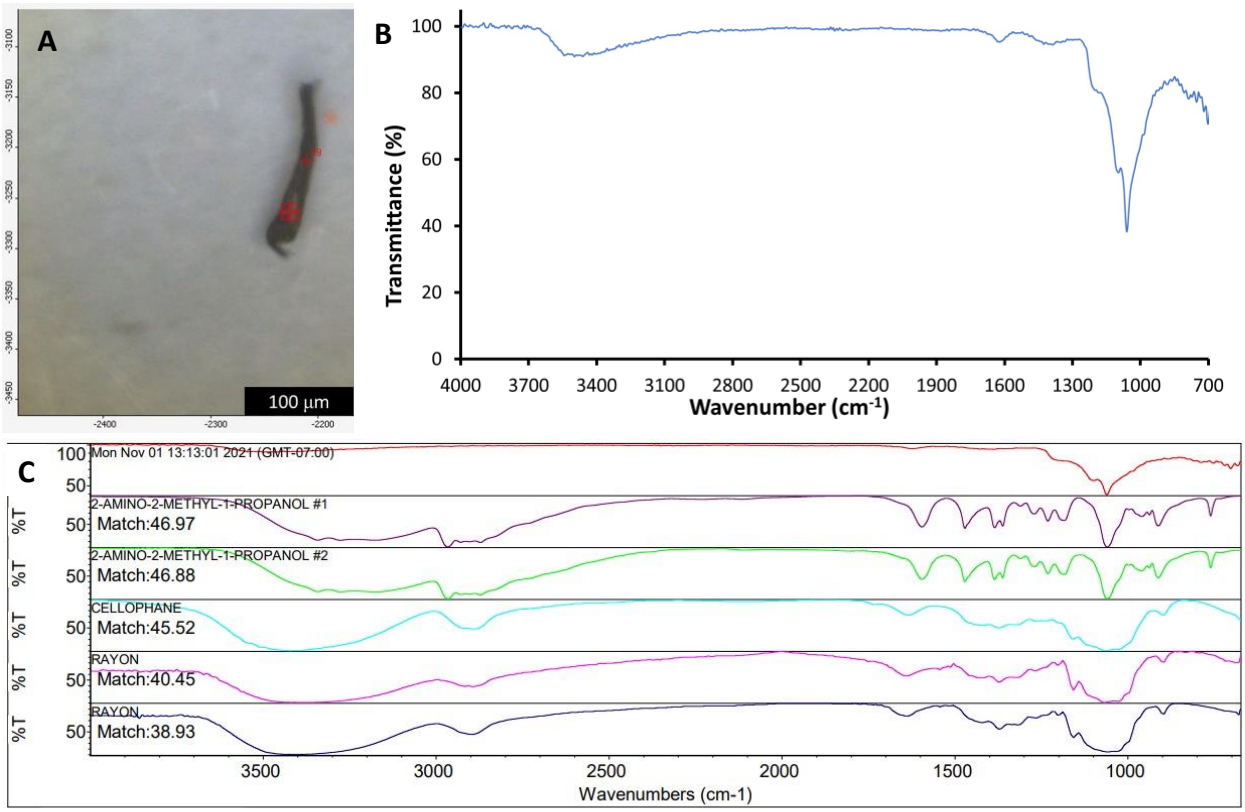

Figure A32. (A) An image of T2-5 particle found from Tingley Beach, New Mexico, (B) ATR-FTIR spectra of T2-5 particle, and (C) ATR-FTIR spectra of T2-45 particle with ~ 47% matched with 2-amino-2-methyl-1-propanol #1.

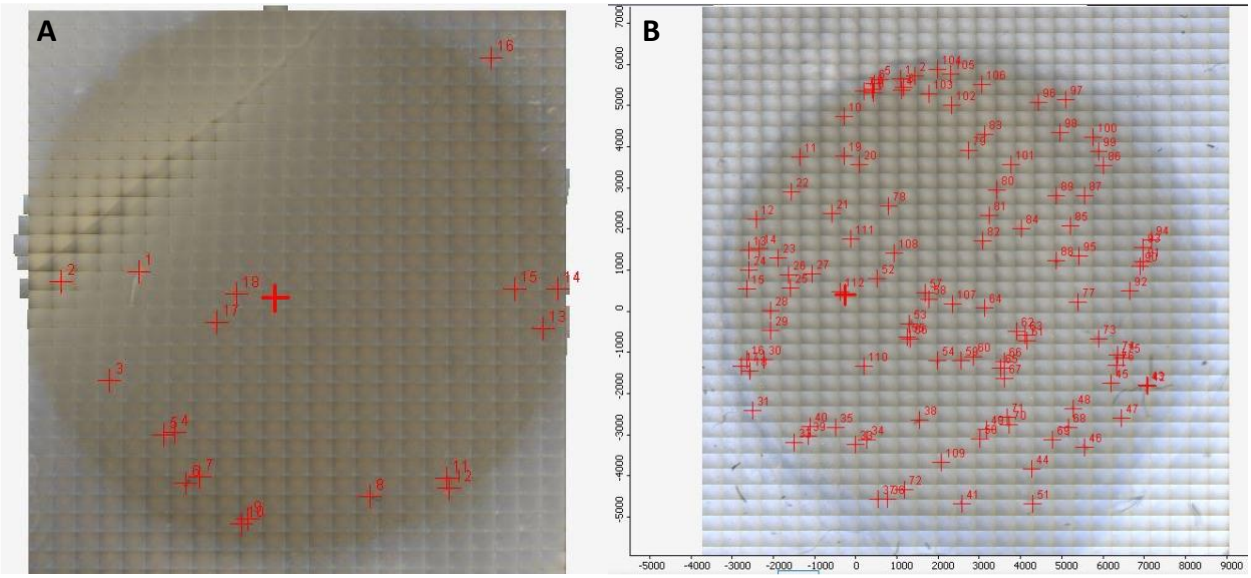

Figure A33. A full mosaic image of the Al2O3 filter with particle count of (A) ~ 18 for Rio Grande Sample 3 (R1) and (B) ~ 112 for Rio Grande Sample 3 (R3).

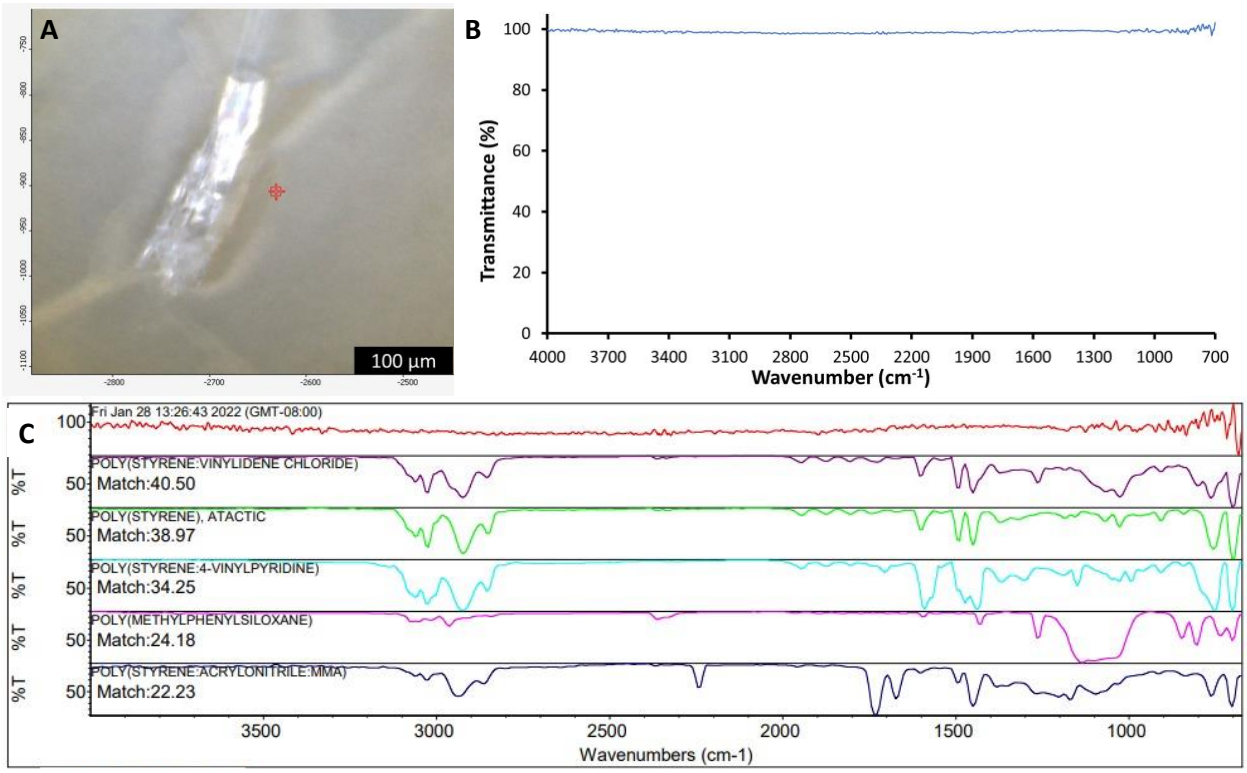

Figure A34. (A) An image of R1-1 particle found from the Rio Grande, (B) ATR-FTIR spectra of R1-1 particle, and (C) ATR-FTIR spectra of R1-1 particle with ~ 41% matched with poly(styrene:vinylidene chloride).

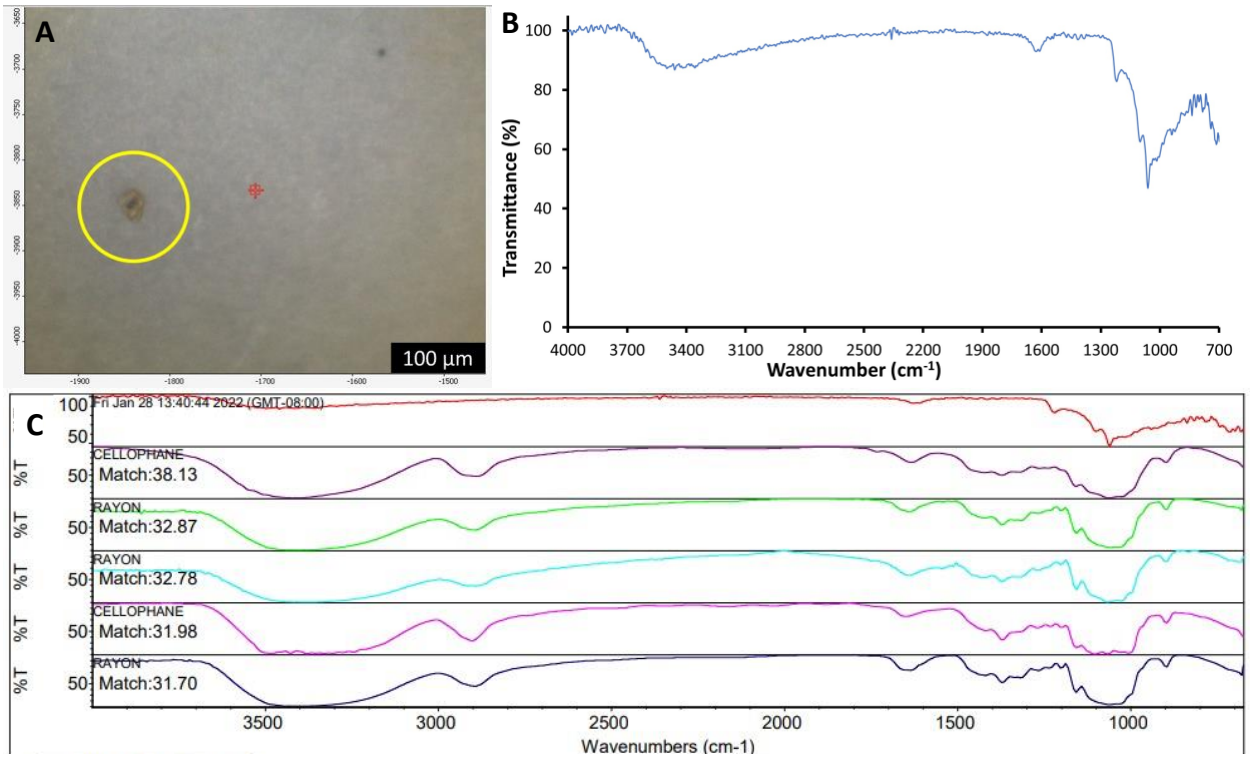

Figure A35. (A) An image of R1-2 particle found from the Rio Grande, (B) ATR-FTIR spectra of R1-2 particle, and (C) ATR-FTIR spectra of R1-2 particle with ~ 38% matched with cellophane.

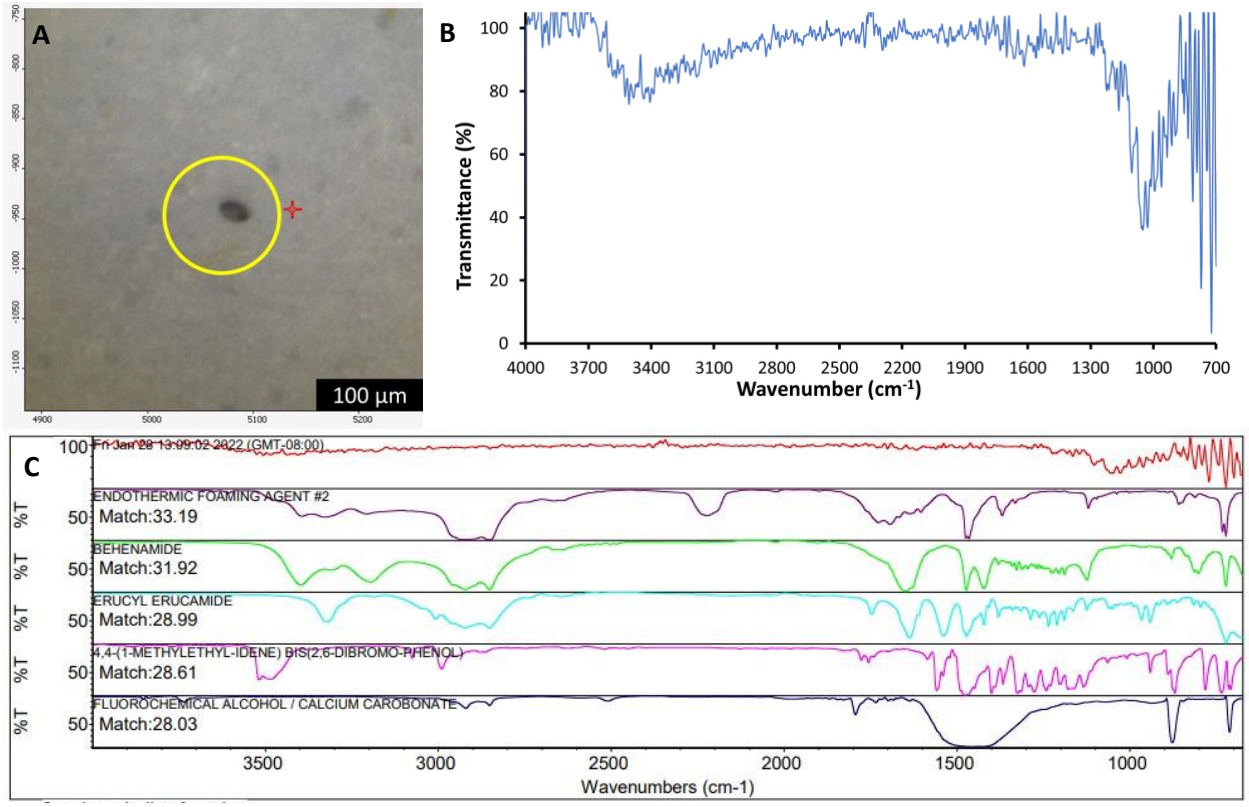

Figure A36. (A) An image of R1-3 particle found from the Rio Grande, (B) ATR-FTIR spectra of R1-3 particle, and (C) ATR-FTIR spectra of R1-3 particle with ~ 33% matched with endothermic foaming agent #2.

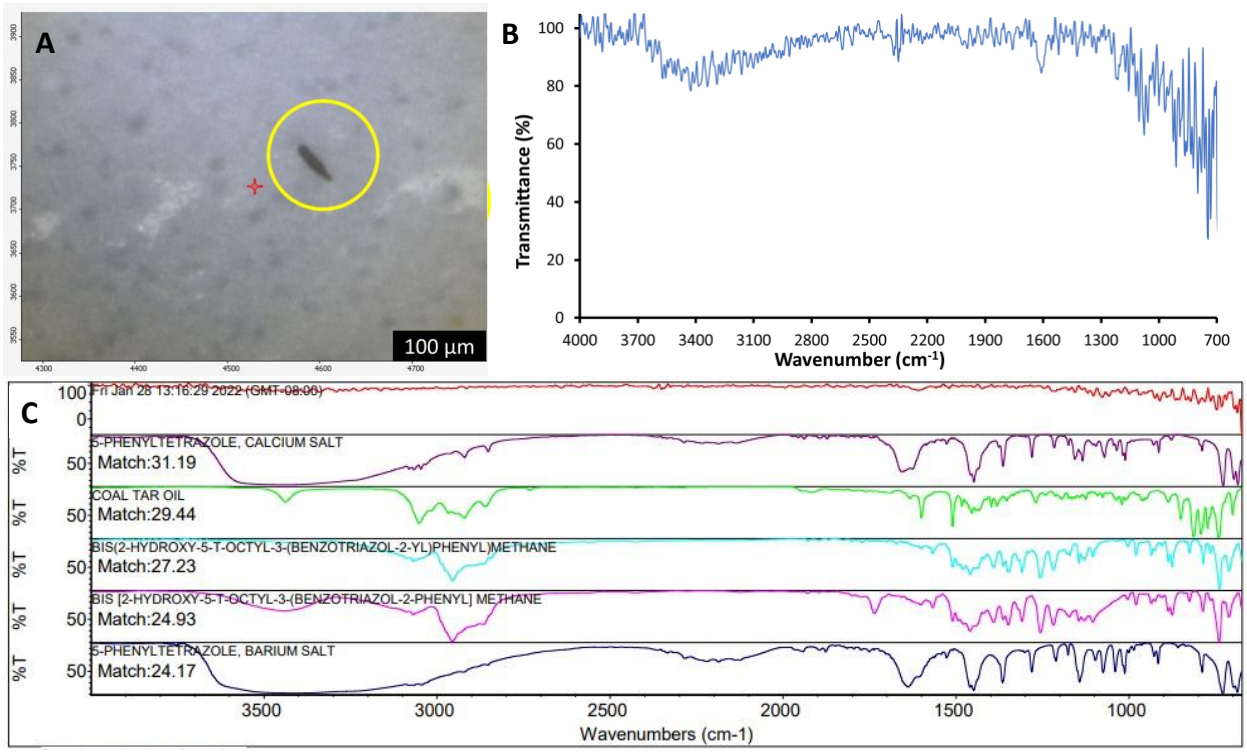

Figure A37. (A) An image of R1-4 particle found from the Rio Grande, (B) ATR-FTIR spectra of R1-4 particle, and (C) ATR-FTIR spectra of R1-4 particle with ~ 31% matched with 5-phenyltetrazole, calcium salt.

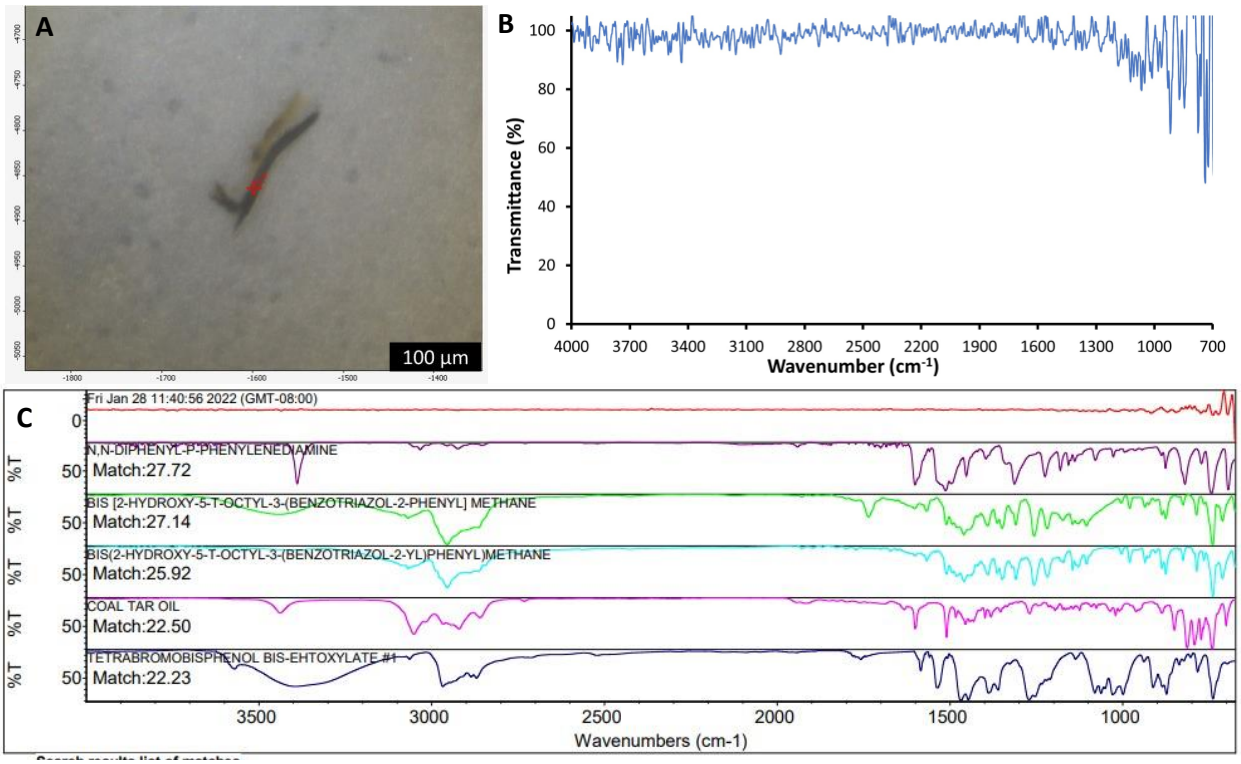

Figure A38. (A) An image of R1-5 particle found from the Rio Grande, (B) ATR-FTIR spectra of R1-5 particle, and (C) ATR-FTIR spectra of R1-5 particle with ~ 28% matched with N,N-diphenyl-p-phenylenediamine.

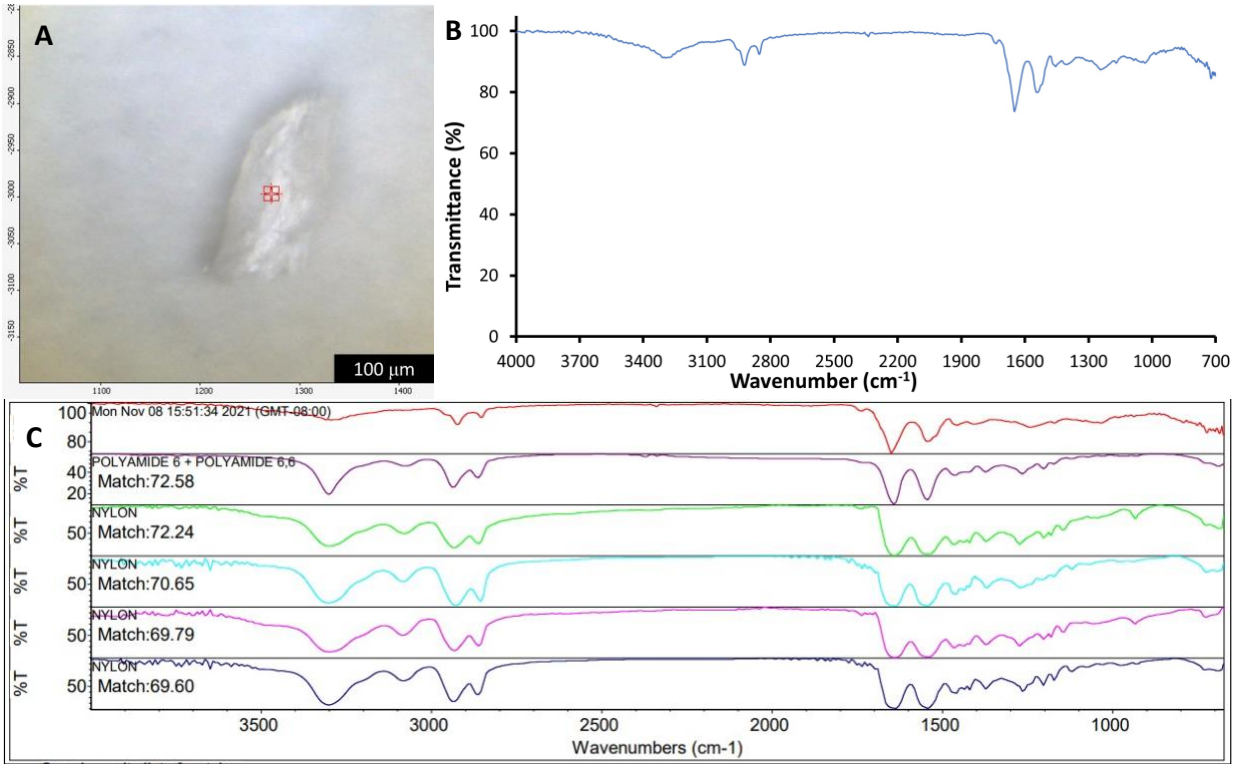

Figure A39. (A) An image of R3-1 particle found from the Rio Grande, (B) ATR-FTIR spectra of R3-1 particle, and (C) ATR-FTIR spectra of R3-1 particle with ~ 73% matched with Polyamide 6 + Polyamide 6,6.

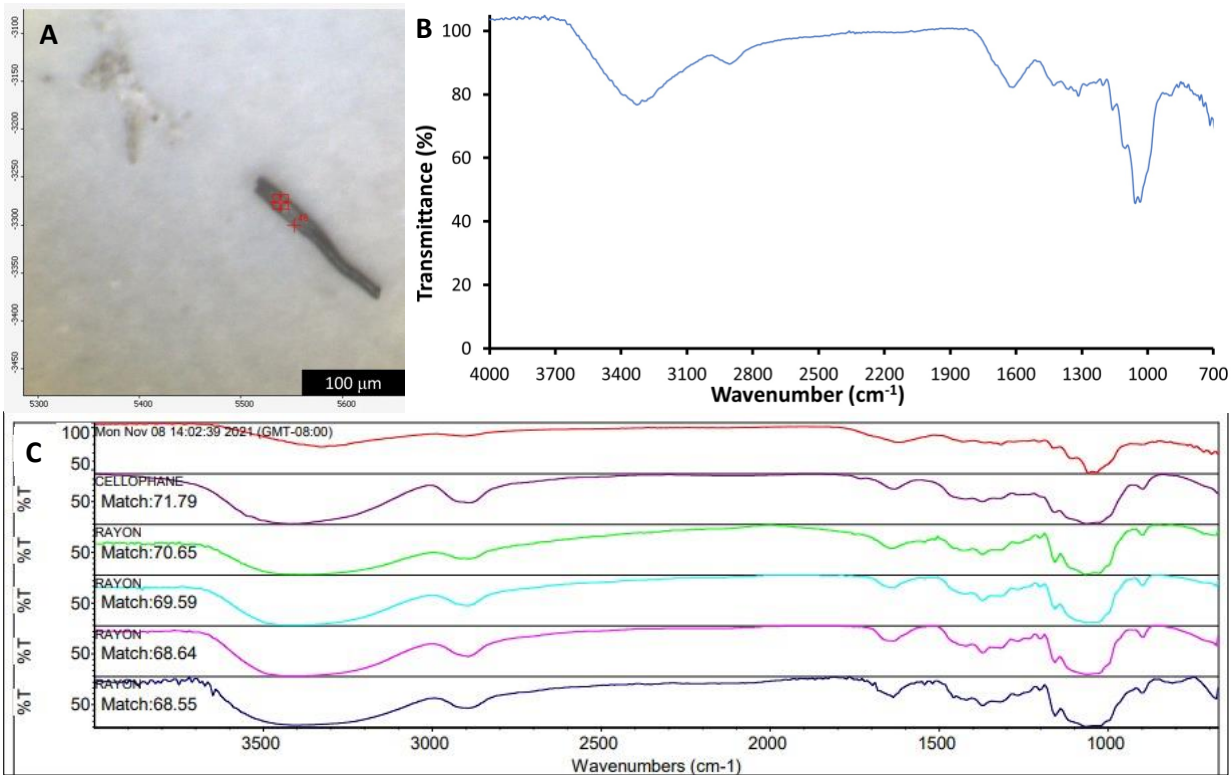

Figure A40. (A) An image of R3-2 particle found from the Rio Grande, (B) ATR-FTIR spectra of R3-2 particle, and (C) ATR-FTIR spectra of R3-2 particle with ~ 72% matched with cellophane.

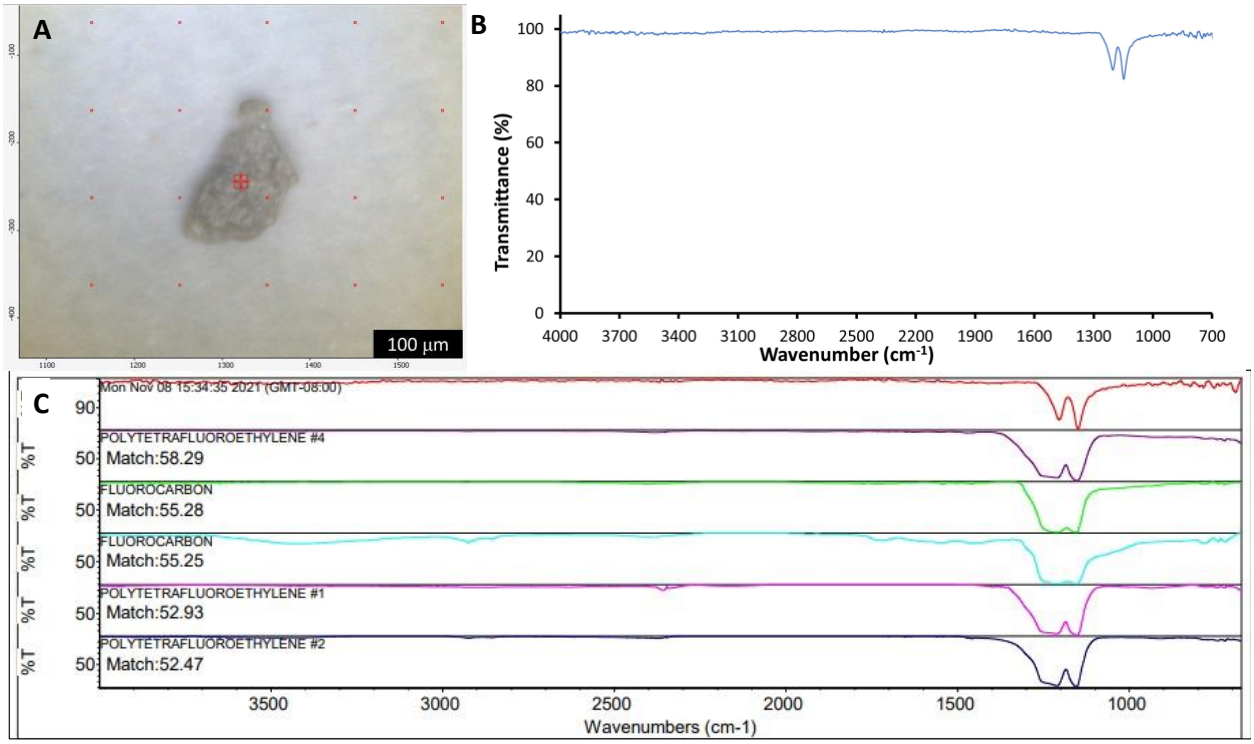

Figure A41. (A) An image of R3-3 particle found from the Rio Grande, (B) ATR-FTIR spectra of R3-3 particle, and (C) ATR-FTIR spectra of R3-3 particle with ~ 58% matched with polytetrafluoroethylene #4.

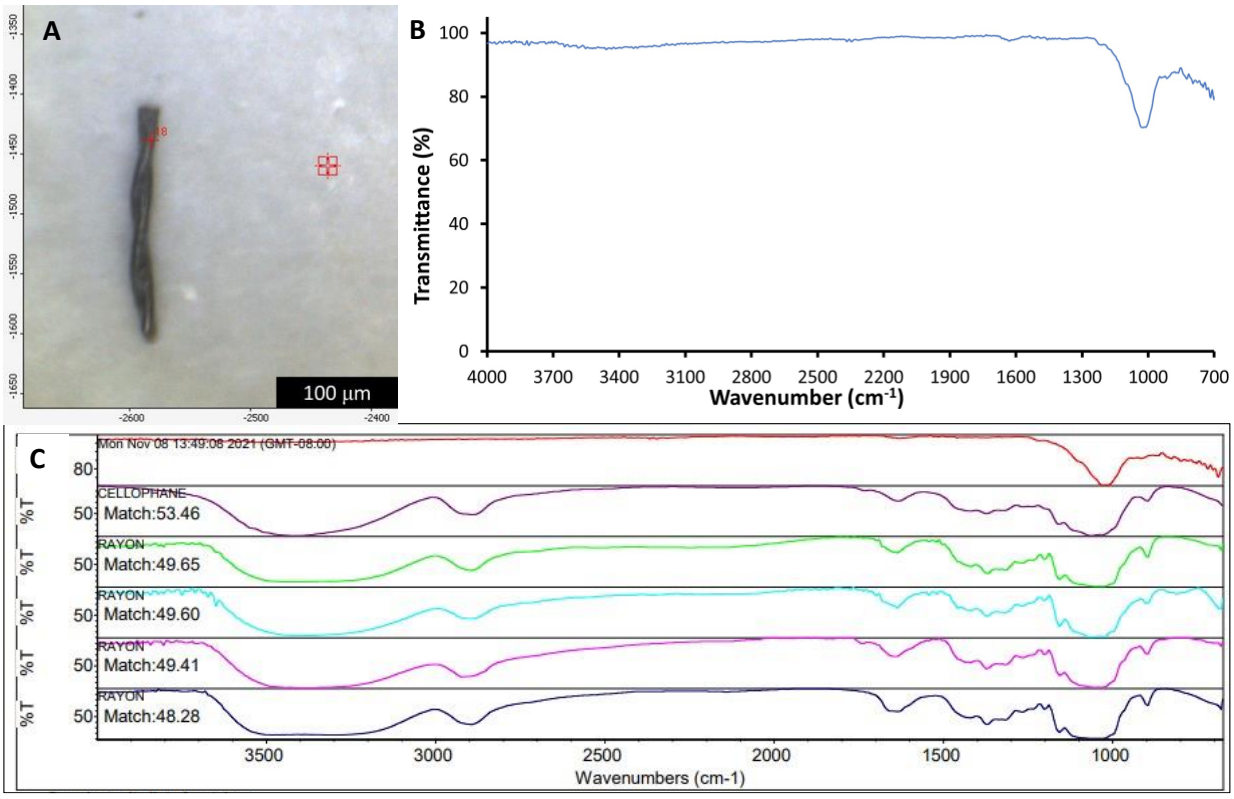

Figure A42. (A) An image of R3-4 particle found from the Rio Grande, (B) ATR-FTIR spectra of R3-4 particle, and (C) ATR-FTIR spectra of R3-4 particle with ~ 53% matched with cellophane.

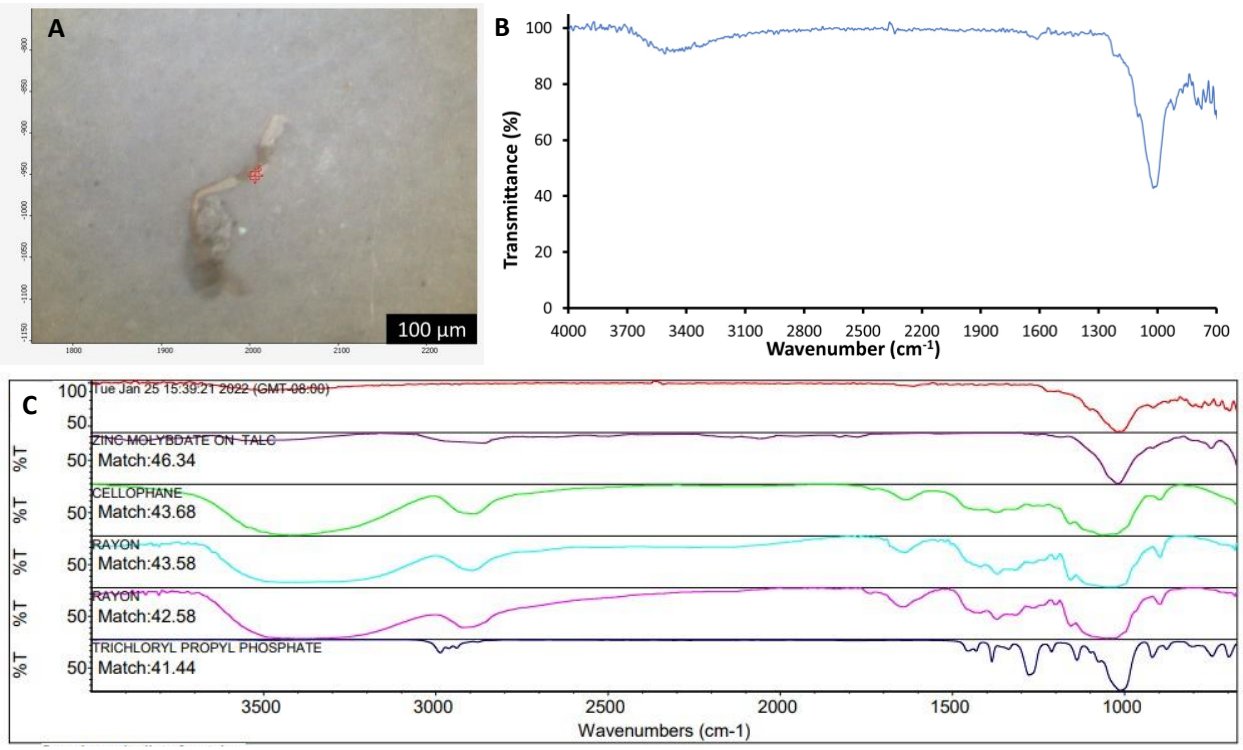

Figure A43. (A) An image of R3-5 particle found from the Rio Grande, (B) ATR-FTIR spectra of R3-5 particle, and (C) ATR-FTIR spectra of R3-5 particle with ~ 46% matched with zinc molybdate on TALC.

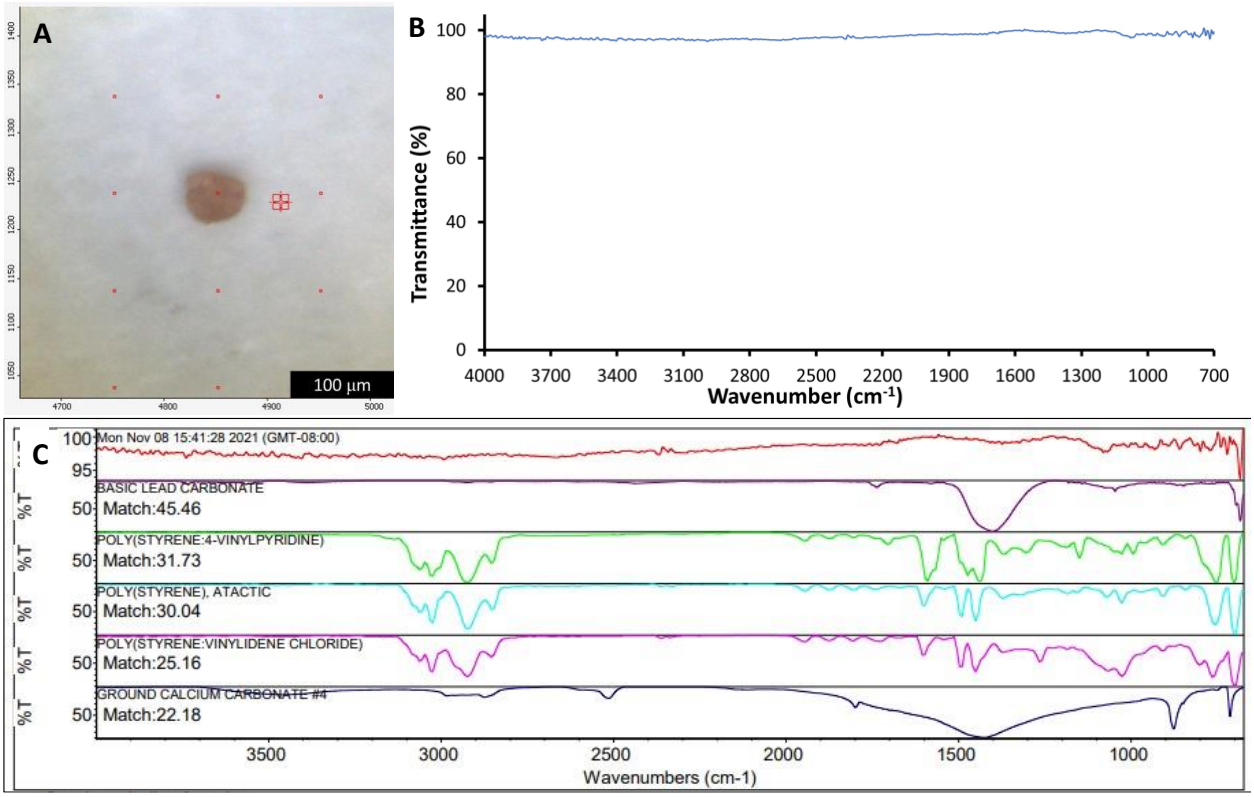

Figure A44. (A) An image of R3-6 particle found from the Rio Grande, (B) ATR-FTIR spectra of R3-6 particle, and (C) ATR-FTIR spectra of R3-6 particle with ~ 45% matched with basic lead carbonate.

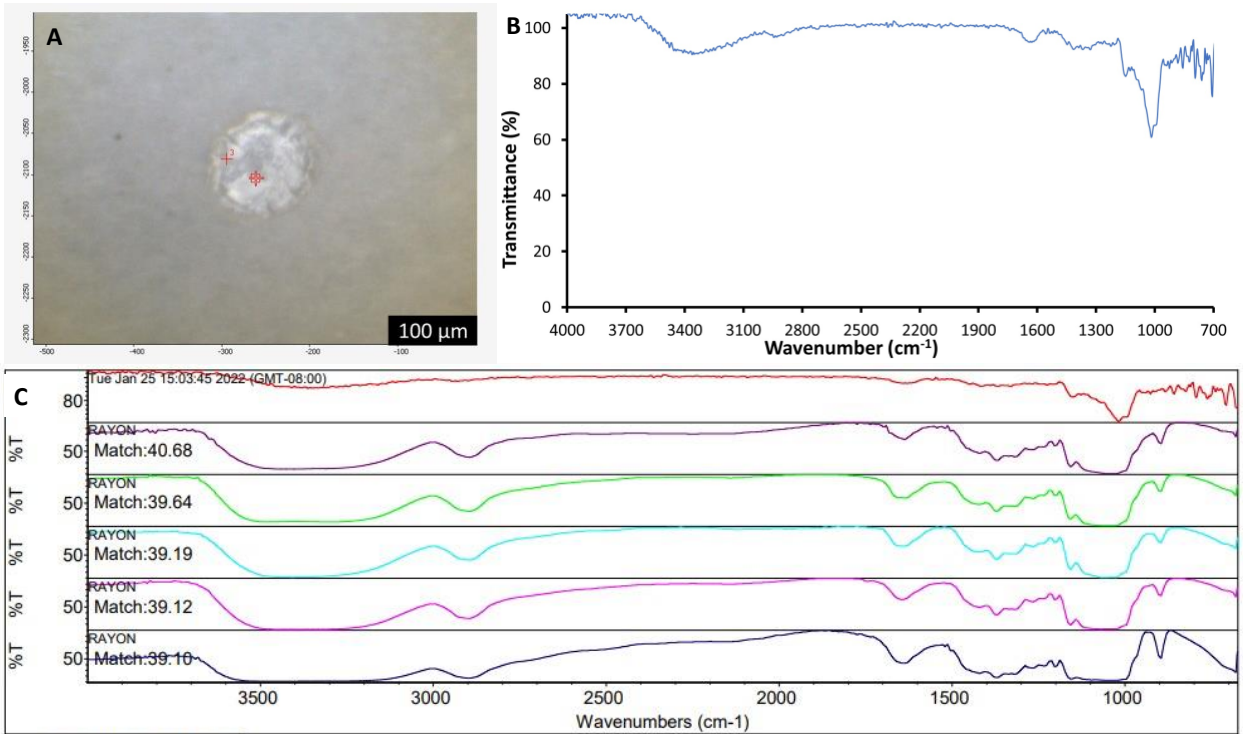

Figure A45. (A) An image of R3-7 particle found from the Rio Grande, (B) ATR-FTIR spectra of R3-7 particle, and (C) ATR-FTIR spectra of R3-7 particle with ~ 41% matched with rayon.

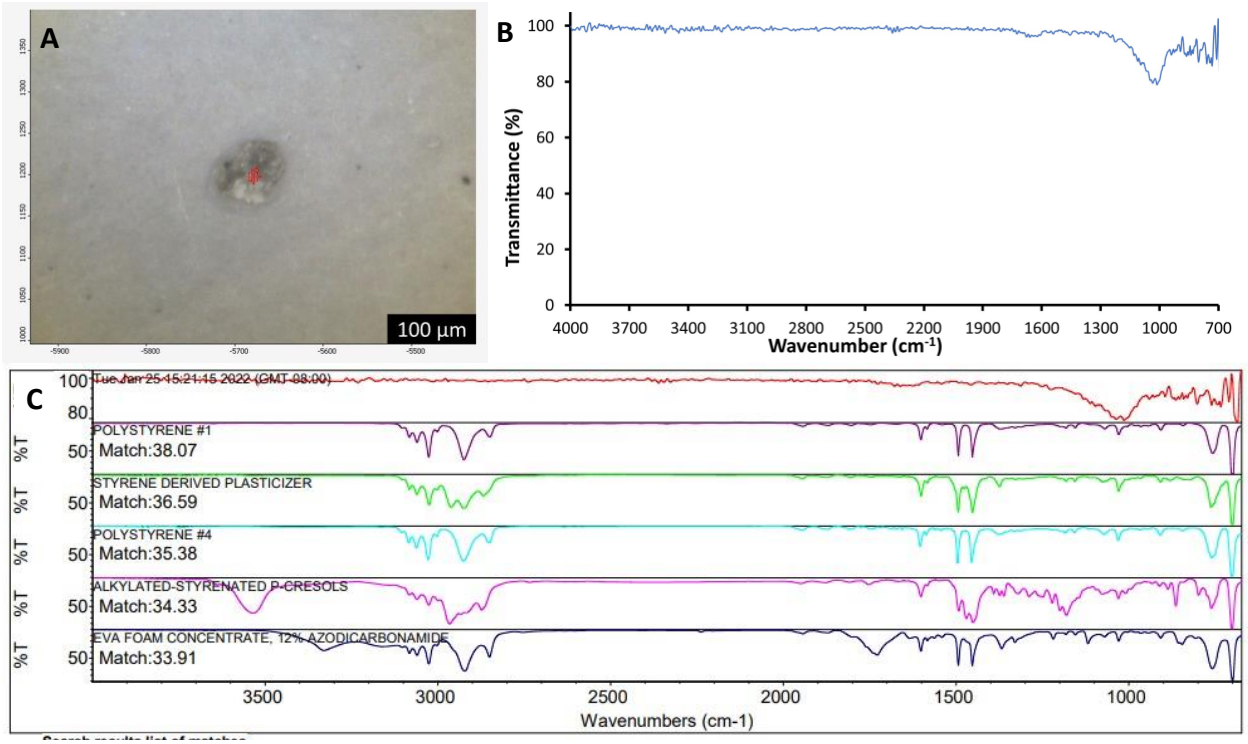

Figure A46. (A) An image of R3-8 particle found from the Rio Grande, (B) ATR-FTIR spectra of R3-8 particle, and (C) ATR-FTIR spectra of R3-8 particle with ~ 38% matched with polystyrene #1.

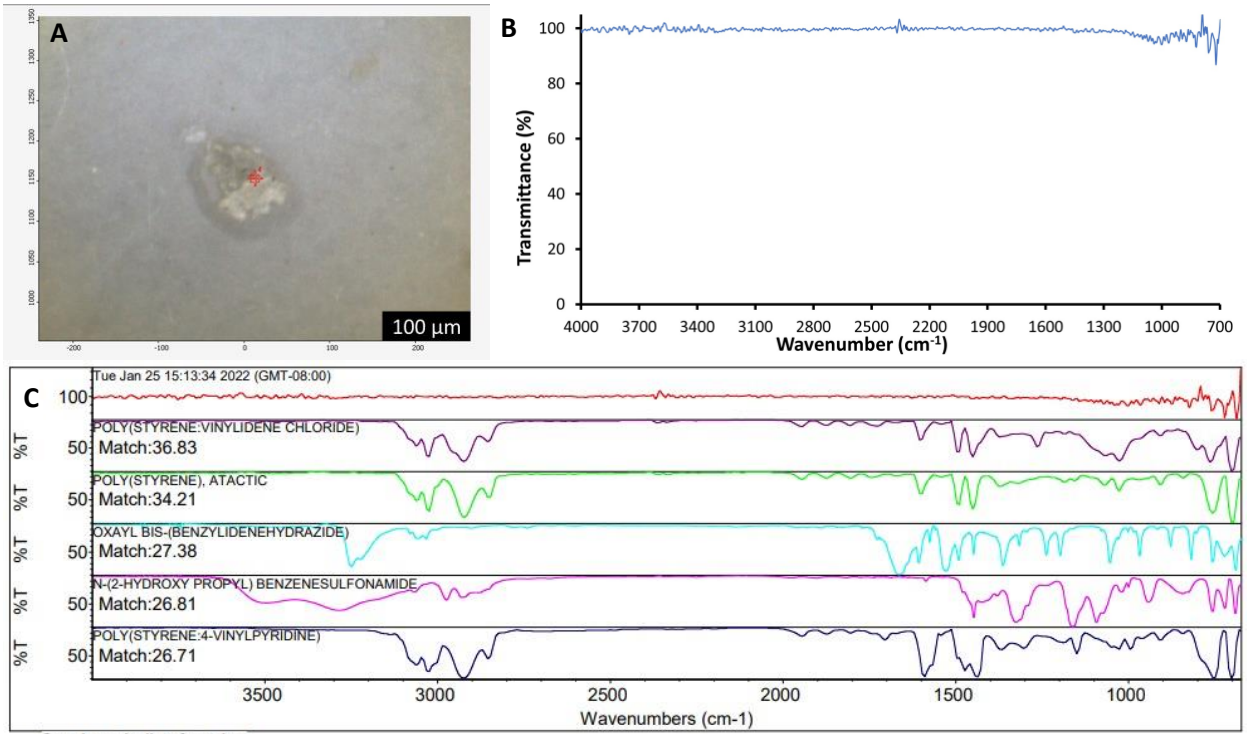

Figure A47. (A) An image of R3-9 particle found from the Rio Grande, (B) ATR-FTIR spectra of R3-9 particle, and (C) ATR-FTIR spectra of R3-9 particle with ~ 37% matched with poly(styrene:vinylidene chloride).

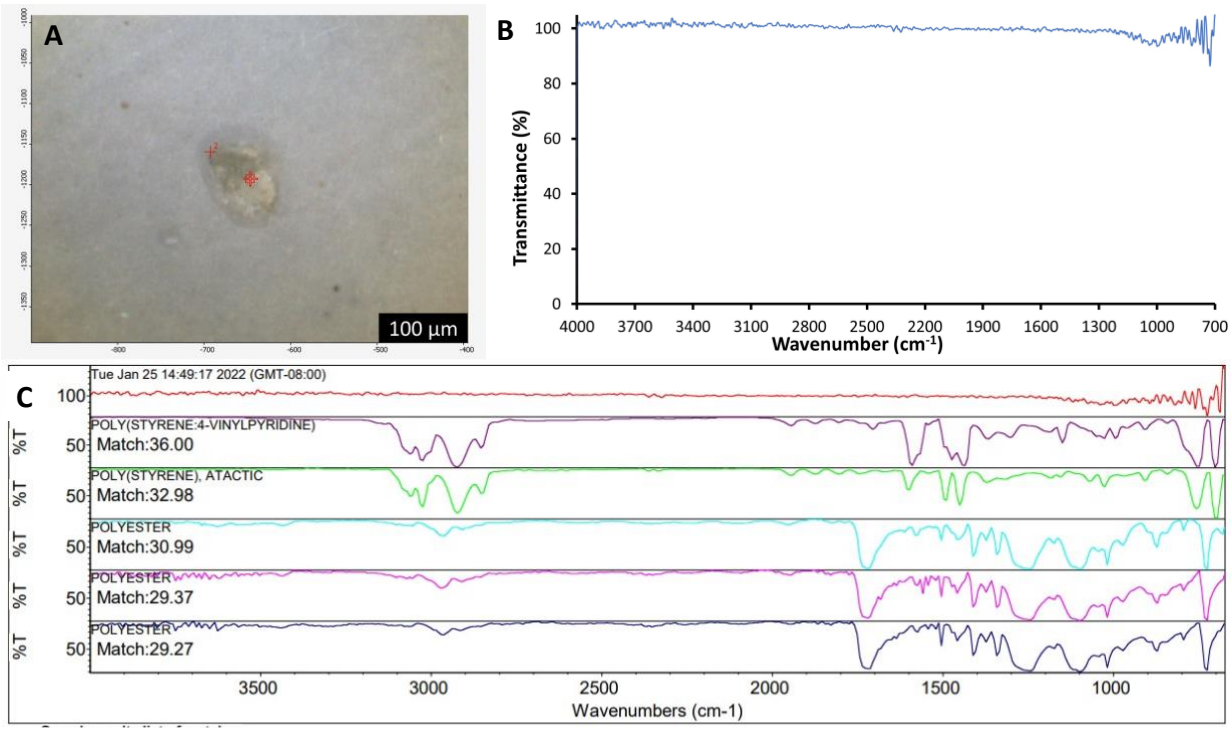

Figure A48. (A) An image of R3-10 particle found from the Rio Grande, (B) ATR-FTIR spectra of R3-10 particle, and (C) ATR-FTIR spectra of R3-10 particle with ~ 36% matched with poly(styrene:4-vinylpyridine).

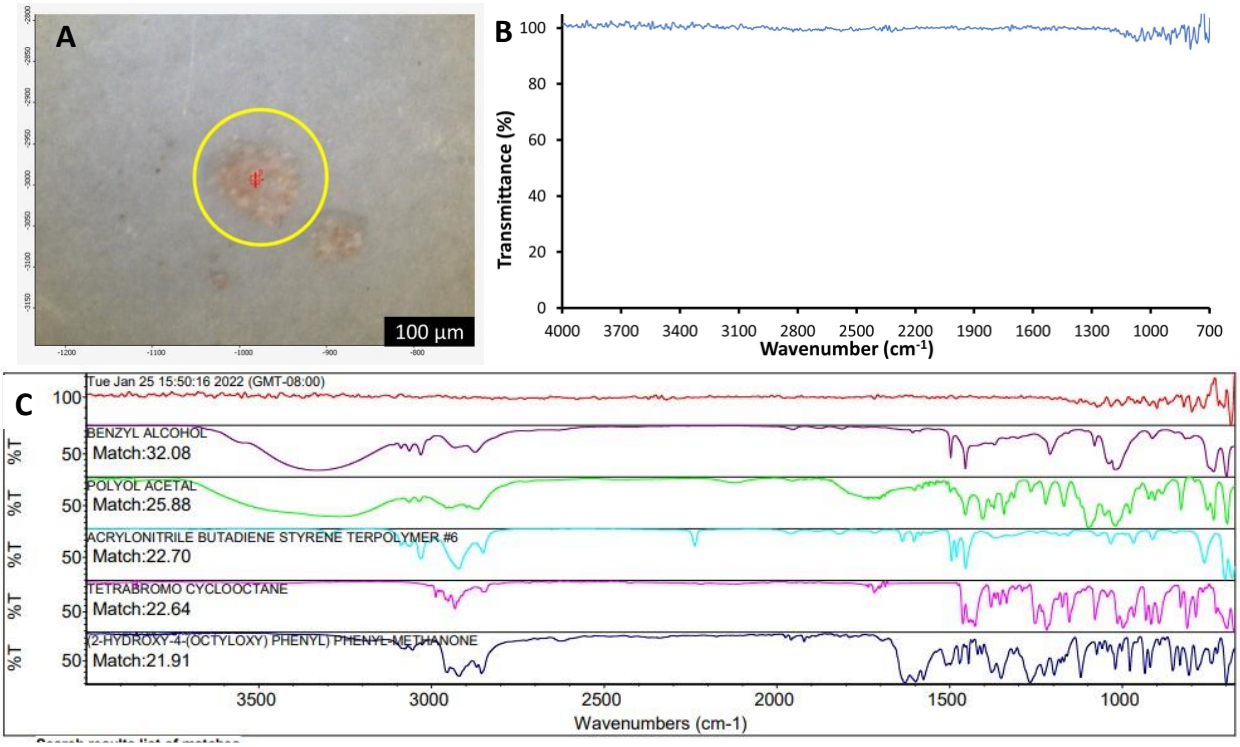

Figure A49. (A) An image of R3-11 particle found from the Rio Grande, (B) ATR-FTIR spectra of R3-11 particle, and (C) ATR-FTIR spectra of R3-11 particle with ~ 32% matched with benzyl alcohol.

Appendix B

Interfacial Interactions of U, As, and Microplastics: Influence of Precipitation Reactions

*Jasmine Quiambao[*1], Kendra Hess[4], Sloane Johnston[4], Achraf Noureddine[2], Michael Spilde[3], Adrian Brearley[3], José M. Cerrato[1], Kerry J. Howe[1], and Jorge Gonzalez-Estrella[*4]*

*Corresponding email addresses: jorgego@okstate.edu; jannequiambao@unm.edu

[1] Department of Civil Engineering, MSC01 1070, University of New Mexico, Albuquerque, New Mexico 87131, USA

[2] Department of Chemical & Biological Engineering, MSC01 1120, 1 University of New Mexico Albuquerque, NM 87131, USA

[3] Department of Earth and Planetary Sciences, MSC03 2040, University of New Mexico, Albuquerque, New Mexico 87131, USA

[4] School of Civil & Environmental Engineering, 248 Engineering North, Oklahoma State University, Stillwater, Oklahoma 74078

Summary of Supporting Information

Journal: Environmental Science and Technology

Table B1. Chemical equilibrium analyses performed on 500 mL stock solution of 0.3 mM U with 1.13 mM Na and 1.09 mM NO3 added at pH 7.

Results U Minerals Formed at pH 7

U Mineral	Log Saturation Index (SI)
Sodium-compreignacite	3.39
Schoepite	0.82
Clarkeite	0.36
Schoepite	-0.14
Rutherfordine	-1.07

Table B2. Chemical equilibrium analyses performed on 200 mL stock solution of 0.2 mM U with 0.83 mM Na and 0.89 mM NO3 added at pH 7.

Results U Minerals Formed at pH 7

U Mineral	Log Saturation Index (SI)
Sodium-compreignacite	2.56
Schoepite	0.59
Clarkeite	0.40
Schoepite	-0.40
Rutherfordine	-1.30

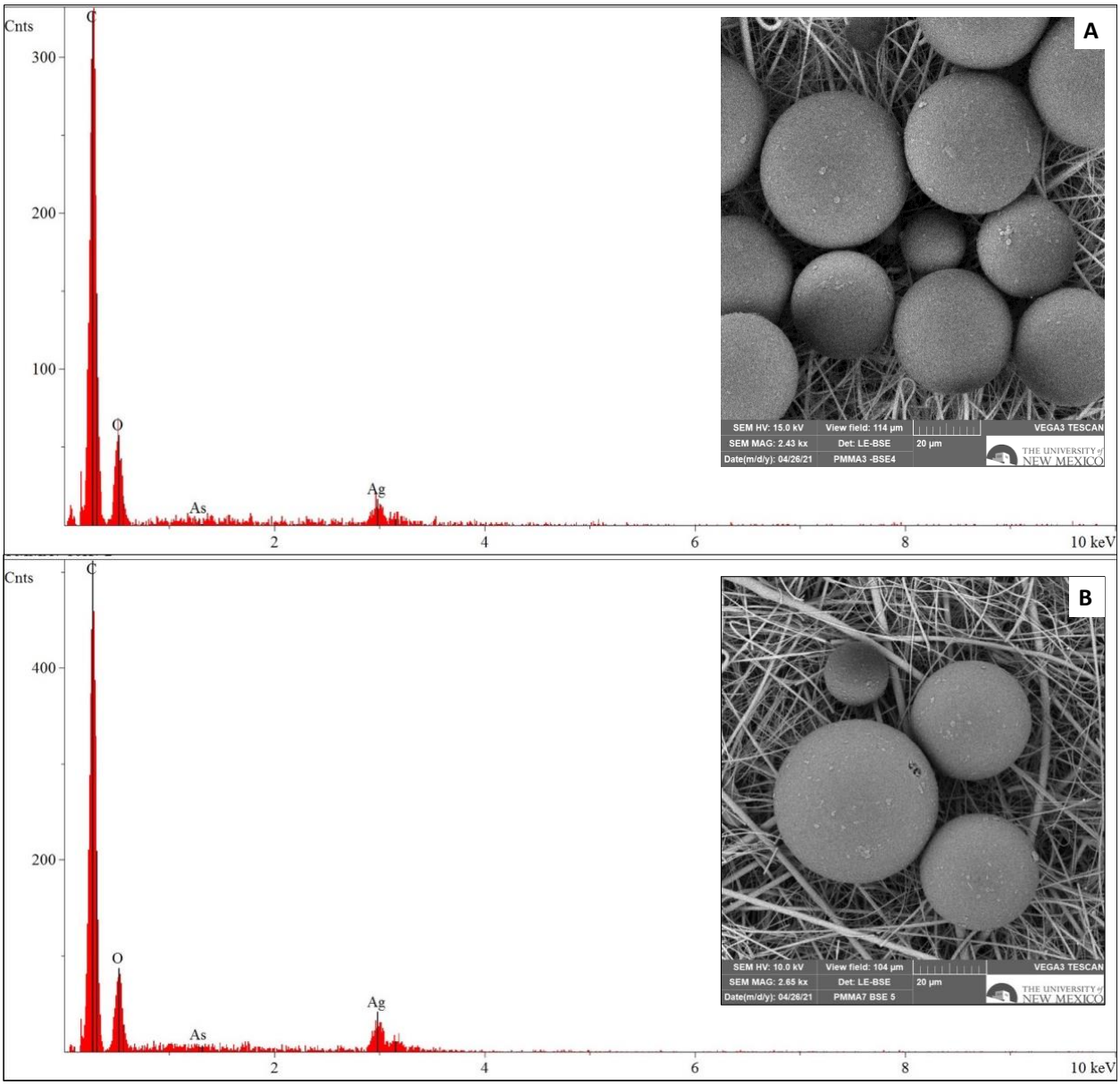

Figure B1. Backscatter (BSE)/EDS analyses of 0.2 mM As exposed to commercial PMMA at (A) pH 3 and (B) pH 7.

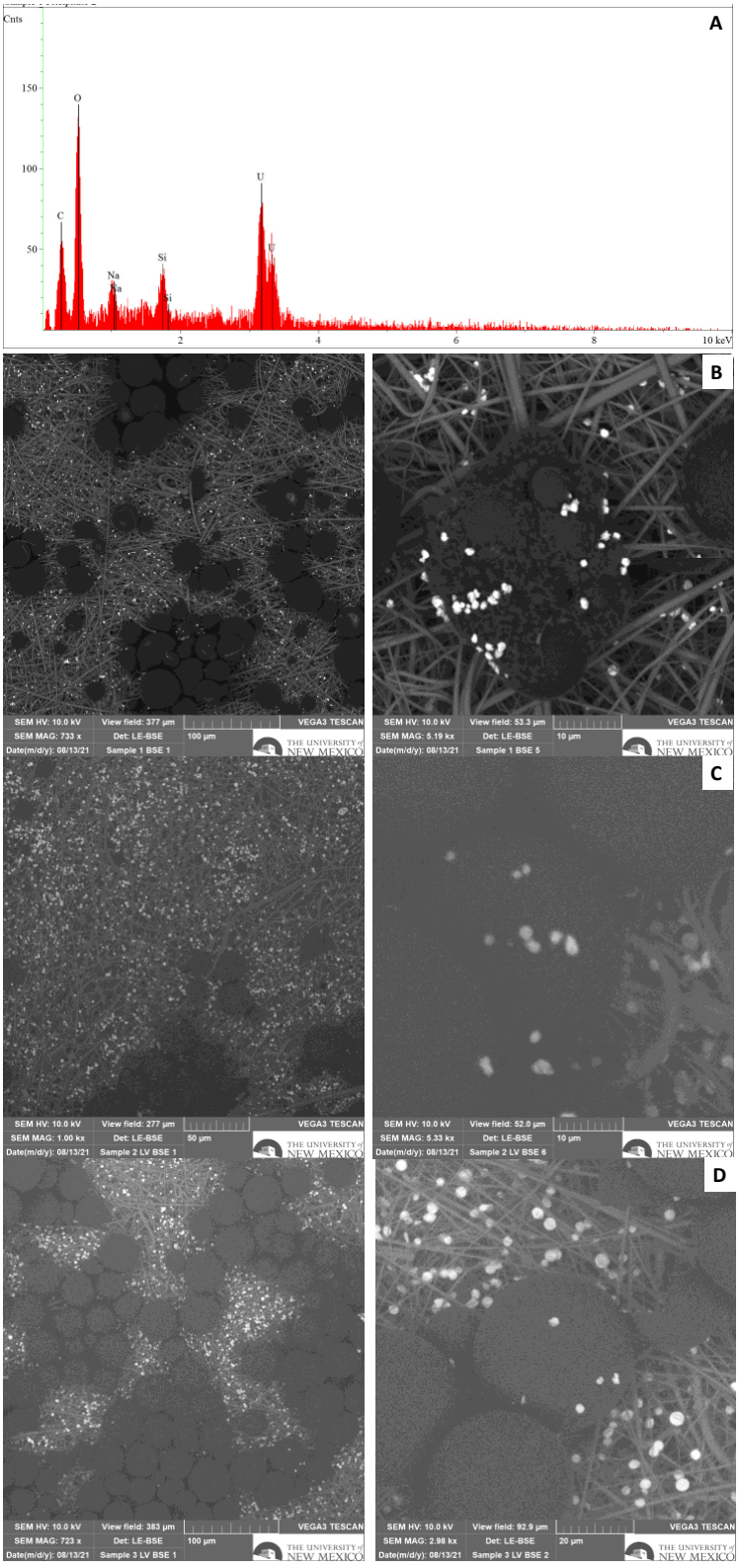

Figure B2. U exposed to PMMA at pH 7. (A) EDS spectra of U precipitate on the microplastic surface and BSE images of (B) 0.05 mM U and PMMA experiments, (C) 0.1 mM U and PMMA experiments, and (D) 0.2 mM U and PMMA experiments.

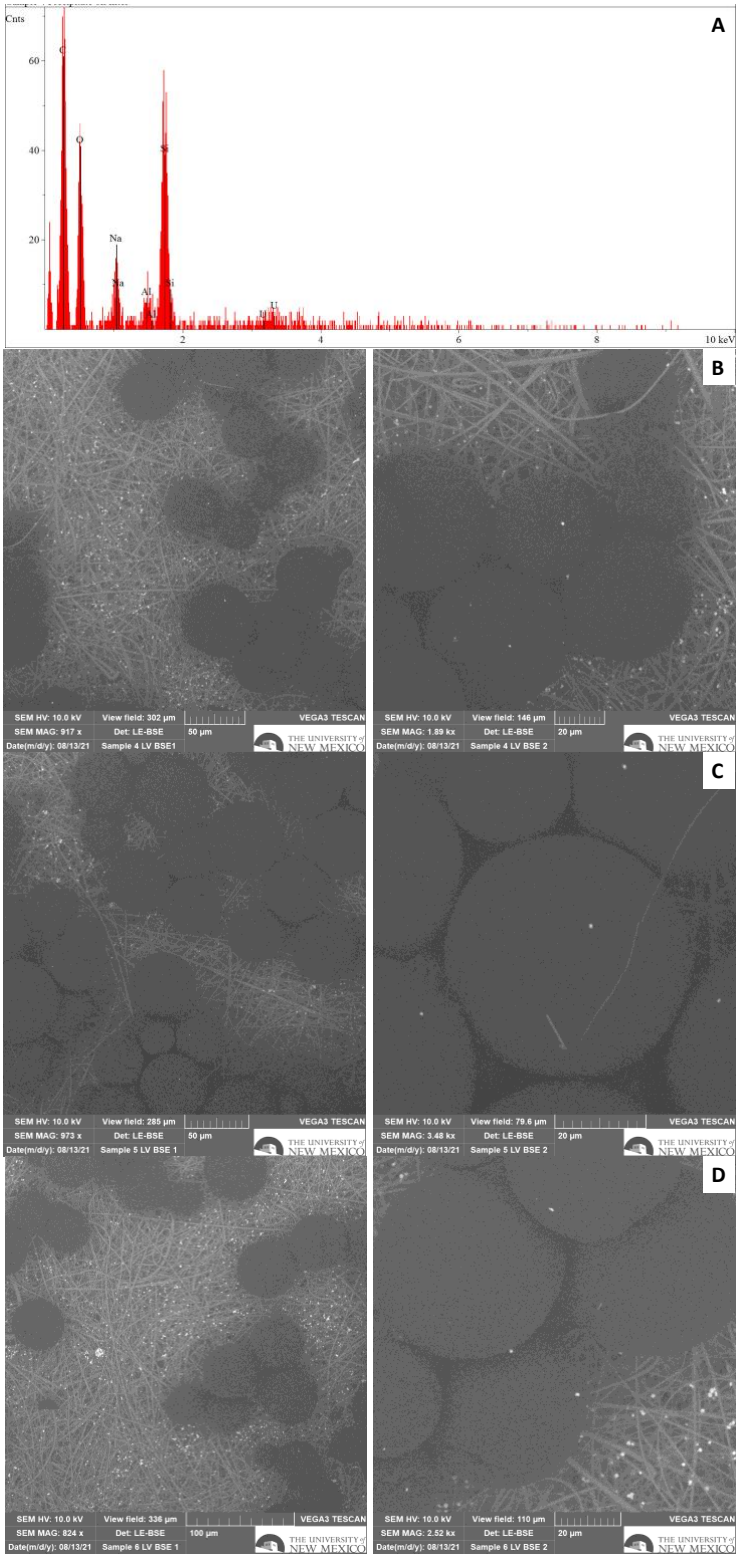

Figure B3. U exposed to PE at pH 7. (A) EDS spectra of U precipitate on the microplastic surface and BSE images of (B) 0.05 mM U and PE experiments, (C) 0.1 mM U and PE experiments, and (D) 0.2 mM U and PMMA experiments.

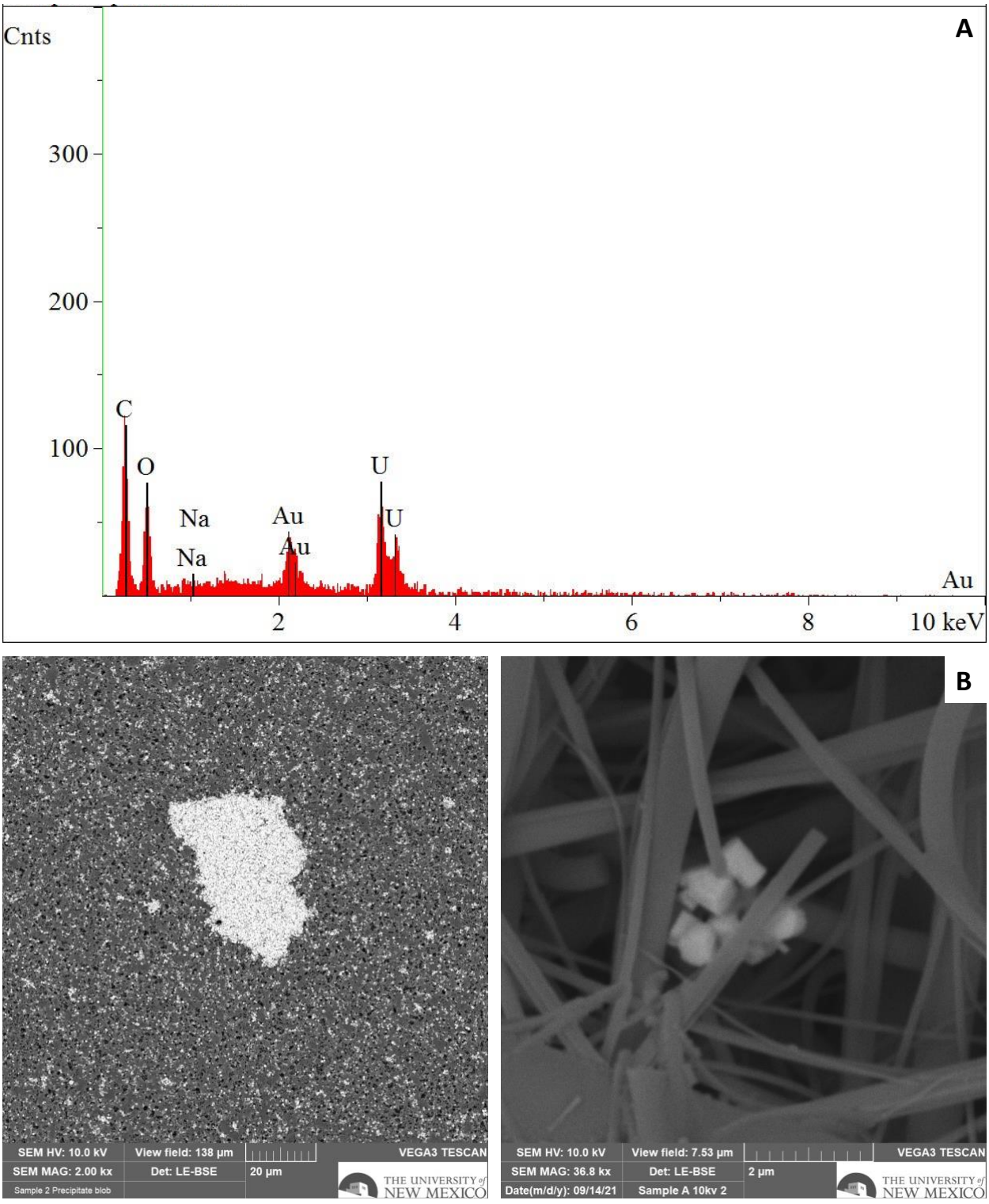

Figure B4. 0.1 mM U without microplastics at pH 7. (A) EDS spectra of U precipitate on the filter and (B) BSE images of U precipitate at 0.1 mM.

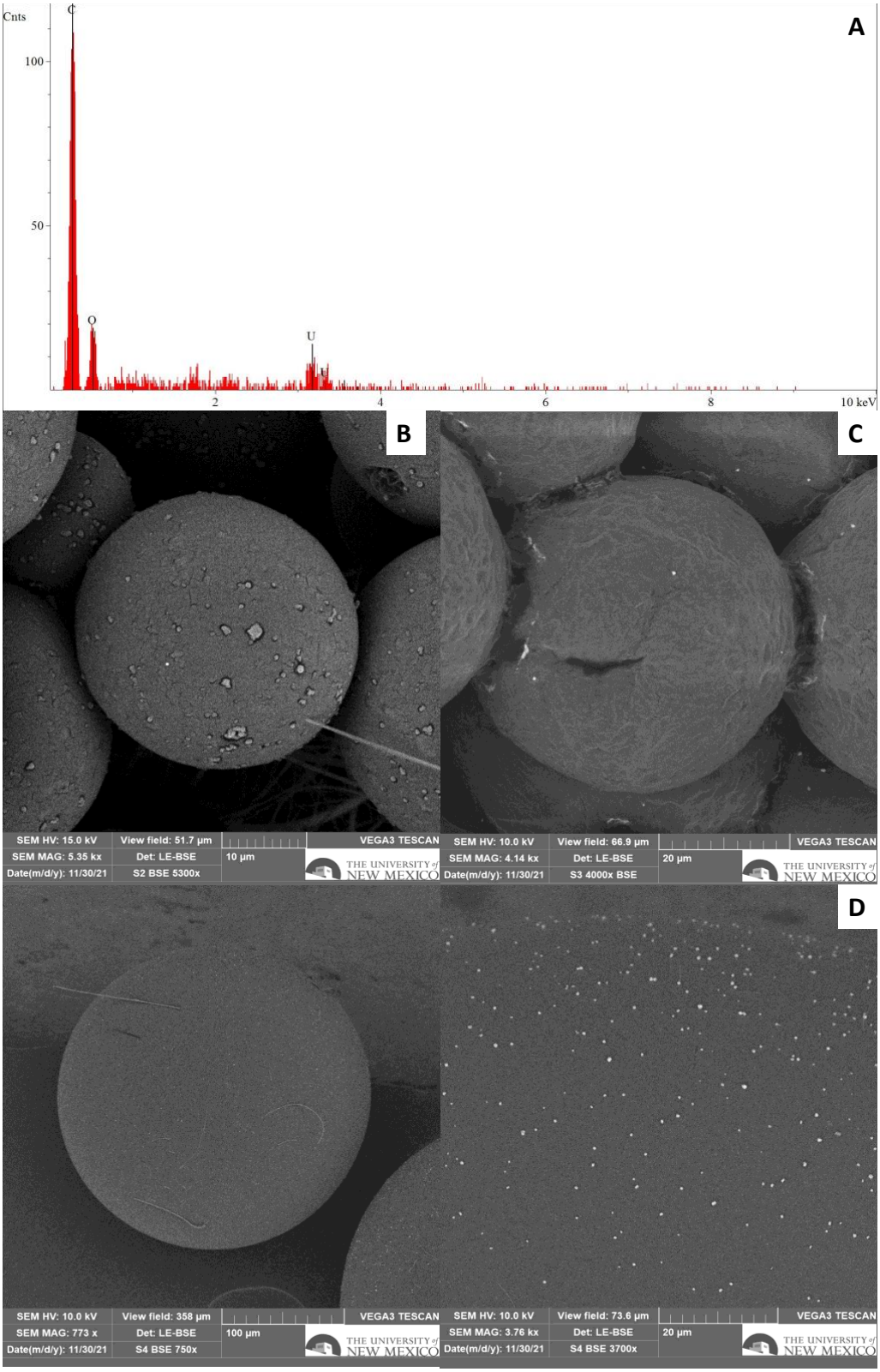

Figure B5. (A) EDS spectra of U precipitate on the microplastics surface and BSE images of 0.06 mM U exposed to (B) PMMA, (C) PE, and (D) PS.

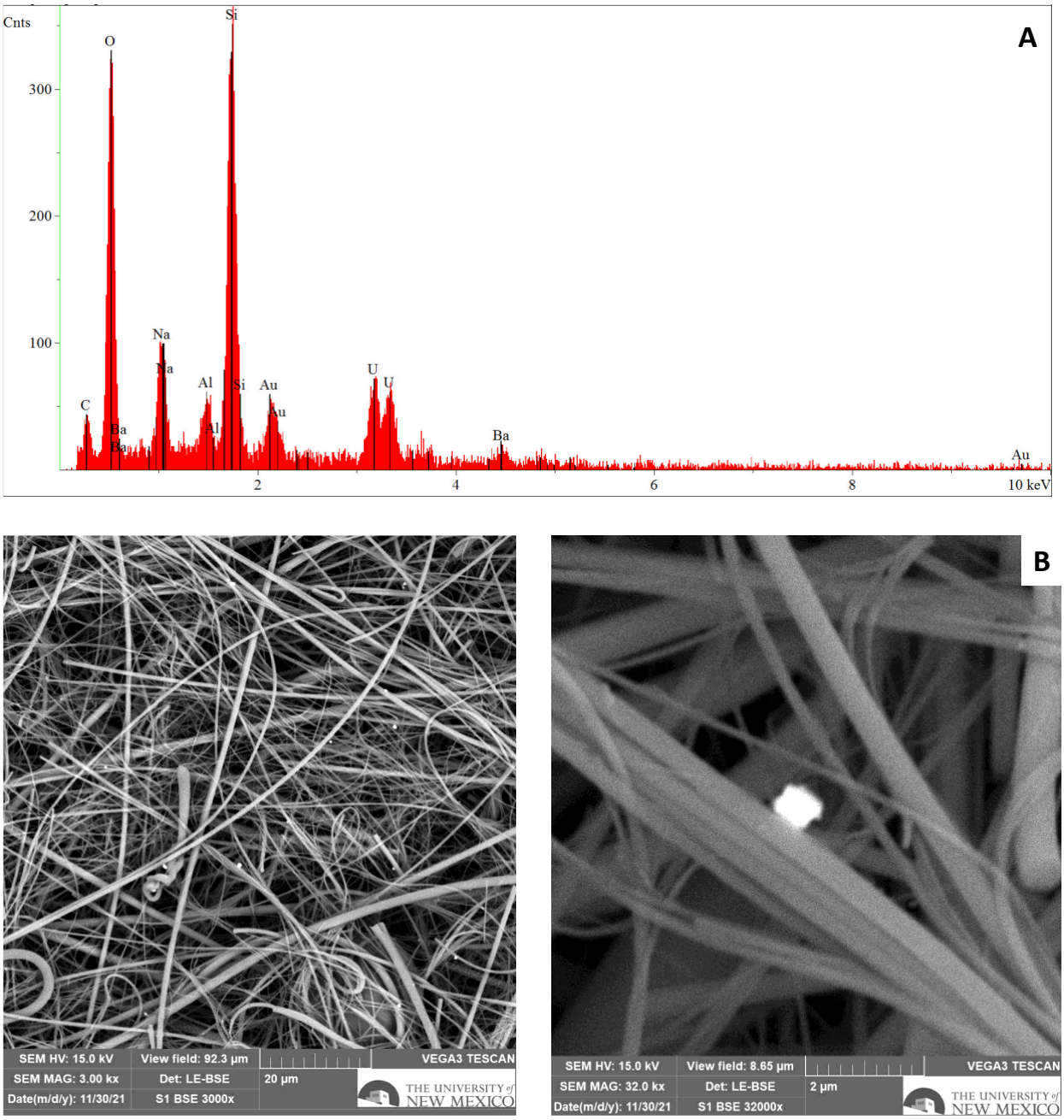

Figure B6. 0.05 mM U without microplastics at pH 7. (A) EDS spectra of U precipitate on the filter and (B) BSE images of U precipitate.

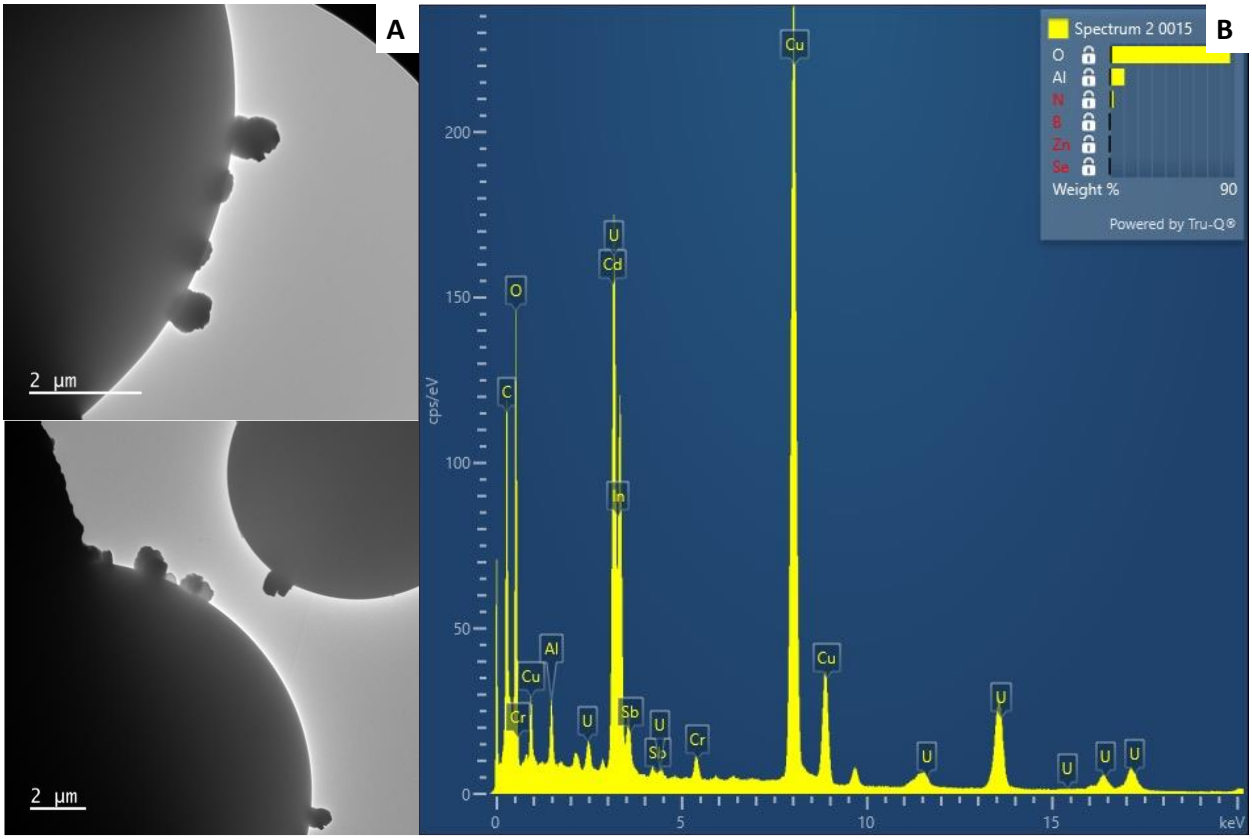

Figure B7. (A) TEM and (B) EDS images of 0.06 mM U exposed to PMMA.

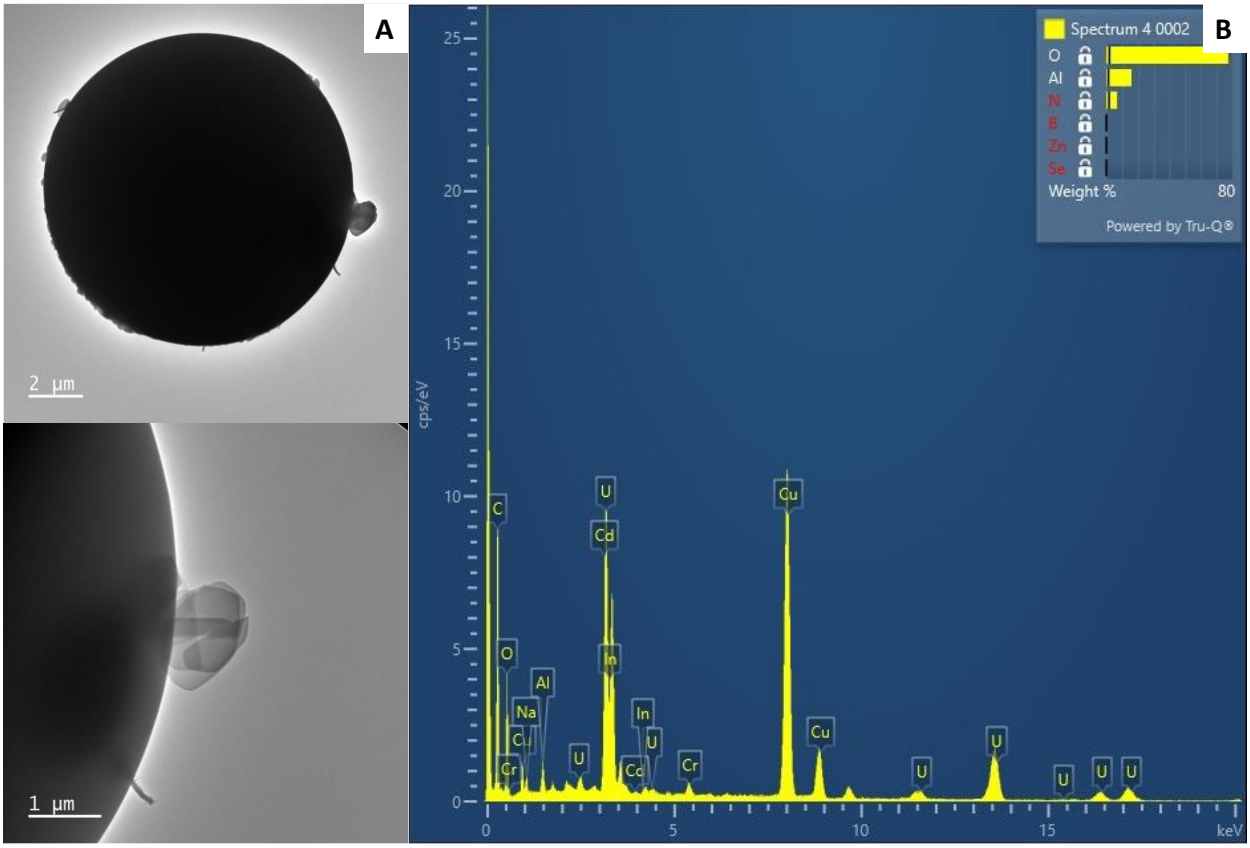

Figure B8. (A) TEM and (B) EDS images of 0.1 mM U exposed to PMMA.

References

Adamcová, D., Radziemska, M., Fronczyk, J., Zloch, J., & Vaverková, M. D. (2017). Research of the biodegradability of degradable/biodegradable plastic material in various types of environments. *Scientific Review Engineering and Environmental Sciences*, *26*(1), 3–14. https://doi.org/10.22630/PNIKS.2017.26.1.01

Ahechti, M., Benomar, M., El Alami, M., & Mendiguchía, C. (2020). Metal adsorption by microplastics in aquatic environments under controlled conditions: exposure time, pH and salinity. *International Journal of Environmental Analytical Chemistry*, *00*(00), 1–8. https://doi.org/10.1080/03067319.2020.1733546

Ali, U., Karim, K. J. B. A., & Buang, N. A. (2015). A Review of the Properties and Applications of Poly (Methyl Methacrylate) (PMMA). *Https://Doi-Org.Libproxy.Unm.Edu/10.1080/15583724.2015.1031377*, *55*(4), 678–705. https://doi.org/10.1080/15583724.2015.1031377

Allsopp, M., Walters, A., Santillo, D., & Johnston, P. (2006). *Plastic Debris in the World's Oceans*.

Andrady, A. L. (2011). Microplastics in the marine environment. *Marine Pollution Bulletin*, *62*(8), 1596–1605. https://doi.org/10.1016/J.MARPOLBUL.2011.05.030

Andrady, A. L., & Neal, M. A. (2009). *Applications and societal benefits of plastics*. https://doi.org/10.1098/rstb.2008.0304

Ateia, M., Ersan, G., Gar Alalm, M., Boffito, D. C., & Karanfil, T. (2022). Emerging investigator series: Microplastics Sources, Fate, Toxicity, Detection, and Interactions with Micropollutants in Aquatic Ecosystems – A Review of Reviews. *Environmental Science: Processes & Impacts*. https://doi.org/10.1039/d1em00443c

Barnes, D. K. A., Galgani, F., Thompson, R. C., & Barlaz, M. (2009). *Accumulation and fragmentation of plastic debris in global environments*. https://doi.org/10.1098/rstb.2008.0205

Benjamin, M. M. (2015). *Water chemistry*. Waveland Press.

Blake, J. M., Avasarala, S., Artyushkova, K., Ali, A. M. S., Brearley, A. J., Shuey, C., Robinson, W. P., Nez, C., Bill, S., Lewis, J., Hirani, C., Pacheco, J. S. L., & Cerrato, J. M. (2015). Elevated Concentrations of U and Co-occurring Metals in Abandoned Mine Wastes in a Northeastern Arizona Native American Community. *Environmental Science and Technology*, *49*(14), 8506–8514. https://doi.org/10.1021/acs.est.5b01408

Blake, J. M., De Vore, C. L., Avasarala, S., Ali, A.-M., Roldan, C., Bowers, F., Spilde, M. N., Artyushkova, K., Kirk, M. F., Peterson, E., Rodriguez-Freire, L., Jos´, J., & Cerrato, J. M. (2017). *Uranium mobility and accumulation along the Rio Paguate, Jackpile Mine in Laguna Pueblo, NM †*. https://doi.org/10.1039/c6em00612d

Blettler, M. C. M., Abrial, E., Khan, F. R., Sivri, N., & Espinola, L. A. (2018). Freshwater plastic pollution: Recognizing research biases and identifying knowledge gaps. *Water Research*, *143*, 416–424. https://doi.org/10.1016/j.watres.2018.06.015

Brennecke, D., Duarte, B., Paiva, F., Caçador, I., & Canning-Clode, J. (2016). Microplastics as vector for heavy metal contamination from the marine environment. *Estuarine, Coastal and Shelf Science*, *178*, 189–195. https://doi.org/10.1016/j.ecss.2015.12.003

Browne, M. A., & Browne, M. A. (2015). Sources and Pathways of Microplastics to Habitats. *Marine Anthropogenic Litter*, *334*, 229–244. https://doi.org/10.1007/978-3-319-16510-3_9

Carbery, M., O'Connor, W., & Palanisami, T. (2018). Trophic transfer of microplastics and mixed contaminants in the marine food web and implications for human health.

Environment International, *115*(March), 400–409. https://doi.org/10.1016/j.envint.2018.03.007

Carr, S. A., Liu, J., & Tesoro, A. G. (2016). Transport and fate of microplastic particles in wastewater treatment plants. *Water Research*, *91*, 174–182. https://doi.org/10.1016/j.watres.2016.01.002

Cheremisinoff, N. P. (1989). *Handbook of Polymer Science and Technology - Cheremisinoff - Google Books* (Nicholas P. Cheremisinoff (ed.); Vol. 1). https://books.google.com/books?hl=en&lr=&id=8r7ZMuazAw0C&oi=fnd&pg=PA341&dq=uses+of+polyethylene&ots=n3KqxmY8ss&sig=9acGkuODDizs3loaCdRuFFXyWco#v=onepage&q=uses&f=false

Choi, J. S., Jung, Y. J., Hong, N. H., Hong, S. H., & Park, J. W. (2018). Toxicological effects of irregularly shaped and spherical microplastics in a marine teleost, the sheepshead minnow (Cyprinodon variegatus). *Marine Pollution Bulletin*, *129*(1), 231–240. https://doi.org/10.1016/J.MARPOLBUL.2018.02.039

Cole, M., Lindeque, P., Halsband, C., & Galloway, T. S. (2011). Microplastics as contaminants in the marine environment: A review. *Marine Pollution Bulletin*, *62*(12), 2588–2597. https://doi.org/10.1016/J.MARPOLBUL.2011.09.025

Cox, K. D., Covernton, G. A., Davies, H. L., Dower, J. F., Juanes, F., & Dudas, S. E. (2019). Human Consumption of Microplastics. *Environmental Science and Technology*, *53*(12), 7068–7074. https://doi.org/10.1021/acs.est.9b01517

Demirors, M. (2011). The History of Polyethylene. In *100+ Years of Plastics. <break></break>Leo Baekeland and Beyond* (Vol. 1080, pp. 115-145 SE – 9). American Chemical Society. https://doi.org/doi:10.1021/bk-2011-1080.ch009

Dong, Y., Gao, M., Song, Z., & Qiu, W. (2019). Adsorption mechanism of As(III) on polytetrafluoroethylene particles of different size. *Environmental Pollution*, *254*, 112950. https://doi.org/10.1016/j.envpol.2019.07.118

Dong, Y., Gao, M., Song, Z., & Qiu, W. (2020). As(III) adsorption onto different-sized polystyrene microplastic particles and its mechanism. *Chemosphere*, *239*, 124792. https://doi.org/10.1016/j.chemosphere.2019.124792

Duis, K., & Coors, A. (2016). Microplastics in the aquatic and terrestrial environment: sources (with a specific focus on personal care products), fate and effects. *Environmental Sciences Europe*, *28*(2). https://doi.org/10.1186/s12302-015-0069-y

Eerkes-Medrano, D., Thompson, R. C., & Aldridge, D. C. (2015). Microplastics in freshwater systems: A review of the emerging threats, identification of knowledge gaps and prioritisation of research needs. *Water Research*, *75*, 63–82. https://doi.org/10.1016/j.watres.2015.02.012

Espinosa, C., Cuesta, A., & Esteban, M. Á. (2017). Effects of dietary polyvinylchloride microparticles on general health, immune status and expression of several genes related to stress in gilthead seabream (Sparus aurata L.). *Fish & Shellfish Immunology*, *68*, 251–259. https://doi.org/10.1016/J.FSI.2017.07.006

Febrianto, J., Kosasih, A. N., Sunarso, J., Ju, Y. H., Indraswati, N., & Ismadji, S. (2009). Equilibrium and kinetic studies in adsorption of heavy metals using biosorbent: A summary of recent studies. *Journal of Hazardous Materials*, *162*(2–3), 616–645. https://doi.org/10.1016/j.jhazmat.2008.06.042

Fu, W., Min, J., Jiang, W., Li, Y., & Zhang, W. (2020). Separation, characterization and identification of microplastics and nanoplastics in the environment. *Science of the Total*

Environment, *721*, 137561. https://doi.org/10.1016/j.scitotenv.2020.137561

Fu, Z., & Wang, J. (2019). Current practices and future perspectives of microplastic pollution in freshwater ecosystems in China. *Science of the Total Environment*, *691*, 697–712. https://doi.org/10.1016/j.scitotenv.2019.07.167

Gao, X., Hassan, I., Peng, Y., Huo, S., & Ling, L. (2021). Behaviors and influencing factors of the heavy metals adsorption onto microplastics: A review. *Journal of Cleaner Production*, *319*(August), 128777. https://doi.org/10.1016/j.jclepro.2021.128777

Geyer, R., Jambeck, J. R., & Law, K. L. (2017). Production, use, and fate of all plastics ever made. *Science Advances*, *3*(7). https://doi.org/10.1126/SCIADV.1700782/SUPPL_FILE/1700782_SM.PDF

Godoy, V., Blázquez, G., Calero, M., Quesada, L., & Martín-Lara, M. A. (2019). The potential of microplastics as carriers of metals. *Environmental Pollution*, *255*. https://doi.org/10.1016/j.envpol.2019.113363

Gonzalez-Estrella, J., Meza, I., Burns, A. J., Ali, A. M. S., Lezama-Pacheco, J. S., Lichtner, P., Shaikh, N., Fendorf, S., & Cerrato, J. M. (2020). Effect of Bicarbonate, Calcium, and pH on the Reactivity of As(V) and U(VI) Mixtures. *Environmental Science and Technology*, *54*(7), 3979–3987. https://doi.org/10.1021/acs.est.9b06063

Gorman-Lewis, D., Burns, P. C., & Fein, J. B. (2008). Review of uranyl mineral solubility measurements. *Journal of Chemical Thermodynamics*, *40*(3), 335–352. https://doi.org/10.1016/j.jct.2007.12.004

Gorman-Lewis, D., Fein, J. B., Burns, P. C., Szymanowski, J. E. S., & Converse, J. (2008). Solubility measurements of the uranyl oxide hydrate phases metaschoepite, compreignacite, Na-compreignacite, becquerelite, and clarkeite. *Journal of Chemical Thermodynamics*,

40(6), 980–990. https://doi.org/10.1016/j.jct.2008.02.006

Greven, A. C., Merk, T., Karagöz, F., Mohr, K., Klapper, M., Jovanović, B., & Palić, D. (2016). Polycarbonate and polystyrene nanoplastic particles act as stressors to the innate immune system of fathead minnow (Pimephales promelas). *Environmental Toxicology and Chemistry*, *35*(12), 3093–3100. https://doi.org/10.1002/ETC.3501

Harrison, J. P., Hoellein, T. J., Sapp, M., Tagg, A. S., Ju-Nam, Y., & Ojeda, J. J. (2018). Microplastic-associated biofilms: A comparison of freshwater and marine environments. In *Handbook of Environmental Chemistry* (Vol. 58). https://doi.org/10.1007/978-3-319-61615-5_9

Hauser, R., Calafat, A. M., & Hauser, A. R. (2005). PHTHALATES AND HUMAN HEALTH. *Environ Med*. https://doi.org/10.1136/oem.2004.017590

Holmes, L. A., Turner, A., & Thompson, R. C. (2012). Adsorption of trace metals to plastic resin pellets in the marine environment. *Environmental Pollution*, *160*(1), 42–48. https://doi.org/10.1016/j.envpol.2011.08.052

Holmes, L. A., Turner, A., & Thompson, R. C. (2014). Interactions between trace metals and plastic production pellets under estuarine conditions. *Marine Chemistry*, *167*, 25–32. https://doi.org/10.1016/j.marchem.2014.06.001

Horton, A. A., & Barnes, D. K. A. (2020). Microplastic pollution in a rapidly changing world: Implications for remote and vulnerable marine ecosystems. *Science of the Total Environment*, *738*, 140349. https://doi.org/10.1016/j.scitotenv.2020.140349

Horton, A. A., Walton, A., Spurgeon, D. J., Lahive, E., & Svendsen, C. (2017). Microplastics in freshwater and terrestrial environments: Evaluating the current understanding to identify the knowledge gaps and future research priorities. *Science of the Total Environment*, *586*, 127–

141. https://doi.org/10.1016/j.scitotenv.2017.01.190

Kanematsu, M., Perdrial, N., Um, W., Chorover, J., & O'Day, P. A. (2014). Influence of phosphate and silica on U(VI) precipitation from acidic and neutralized wastewaters. *Environmental Science and Technology*, *48*(11), 6097–6106. https://doi.org/10.1021/es4056559

Kataoka, T., Nihei, Y., Kudou, K., & Hinata, H. (2019). Assessment of the sources and inflow processes of microplastics in the river environments of Japan. *Environmental Pollution*, *244*, 958–965. https://doi.org/10.1016/j.envpol.2018.10.111

Koelmans, A. A., Mohamed Nor, N. H., Hermsen, E., Kooi, M., Mintenig, S. M., & De France, J. (2019). Microplastics in freshwaters and drinking water: Critical review and assessment of data quality. *Water Research*, *155*, 410–422. https://doi.org/10.1016/j.watres.2019.02.054

Lee, A., Mondon, J., Merenda, A., Dumée, L. F., & Callahan, D. L. (2021). Surface adsorption of metallic species onto microplastics with long-term exposure to the natural marine environment. *Science of the Total Environment*, *780*. https://doi.org/10.1016/j.scitotenv.2021.146613

Lei, L., Wu, S., Lu, S., Liu, M., Song, Y., Fu, Z., Shi, H., Raley-Susman, K. M., & He, D. (2018). Microplastic particles cause intestinal damage and other adverse effects in zebrafish Danio rerio and nematode Caenorhabditis elegans. *Science of The Total Environment*, *619–620*, 1–8. https://doi.org/10.1016/J.SCITOTENV.2017.11.103

Lewis, J., Hoover, J., & MacKenzie, D. (2017). Mining and Environmental Health Disparities in Native American Communities. *Current Environmental Health Reports*, *4*(2), 130–141. https://doi.org/10.1007/s40572-017-0140-5

Li, C., Busquets, R., & Campos, L. C. (2020). Assessment of microplastics in freshwater systems: A review. *Science of the Total Environment*, *707*, 135578. https://doi.org/10.1016/j.scitotenv.2019.135578

Li, Jia, Zhang, K., & Zhang, H. (2018). Adsorption of antibiotics on microplastics. *Environmental Pollution*, *237*, 460–467. https://doi.org/10.1016/J.ENVPOL.2018.02.050

Li, Jingyi, Liu, H., & Paul Chen, J. (2018). Microplastics in freshwater systems: A review on occurrence, environmental effects, and methods for microplastics detection. *Water Research*, *137*, 362–374. https://doi.org/10.1016/j.watres.2017.12.056

Li, L., Geng, S., Wu, C., Song, K., Sun, F., Visvanathan, C., Xie, F., & Wang, Q. (2019). Microplastics contamination in different trophic state lakes along the middle and lower reaches of Yangtze River Basin. *Environmental Pollution*, *254*, 112951. https://doi.org/10.1016/j.envpol.2019.07.119

Liu, X., Zheng, M., Wang, L., Ke, R., Lou, Y., Zhang, X., Dong, X., & Zhang, Y. (2018). Sorption behaviors of tris-(2,3-dibromopropyl) isocyanurate and hexabromocyclododecanes on polypropylene microplastics. *Marine Pollution Bulletin*, *135*, 581–586. https://doi.org/10.1016/J.MARPOLBUL.2018.07.061

Lu, Y., Zhang, Y., Deng, Y., Jiang, W., Zhao, Y., Geng, J., Ding, L., & Ren, H. (2016). *Uptake and Accumulation of Polystyrene Microplastics in Zebrafish (Danio rerio) and Toxic Effects in Liver*. https://doi.org/10.1021/acs.est.6b00183

Luís, L. G., Ferreira, P., Fonte, E., Oliveira, M., & Guilhermino, L. (2015). Does the presence of microplastics influence the acute toxicity of chromium(VI) to early juveniles of the common goby (Pomatoschistus microps)? A study with juveniles from two wild estuarine populations. *Aquatic Toxicology*, *164*, 163–174.

https://doi.org/10.1016/J.AQUATOX.2015.04.018

Luo, W., Su, L., Craig, N. J., Du, F., Wu, C., & Shi, H. (2019). Comparison of microplastic pollution in different water bodies from urban creeks to coastal waters. *Environmental Pollution*, *246*, 174–182. https://doi.org/10.1016/J.ENVPOL.2018.11.081

Lwanga, E. H., Mendoza Vega, J., Quej, V. K., De Los, J., Chi, A., Sanchez Del Cid, L., Chi, C., Segura, G. E., Gertsen, H., Salánki, T., Van Der Ploeg, M., Koelmans, A. A., & Geissen, V. (2017). *Field evidence for transfer of plastic debris along a terrestrial food chain*. https://doi.org/10.1038/s41598-017-14588-2

Mao, R., Lang, M., Yu, X., Wu, R., Yang, X., & Guo, X. (2020). Aging mechanism of microplastics with UV irradiation and its effects on the adsorption of heavy metals. *Journal of Hazardous Materials*, *393*(February), 122515. https://doi.org/10.1016/j.jhazmat.2020.122515

Microplastics in drinking-water. (2019).

Munier, B., & Bendell, L. I. (2018). Macro and micro plastics sorb and desorb metals and act as a point source of trace metals to coastal ecosystems. *PLoS ONE*, *13*(2), 1–13. https://doi.org/10.1371/journal.pone.0191759

Naqash, N., Prakash, S., Kapoor, D., & Singh, R. (2020). Interaction of freshwater microplastics with biota and heavy metals: a review. *Environmental Chemistry Letters*, *18*(6), 1813–1824. https://doi.org/10.1007/s10311-020-01044-3

National Primary Drinking Water Regulations | Ground Water and Drinking Water | US EPA. (n.d.). Retrieved May 28, 2021, from https://www.epa.gov/ground-water-and-drinking-water/national-primary-drinking-water-regulations

Nuelle, M. T., Dekiff, J. H., Remy, D., & Fries, E. (2014). A new analytical approach for

monitoring microplastics in marine sediments. *Environmental Pollution*, *184*, 161–169. https://doi.org/10.1016/j.envpol.2013.07.027

O'Brine, T., & Thompson, R. C. (2010). Degradation of plastic carrier bags in the marine environment. *Marine Pollution Bulletin*, *60*(12), 2279–2283. https://doi.org/10.1016/j.marpolbul.2010.08.005

Rochman, C. M., Hentschel, B. T., & The, S. J. (2014). Long-term sorption of metals is similar among plastic types: Implications for plastic debris in aquatic environments. *PLoS ONE*, *9*(1). https://doi.org/10.1371/journal.pone.0085433

Rodrigues, M. O., Abrantes, N., Gonçalves, F. J. M., Nogueira, H., Marques, J. C., & Gonçalves, A. M. M. (2018). Spatial and temporal distribution of microplastics in water and sediments of a freshwater system (Antuã River, Portugal). *Science of the Total Environment*, *633*, 1549–1559. https://doi.org/10.1016/j.scitotenv.2018.03.233

Schymanski, D., Goldbeck, C., Humpf, H. U., & Fürst, P. (2018). Analysis of microplastics in water by micro-Raman spectroscopy: Release of plastic particles from different packaging into mineral water. *Water Research*, *129*, 154–162. https://doi.org/10.1016/j.watres.2017.11.011

Smedley, P. L., & Kinniburgh, D. G. (2002). A review of the source, behaviour and distribution of arsenic in natural waters. *Applied Geochemistry*, *17*(5), 517–568. https://doi.org/10.1016/S0883-2927(02)00018-5

Song, Y. K., Hong, S. H., Jang, M., Han, G. M., Rani, M., Lee, J., & Shim, W. J. (2015a). A comparison of microscopic and spectroscopic identification methods for analysis of microplastics in environmental samples. *Marine Pollution Bulletin*, *93*(1–2), 202–209. https://doi.org/10.1016/j.marpolbul.2015.01.015

Song, Y. K., Hong, S. H., Jang, M., Han, G. M., Rani, M., Lee, J., & Shim, W. J. (2015b). A comparison of microscopic and spectroscopic identification methods for analysis of microplastics in environmental samples. *Marine Pollution Bulletin*, *93*(1–2), 202–209. https://doi.org/10.1016/j.marpolbul.2015.01.015

Sruthy, S., & Ramasamy, E. V. (2017). Microplastic pollution in Vembanad Lake, Kerala, India: The first report of microplastics in lake and estuarine sediments in India. *Environmental Pollution*, *222*, 315–322. https://doi.org/10.1016/j.envpol.2016.12.038

Su, L., Cai, H., Kolandhasamy, P., Wu, C., Rochman, C. M., & Shi, H. (2018). Using the Asian clam as an indicator of microplastic pollution in freshwater ecosystems. *Environmental Pollution*, *234*, 347–355. https://doi.org/10.1016/J.ENVPOL.2017.11.075

Su, L., Xue, Y., Li, L., Yang, D., Kolandhasamy, P., Li, D., & Shi, H. (2016). Microplastics in Taihu Lake, China. *Environmental Pollution*, *216*, 711–719. https://doi.org/10.1016/J.ENVPOL.2016.06.036

Tourinho, P. S., Kočí, V., Loureiro, S., & van Gestel, C. A. M. (2019). Partitioning of chemical contaminants to microplastics: Sorption mechanisms, environmental distribution and effects on toxicity and bioaccumulation. *Environmental Pollution*, *252*, 1246–1256. https://doi.org/10.1016/j.envpol.2019.06.030

Trainic, M., Flores, J. M., Pinkas, I., Pedrotti, M. L., Lombard, F., Bourdin, G., Gorsky, G., Boss, E., Rudich, Y., Vardi, A., & Koren, I. (2020). Airborne microplastic particles detected in the remote marine atmosphere. *Communications Earth & Environment*, *1*(1), 1–9. https://doi.org/10.1038/s43247-020-00061-y

Triebskorn, R., Braunbeck, T., Grummt, T., Hanslik, L., Huppertsberg, S., Jekel, M., Knepper, T. P., Krais, S., Müller, Y. K., Pittroff, M., Ruhl, A. S., Schmieg, H., Schür, C., Strobel, C.,

Wagner, M., Zumbülte, N., & Köhler, H. R. (2019). Relevance of nano- and microplastics for freshwater ecosystems: A critical review. *TrAC - Trends in Analytical Chemistry*, *110*, 375–392. https://doi.org/10.1016/j.trac.2018.11.023

Turner, A., & Holmes, L. A. (2015). Adsorption of trace metals by microplastic pellets in fresh water. *Environmental Chemistry*, *12*(5), 600–610. https://doi.org/10.1071/EN14143

Veerappapillai, S., & Muthukumar, A. (2015). Biodegradation of Plastics-A Brief Review. *International Journal of Pharmaceutical Sciences Review and Research*, *31*(2), 204–209. www.globalresearchonline.net

Verla, A. W., Enyoh, C. E., Verla, E. N., & Nwarnorh, K. O. (2019). Microplastic–toxic chemical interaction: a review study on quantified levels, mechanism and implication. *SN Applied Sciences*, *1*(11), 1–30. https://doi.org/10.1007/s42452-019-1352-0

Wang, Fayuan, Yang, W., Cheng, P., Zhang, S., Zhang, S., Jiao, W., & Sun, Y. (2019). Adsorption characteristics of cadmium onto microplastics from aqueous solutions. *Chemosphere*, *235*, 1073–1080. https://doi.org/10.1016/j.chemosphere.2019.06.196

Wang, Fen, Wong, C. S., Chen, D., Lu, X., Wang, F., & Zeng, E. Y. (2018). Interaction of toxic chemicals with microplastics: A critical review. *Water Research*, *139*, 208–219. https://doi.org/10.1016/J.WATRES.2018.04.003

Wang, J., Peng, J., Tan, Z., Gao, Y., Zhan, Z., Chen, Q., & Cai, L. (2017). Microplastics in the surface sediments from the Beijiang River littoral zone: Composition, abundance, surface textures and interaction with heavy metals. *Chemosphere*, *171*, 248–258. https://doi.org/10.1016/j.chemosphere.2016.12.074

Wang, Q., Zhang, Y., Wangjin, X., Wang, Y., Meng, G., & Chen, Y. (2020). The adsorption behavior of metals in aqueous solution by microplastics effected by UV radiation. *Journal*

of Environmental Sciences (China), *87*, 272–280. https://doi.org/10.1016/j.jes.2019.07.006

Wang, T., Wang, L., Chen, Q., Kalogerakis, N., Ji, R., & Ma, Y. (2020). Interactions between microplastics and organic pollutants: Effects on toxicity, bioaccumulation, degradation, and transport. *Science of The Total Environment*, *748*, 142427. https://doi.org/10.1016/J.SCITOTENV.2020.142427

Wang, Z., Qin, Y., Li, W., Yang, W., Meng, Q., & Yang, J. (2019). Microplastic contamination in freshwater: first observation in Lake Ulansuhai, Yellow River Basin, China. *Environmental Chemistry Letters*, *17*(4), 1821–1830. https://doi.org/10.1007/s10311-019-00888-8

Wong, J. K. H., Lee, K. K., Tang, K. H. D., & Yap, P. S. (2020). Microplastics in the freshwater and terrestrial environments: Prevalence, fates, impacts and sustainable solutions. *Science of the Total Environment*, *719*, 137512. https://doi.org/10.1016/j.scitotenv.2020.137512

Wright, S. L., & Kelly, F. J. (2017). *Plastic and Human Health: A Micro Issue?* https://doi.org/10.1021/acs.est.7b00423

Yang, D., Shi, H., Li, L., Li, J., Jabeen, K., & Kolandhasamy, P. (2015). Microplastic Pollution in Table Salts from China. *Environmental Science and Technology*, *49*(22), 13622–13627. https://doi.org/10.1021/acs.est.5b03163

Yao, L., Hui, L., Yang, Z., Chen, X., & Xiao, A. (2020). Freshwater microplastics pollution: Detecting and visualizing emerging trends based on Citespace II. *Chemosphere*, *245*, 125627. https://doi.org/10.1016/j.chemosphere.2019.125627

Yonkos, L. T., Friedel, E. A., Perez-Reyes, A. C., Ghosal, S., & Arthur, C. D. (2014). Microplastics in four estuarine rivers in the chesapeake bay, U.S.A. *Environmental Science and Technology*, *48*(24), 14195–14202. https://doi.org/10.1021/es5036317

Yuan, W., Liu, X., Wang, W., Di, M., & Wang, J. (2019). Microplastic abundance, distribution and composition in water, sediments, and wild fish from Poyang Lake, China. *Ecotoxicology and Environmental Safety*, *170*(November 2018), 180–187. https://doi.org/10.1016/j.ecoenv.2018.11.126

Zhang, K., Shi, H., Peng, J., Wang, Y., Xiong, X., Wu, C., & Lam, P. K. S. (2018). Microplastic pollution in China's inland water systems: A review of findings, methods, characteristics, effects, and management. *Science of the Total Environment*, *630*, 1641–1653. https://doi.org/10.1016/j.scitotenv.2018.02.300

Zhao, S., Zhu, L., Wang, T., & Li, D. (2014). Suspended microplastics in the surface water of the Yangtze Estuary System, China: First observations on occurrence, distribution. *Marine Pollution Bulletin*, *86*(1–2), 562–568. https://doi.org/10.1016/j.marpolbul.2014.06.032

Zhu, X., Qiang, L., Shi, H., & Cheng, J. (2020). Bioaccumulation of microplastics and its in vivo interactions with trace metals in edible oysters. *Marine Pollution Bulletin*, *154*(March), 111079. https://doi.org/10.1016/j.marpolbul.2020.111079

Zou, J., Liu, X., Zhang, D., & Yuan, X. (2020). Adsorption of three bivalent metals by four chemical distinct microplastics. *Chemosphere*, *248*, 126064. https://doi.org/10.1016/j.chemosphere.2020.126064